File Copy

UM-HSRI-PF-74-13-1

BRAKING EFFICIENCY TEST TECHNIQUE

FINAL REPORT

CONTRACT DOT-HS-031-3-765

R. D. ERVIN

C. B. WINKLER

HIGHWAY SAFETY RESEARCH INSTITUTE
THE UNIVERSITY OF MICHIGAN
ANN ARBOR, MICHIGAN 48105

DECEMBER 1974

TECHNICAL REPORT STANDARD TITLE PAGE

1. Report No.	2. Government Accession No.	3. Recipient's Catalog No.

4. Title and Subtitle	5. Report Date
BRAKING EFFICIENCY TEST TECHNIQUE	December 1974
	6. Performing Organization Code

7. Author(s)	8. Performing Organization Report No.
R. D. Ervin and C. B. Winkler	UM-HSRI-PF-74-13-1

9. Performing Organization Name and Address	10. Work Unit No.
Highway Safety Research Institute The University of Michigan Huron Parkway & Baxter Road Ann Arbor, Michigan 48105	11. Contract or Grant No. DOT-HS-031-3-765
	13. Type of Report and Period Covered Final Report 7/73 - 11/74
12. Sponsoring Agency Name and Address U.S. Department of Transportation National Highway Traffic Safety Administration Nassif Building 400 Seventh Street, S.W. Washington, D.C. 20590	14. Sponsoring Agency Code

15. Supplementary Notes

16. Abstract

"A Braking Efficiency Test Technique" provides a method whereby vehicle stopping performance can be specified, measured, and compared independently of the test surface. The method provides for an independent measure of the prevailing friction potential of the test surface. This measure is used to normalize the measured stopping performance of the test vehicle. The concept presented is tailored toward a safety argument and toward rulemaking as a potential adaptation to braking effectiveness requirements which currently exist. A new mobile tire dynamometer, developed for this program, is discussed, as are the results of a demonstration test program carried out at the Bendix Automotive Development Center.

17. Key Words	18. Distribution Statement
Braking Efficiency, normalize, traction, stopping distance, measure, safety, rulemaking	Unlimited

19. Security Classif. (of this report)	20. Security Classif. (of this page)	21. No. of Pages	22. Price
None	None	215	

Form DOT F 1700.7 (8-69)

FORWARD

This final technical report summarizes the results of a program of research devoted to the development of a braking performance test technique based on the concept of braking efficiency. It is submitted in fulfillment of Contract No. DOT-HS-031-3-765 for the National Highway Traffic Safety Administration by the Highway Safety Research Institute of The University of Michigan.

The authors would like to acknowledge the support and assistance of the various individuals and groups who participated in this research effort; in particular, Mr. George Parker of NHTSA, the Contract Technical Manager, Mr. Joseph Boissonneault and his staff at HSRI who fabricated the hardware used in this program, and the personnel of the Bendix Automotive Development Center where the vehicle testing activity took place.

The opinions and findings expressed in this document are those of the authors and not necessarily those of the National Highway Traffic Safety Administration.

TABLE OF CONTENTS

1. INTRODUCTION. 1

2. CONCEPTUAL BASIS FOR THE STUDY. 3

3. THE ELEMENTS OF A BRAKING EFFICIENCY TEST TECHNIQUE. 11

3.1 The Definition of the Reference Vehicle. 12

3.2 Computation of Ideal Stopping Distance . . . 24

3.3 The Measurement of the Reference Tire's Traction Performance. 30

3.4 The Conduct of Limit Braking Tests of Actual Vehicles 42

4. CONDUCT AND RESULTS OF THE DEMONSTRATION TEST PROGRAM. 57

4.1 The Test Vehicles. 57

4.2 The Test Matrix. 60

4.3 Test Procedure 66

4.4 Test Program Results 69

5. APPLICATION OF THE BRAKING EFFICIENCY TEST TECHNIQUE TO RULEMAKING 85

6. CONCLUSIONS AND RECOMMENDATIONS 92

6.1 Conclusions. 92

6.2 Recommendations. 94

APPENDIX A - LITERATURE SURVEY 98

APPENDIX B - DESIGN OF THE SURFACE FRICTION DYNAMOMETER AND PROCEDURES FOR ITS USE 142

APPENDIX C - PROCEDURE AND PROGRAM FOR REDUCING AND HANDLING THE BRAKING EFFICIENCY TEST DATA 185

APPENDIX D - PROCEDURE FOR CONDUCT OF THE BRAKING EFFICIENCY TEST TECHNIQUE 204

APPENDIX E - THE VARIABLE BRAKING VEHICLE. 212

1.0 INTRODUCTION

This document constitutes the final report on U. S. Department of Transportation Contract Number DOT-HS-031-3-765 entitled "Braking Efficiency Test Technique." This research study has been conducted by the Highway Safety Research Institute (HSRI) of The University of Michigan at its facilities in Ann Arbor, Michigan, with certain test activities being conducted at the facilities of the Bendix Automotive Development Center in New Carlisle, Indiana.

The program's primary objective has been the development of a method whereby vehicle stopping performance can be specified, measured, and compared independently of the test surface. The "independence" quality of the method derives from a technique by which a measure of the prevailing frictional "potential" of the test surface is used to normalize a vehicle's stopping performance, as measured on that surface. The normalized characterization thus quantifies the "efficiency" with which the vehicle is capable of utilizing the frictional limitations of the test surface to maximize deceleration. The measure which has been defined, however, involves a specialized concept of "efficiency" which derives from certain convictions concerning the safety relevance of vehicle limit braking capability. Whereas this concept is decidedly removed from "classical" braking efficiency as has been defined, for example, by Rouse (1)*, the body of this report begins, in Section 2, with a discussion of the rationale which forms the conceptual basis for the study. It should be noted that the concept presented here is tailored not only toward a safety argument, but also toward rulemaking as a potential adaptation to braking effectiveness requirements which currently exist within FMVSS 105-75 and 121.

The concept has been developed into a test technique which is comprised of three basic elements. These elements are discussed in Section 3 in the context of the developmental

*Numbers in parentheses indicate references listed in Appendix A.

effort of this program. The technique is defined as requiring two physical measurement activities; one which addresses pavement friction, or more specifically, longitudinal traction potential, and the other which addresses vehicle limit stopping capability. The third element of the method, then, specifies a normalizing formula by which these measurements are combined in the computation of the braking efficiency numeric.

Within this study a demonstration of the developed methodology has been achieved through the conduct of full-scale testing and the accompanying computations of the braking efficiency measure. These tests, described in Section 4, involved the measurement of the limit braking performance of both a passenger car and a heavy truck, as well as the extensive application of a mobile dynamometer for measurement of surface friction. The mobile device, a major development of this study, is especially configured for measurement of the peak traction capability of a reference tire at varying load and velocity conditions.

In Section 5 of the report, the potential application of the developed braking efficiency test technique to rulemaking is examined, together with certain considerations which we feel to be natural outgrowths of the basic concept.

In Section 6, a set of conclusions and recommendation is presented in summary of the program's findings, as well as its implications for future research. The report is structured with five appendices which cover, firstly, a literature survey and then, in the other four sections, the specifically recommended procedures for conducting the braking efficiency technique.

2.0 CONCEPTUAL BASIS FOR THE STUDY

Since the technique which has been developed in this study departs markedly from the classical definition of braking efficiency, it is appropriate that the underlying rationale be carefully articulated. The following discourse serves to establish certain positions upon which the rationale is founded, and to describe the measurement concept which has been pursued.

To begin the discussion in a traffic safety context, the position was adopted that "a vehicle manifests optimum braking performance when it permits the representative driver to achieve the minimum stopping distance while otherwise controlling his vehicle's path under the existing conditions of roadway friction." From this definition, the scope of this study and the form of the desired test method assumed shape. Namely, the "position" suggests the need to (a) characterize minimum stopping distance performance (as opposed to instantaneous deceleration capabilities); (b) to account for the limited ability with which the representative driver can modulate brake pedal effort to maximize braking without suffering wheel lockup; and (c) to attain a meaningful normalization for pavement friction.

As for the characterization of minimum stopping distance performance, this study was not structured to break much new ground. The only substantive departure from current stopping distance measurement practice involved the methodology by which certain concerns about the representative driver were addressed.

It was hypothesized that maximum stopping performance is constrained in service by the degree of brake pedal modulation that is required of the driver to accrue the maximum utilization of a vehicle's braking capability. Since the transient character of the braking process implies continually changing mechanical performance of tires as well as brakes, the brake pedal effort corresponding to maximum deceleration without lockup (Figure 1) may vary markedly over the course of a stop. To the extent that the representative driver seldom, if ever, gathers

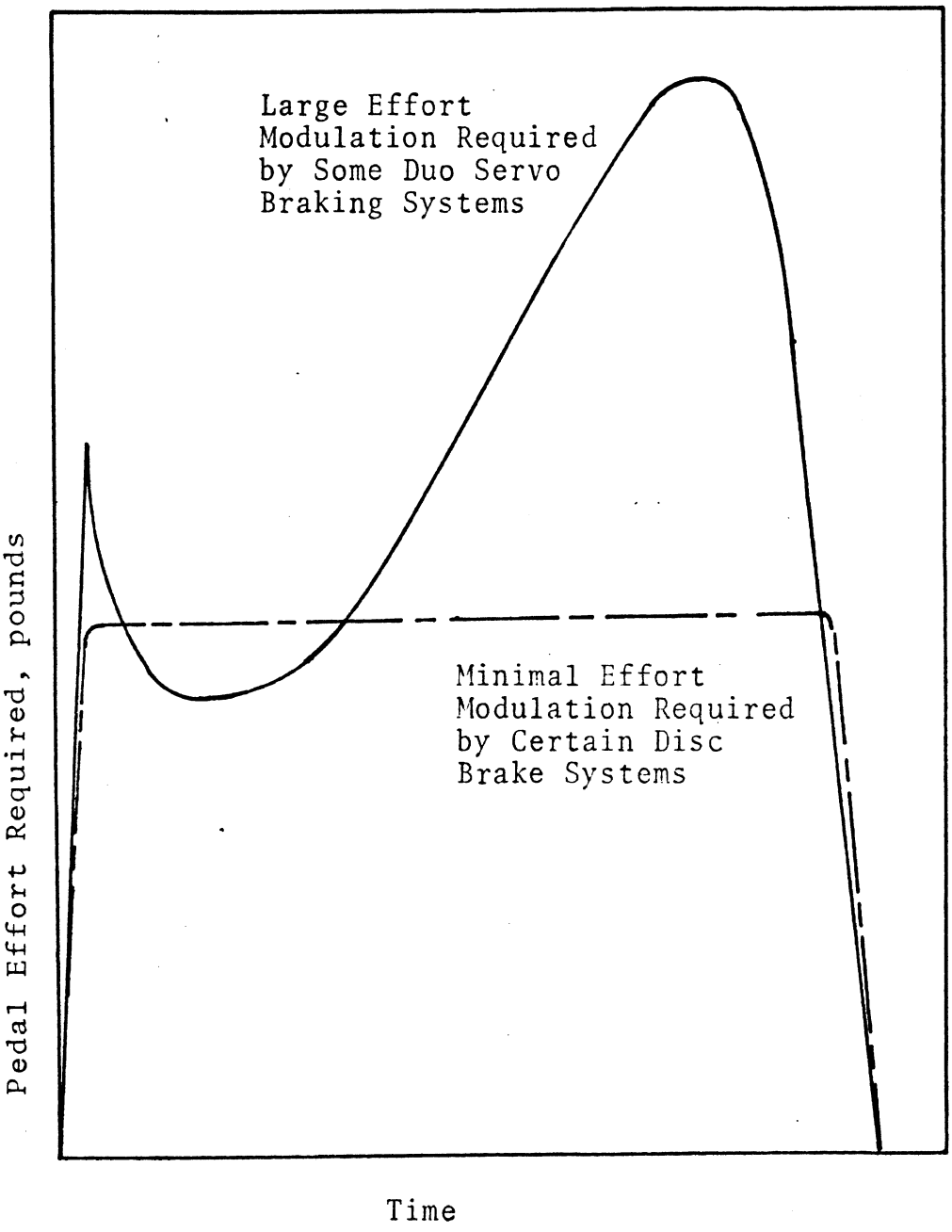

Figure 1. Pedal effort required for a maximum deceleration stop without wheel lock.

experience which would permit him to recognize the need, and thus provide for, appropriate pedal modulation during limit braking, it is hypothesized that safety quality is enhanced by that vehicle system which requires the least modulation or variation in braking effort in achieving complete utilization of the available tire forces.

It follows from the stated hypothesis that, in the absence of comprehensive data describing the brake modulation capability of drivers, braking performance measures should be structured using non-modulated brake pedal effort throughout the stop. Certain tasks were thus devoted in this study to the development of hardware and procedures by which constant-pedal-effort stops could be executed.

The major challenge of the study was to determine a method by which a measure of braking performance would obtain which has safety meaning regardless of the surface employed. Accordingly, the question is raised "What influence does the surface have on determining the stopping distance which can be accrued?" The paved surface comprises only one component of the friction couple which sustains shear force at the tire-road interface. Since the role played by the pavement cannot, within current technology, be distinguished from the role played by the tire, it is not categorically feasible to characterize a pavement's friction force capability as an inherent property residing within the texture and chemistry of the pavement itself. Further, a given tire will generate shear forces on a given surface not only as related to the sum of the mechanical and chemical descriptions of both tire and pavement, but also as influenced markedly by the prevailing velocity and vertical load. Differences in surface texture, chemistry and contamination can cause changes in the relative influence of velocity and tire load on shear force capability.

As a consequence of these facts, the ASTM skid number measure is judged to be an insufficiently comprehensive characterization of the friction-related properties of a

pavement. Whereas the ASTM method utilizes a single vertical load and single test velocity in deriving its measure, no mechanism exists to account for the influence of load and velocity as may be peculiar to the surface being measured. To the extent that the ASTM method represents the only recognized full-scale road friction standard, its shortcomings require that the subject braking efficiency method look to the development of a new tire-road friction measurement.

In determining a position to be taken concerning the tire-road friction characterization which is needed to effect a meaningful normalization of stopping distance, certain implications of a classical version of braking efficiency need to be addressed.

Classical braking efficiency can be defined as a measure of the extent to which a vehicle is capable of accruing the peak longitudinal force capability of each tire throughout the stopping process.

In the simplistic approach which has traditionally been used (for example, in evaluation of a passenger vehicle's front-to-rear brake proportion), the "peak longitudinal force capability" of tires was merely represented by a normalizing constant, μ, where

$$\mu = F_x/F_z \tag{2.1}$$

The μ capability of the tire-pavement couple was utilized in the classical efficiency measure to normalize an average longitudinal acceleration performance, A_x, such that:

$$\frac{A_x/g}{\mu} \times 100\% = \eta \text{ (classical efficiency)} \tag{2.2}$$

A developed interpretation of classical efficiency, such as was applied by Murphy (2), involves a more accurate representation of the road friction capability—substituting a longitudinal force function for the constant characterization, μ. A comprehensive form of this function would include the frictional coupling influences of velocity and vertical tire load, mentioned previously.

If one were to experimentally determine the comprehensive measure of a vehicle's classical braking efficiency, it would require longitudinal shear force measurements of the installed tire while operating on the subject surface at sufficient loads and velocities as to cover all those operating conditions which were experienced by each tire on the vehicle. Following this data acquisition effort, a computation would be conducted in which the running integration of instantaneous acceleration yields the ideal stopping distance which would derive if the perfect anti-lock system was maintaining each tire at its peak force output throughout the stop.

One can quickly perceive that the sensitivity of a tire's normalized longitudinal force to vertical load imposes a host of problems to such a comprehensive classical braking efficiency method, especially for the case of multi-axle commercial vehicles. If one must compute the instantaneous vertical loads of each tire throughout a stop, then one must have a comprehensive knowledge of the manner and degree to which vertical load is distributed about the various axles on a vehicle. For those vehicles with tandem suspensions or with multiple independently-suspended (and thus statically indeterminate) axles, the computation of vertical load distribution requires a complicated and quite non-routine set of parameter measurements. Additionally, a rather complex simulation is then needed to permit the determination of the ideal stopping distance normalizer.

Further, it is clear that any derived classical braking efficiency measure provides no indication of absolute stopping performance capability. A vehicle could score a very high value

of classical braking efficiency by effecting the high utilization of a traction-poor tire. Thus, since good stopping distance capability is not assured through the indication of a high value of classic braking efficiency, it is clear that a tire traction rule would be a necessary adjunct to any classical braking efficiency rule or specification. Further, since tire loading can seriously compromise the accrual of a tire's innate traction capability, it follows that a tire load rating rule would be needed as well.

In light of these observations, it was concluded that classical braking efficiency is unusable as a standard method by which stopping performance can be normalized. Instead, the subject study has pursued the development of a simplified normalization which derives its meaning and validity from a scenario of the safety implications of vehicles distributed serially in traffic streams.

It can be argued, in developing this scenario, that highway travel does not, by its very nature, impose any truly general requirement for the absolute braking performance of vehicles, although in each pure braking application there is an absolute performance requirement to be met if a collision is to be avoided. Accordingly, one can assert that more braking capability is better and, indeed, high levels of capability are probably desirable. However, a specific minimum performance level which is generally essential cannot be identified.

On the other hand, the leading/following distribution of vehicles on the highway does impose an inherently meaningful requirement for relative braking performance. By this prospect, the relative braking capability of serially adjacent vehicles achieves safety meaning due to the likelihood of rear-end collisions as well as the disturbances in traffic flow which arise from the evasive tactics of the less capable braking

performers in the stream. That is, it is generally desirable that all vehicles in the traffic stream have equal braking ability, regardless of their absolute ability.

A braking efficiency measure based upon relative performance departs from classical braking efficiency in that it normalizes a vehicle's stopping performance to account for the extent to which other vehicle-tire systems can utilize the available pavement-limited friction—rather than accounting for the frictional potential of the subject vehicle's own tires on the subject surface. In the development of a standardized technique which involves adjustment for "other vehicle" characteristics, it becomes necessary to standardize the "other vehicle" characteristics. Thus we have defined a braking efficiency characterization which normalizes the stopping distance capability of vehicles against the reference stopping distance capability of "the mean passenger vehicle."

The NHTSA has espoused a comparable rationale in rulemaking which requires a dramatic upgrading of the braking capability of commercial vehicles. Implicit in such rulings has been the notion that the mean passenger vehicle represents the norm, or reference in stopping capability such that it is deemed wiser to upgrade commercial vehicle performance toward passenger vehicles rather than to downgrade passenger car performance. The fact that passenger cars comprise the majority of the vehicle population, and that they generally have exhibited the superior limit braking capability gives basis to the judgment that they represent a de facto norm for braking performance in the traffic system.

In terms of the braking efficiency measurement itself, the concept suggests that two concurrent stopping distance measures will be made on a given surface, using both the subject vehicle and the reference passenger vehicle. Because of concerns over the long-term repeatability of an actual passenger vehicle's performance, however, it was judged more practical to compute

the stopping distance capability of the reference vehicle on the subject surface using tire shear force data which will have been gathered using a special test device. The tire defined to be installed on the hypothetical reference vehicle is one which exhibits a traction performance which is representative of the mean vehicle in the passenger car population.

The exercise of the method outlined here, and developed in the next section, yields a numeric characterization which is novel, but one which is proposed as being specifically addressed to a generally meaningful safety argument.

3.0 THE ELEMENTS OF A BRAKING EFFICIENCY TEST TECHNIQUE

Given the definition of a braking efficiency concept which centers around a reference vehicle scheme for normalization, the bulk of the study was concerned with development of the reference vehicle's performance characterization. Since at the outset we asserted the judgment that no physical vehicle could be used for a reference braking performance measurement, it became necessary to define a computation by which "reference" performance could be derived. The associated computation required the identification of a set of relevant vehicle parameters as well as a mathematical solution to the reference stopping distance expression.

The selection of basic inertial and geometric parameters of the vehicle was complemented by an effort to identify a truly representative reference tire. The reference performance computation would then include a set of parameters describing the traction capability of this tire, as it would be found to operate on the subject test surface. The traction measurements clearly required the development of a new test device—a major task in the program.

Aside from these efforts which were all related to the reference vehicle's performance characterization, additional effort was also devoted to the objectivization of limit stopping distance testing. In this section, we present a digest of the efforts devoted to each of these topics.

3.1 THE DEFINITION OF THE REFERENCE VEHICLE

A scenario was presented in Section 2 in which the differing braking capabilities among vehicles serially disposed in a traffic stream constitute a safety hazard.

In this scenario, a hypothetical "mean" passenger vehicle (as currently exists on the U.S. road system) was seen as representing the reference vehicle. The limit braking capability of this vehicle on any existing road surface was seen, in conceptual terms, as constituting a "friction utilization" level against which the braking performance of other vehicles could be compared.

The computation of the reference vehicle's capability required, as mentioned, that certain parameters be evaluated, viz:

W = total vehicle weight, lbs.

ℓ = vehicle wheelbase, inches

h = height of the vehicle's mass center above the road plane, inches

a = location of the mass center aft of the front axle center.

Clearly, these parameters are significant only in determining the mass which is to be decelerated and the vertical load, F_z, which is imposed upon front and rear tires. Only to the extent that the normalized longitudinal force capability of the vehicle's tires will be sensitive to vertical load is it necessary to be concerned with front versus rear tire loading. This is the case because the computation of the reference vehicle's performance was conceived as representing an ideal braking process by which the maximum available tire shear forces, at the prevailing loads and velocity, would be sustained throughout the stop.

The determination of the cited parameters was guided by an interest in authenticity, in terms of the truly mean representation of modern passenger cars. Thus, in the case of parameters W, ℓ, and a, the American-made portion of the domestic vehicle population was characterized by way of a thorough compilation of data as published for each model year in the Motor Vehicle Manufacturer Association "Specifications." (The parameter h is not generally available from the MVMA or any other source.) The respective vehicle models (and thus parameter values) were each assigned a percentage of the yearly production of the respective manufacturers on the basis of annual sales figures published by the Automotive News. Next, the average value of each parameter was computed for each vehicle model line such as Ford, Chevrolet, Pontiac, etc.

The average parameter values for foreign-manufactured lines of passenger cars were not obtainable from published data. Thus it was necessary to utilize an abbreviated sample of parameters which had been measured previously at HSRI on certain high volume models of foreign vehicles. These vehicle selections, comprising over 60 percent of the foreign car market in the United States, provided average parameter values for each respective foreign manufacturer in a form comparable to that cited for domestic production. (The remaining 40% of foreign vehicles were assumed to possess the average set of foreign vehicle parameters as had been measured.)

At this point, the data consisted of a set of average parameters for the total yearly production for each manufacturing division, both foreign and domestic, for the 1971, 1972, and 1973 model years. Vehicle registration data for all passenger cars were made available by R.L. Polk and Company and were used to assign each manufacturer a percentage of the total vehicle market for each of the three years. By this apportioning, the average value of each of the parameters a, ℓ, and W was then obtained for each model year, as shown in Table 3.1.

TABLE 3-1. COMPILATION OF PARAMETERS OF U.S.-REGISTERED PASSENGER CARS

Production Year	Manufacturers	No. of New Car Registrations in U.S.	Percentage of Total Registrations	Mean Value of Wheelbase, ℓ, (inches)	Mean Value of Normalized Longitudinal Position of c.g. (a/ℓ)	Mean Value of Curb Weight W, lbs.
1971	American	8,263,436	85.0%	116.3	.459	3729
	Foreign	1,465,673	15.0%	94.7	.498	1989
			(Overall Mean)→	113.1	.464	3468
1972	American	8,405,818	85.5%	115.7	.461	3709
	Foreign	1,428,477	14.5%	95.1	.486	2036
			(Overall Mean)→	112.7	.465	3466
1973 (1st 6 mo)	American	4,748,487	84.6%	115.1	.456	3778
	Foreign	867,047	15.4%	94.9	.486	2029
			(Overall Mean)→	112.0	.459	3508

The data compilation and averaging was limited to the three most recent years for which data was available in order to attenuate the influence of older vehicles and thereby effect an extrapolated set of average parameters such as may be more representative of the total vehicle population in the current era (1974-75). Averaging the parameter values over the three years in Table 1, a set of "curb weight" dimensions were defined as follows:

$a = 52.2$ inches

$\ell = 112.6$ inches

$W = 3480$ lbs.

Referring to a limited set of vehicle center of gravity height measurements which had been made at HSRI (122), it was determined that a typical vehicle, whose a, ℓ, and W parameters were as shown above, could be expected to possess a value of $h \approx 22.5$ inches.

The final values specifying the reference "mean" passenger car were further adjusted to include the placement of a 150 lb. driver plus a 75 lb. "half-passenger," yielding the final vehicle configuration shown in Figure 2.

It was recognized, of course, that the indicated mean parameter values represent only a temporary authenticity since certain economic and regulatory influences continue to impact on vehicle design practice, and thus on the configuration of the mean passenger car in the population.

Having established a definition of the reference passenger car, it was necessary to determine a selection for the representative passenger car tire. Since traction capability was the property which would govern selection of the reference tire, it was clear that the tire's representativeness could not be screened with rigor comparable to the car parameter determination. Further, it was clear that limitations in

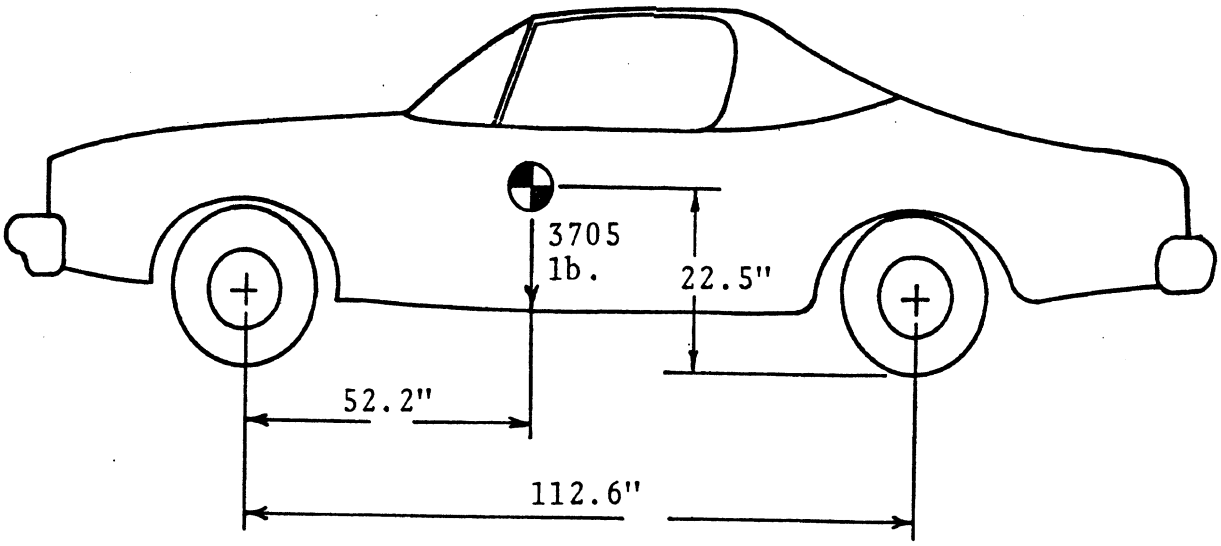

Figure 2. Parameters of the Reference Vehicle

available data describing tire market distribution as well as traction performance would prevent the identification of a tire whose longitudinal shear force capability represented the mean of the operating tire population. Rather, for purposes of this study, a tire would be selected whose traction capability was approximately the average performance of a sample of domestic production tires. The "average" performance characteristic, of course, renders a traction capability which, strictly speaking, is of unknown representativeness to the mean, but one which can be argued to be reasonably representative, given the nature of the traction differences which are observed among tires.

Shown in Figure 3 is a set of data which was generated in a previous study using the HSRI Mobile Tire Tester (21). These data illustrate the distribution of peak normalized longitudinal shear forces measured over a matrix of surface and velocity conditions for each of a sample of eleven tires. The dotted bar within each data sample at a given velocity and surface indicates the average performance for that condition.

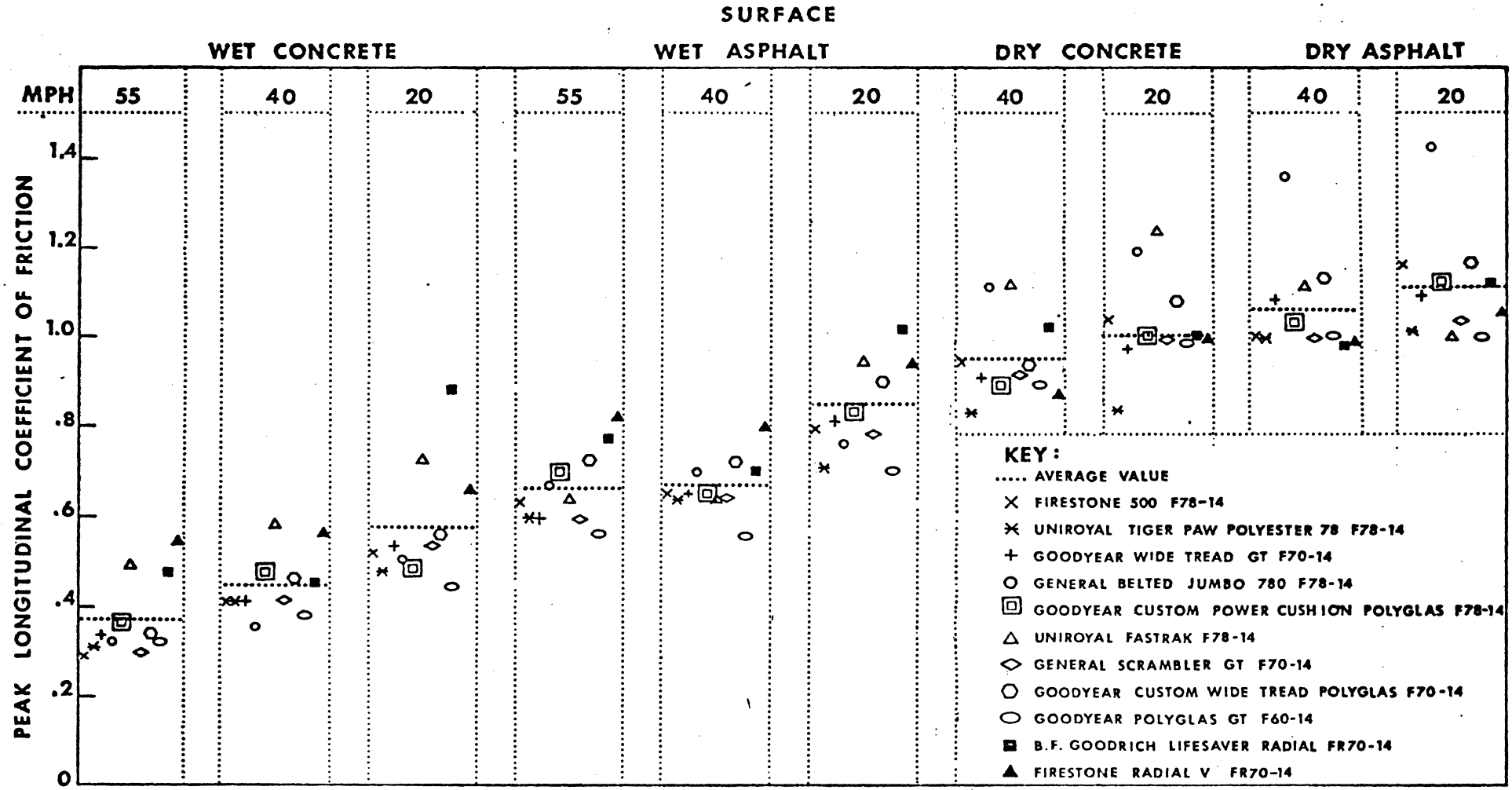

Figure 3. Peak Longitudinal Friction Coefficient Tire Data.

Using these data as the only available reference covering a reasonably broad sample of tires and conditions, the Goodyear Custom Power Cushion Polyglas was identified as the tire construction which was most representative of the average performance.

While the ASTM tire was not included in the eleven-tire sample, there was an interest in determining its degree of representativeness—either as compared to the average of the tire sample performances, or, more conveniently, as compared to the traction capability of the Goodyear Polyglas tire. In the latter comparison, a rationale was espoused by which an adequate match between the performance of the ASTM tire and the Goodyear Polyglas tire would be seen as grounds for selection of the ASTM standard—given that this tire is produced in a controlled fashion and has been designed for maximum stability of tread compound and minimum influence of "reversion" alterations of the tread surface. For purposes, then, of selecting a reference tire for use in this study, the candidate ASTM and Goodyear Polyglas tires were tested, under a variety of pavement and velocity conditions, using the newly-developed Surface Friction Dynamometer device—to be discussed in Section 3.2.

Prior to the gathering of these data, a set of tests were performed using both candidate tires to determine a practice to be observed in preparing tire samples for testing. Of particular interest was the tire break-in procedure which would be required to assure the elimination of mold contaminant effects and the achievement of a stabilized shear force performance. The Goodyear Polyglas tire sample used in these experiments was an E78-14 size, chosen as representative of the size class likely to be installed on a vehicle whose dimensions were comparable to the defined reference vehicle. The test tire's loading, 925 lbs., was determined as the average wheel load on the reference vehicle. As shown in Figure 4, the Goodyear tire was found to exhibit a significant transient in

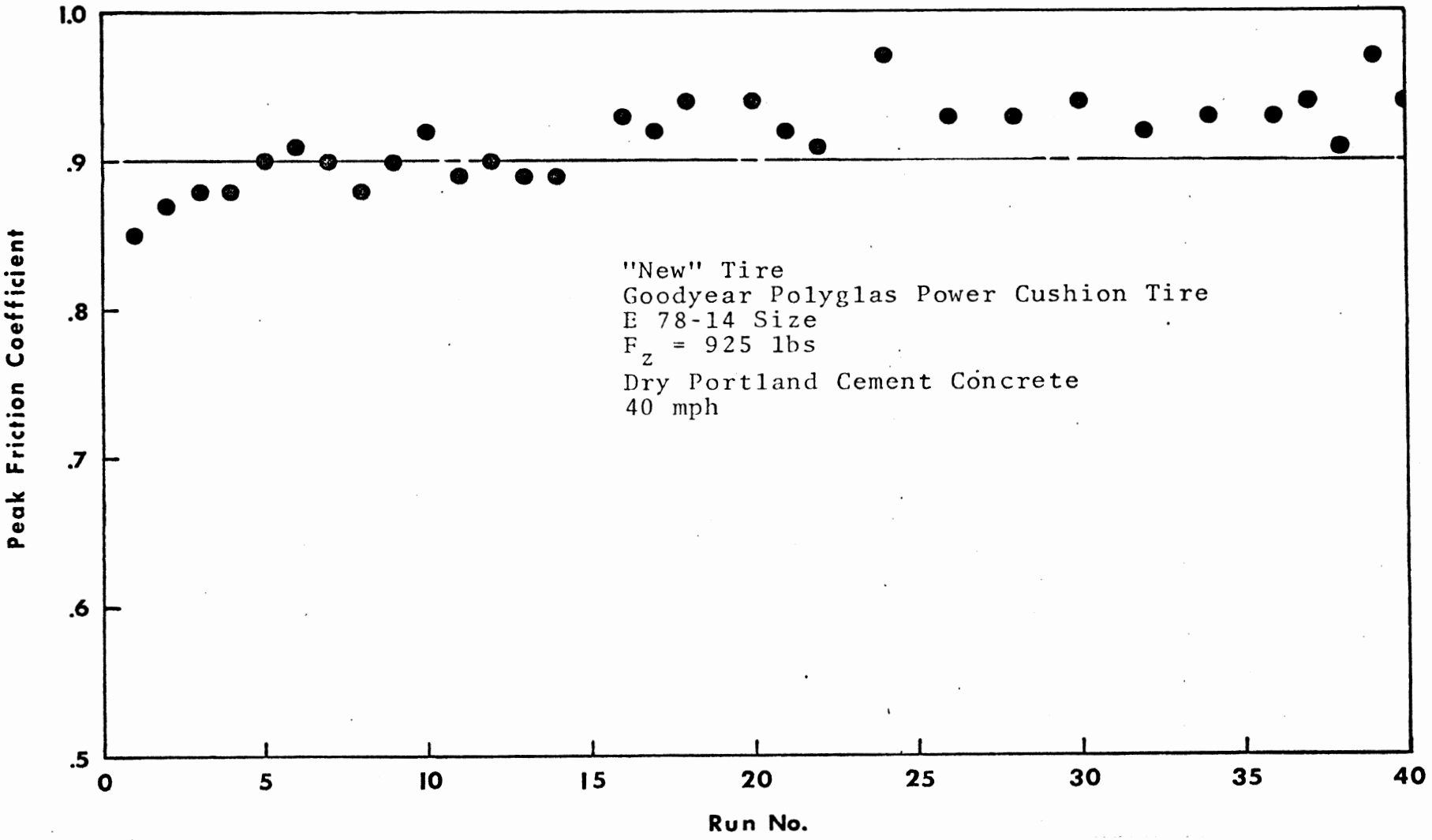

Figure 4. Sensitivity of Peak F_x/F_z Performance of the Polyglas Tire to Cumulative Work History—Beginning with Tire in its New Condition

peak normalized longitudinal force capability as successive lockup cycles were accumulated, beginning with the as-new condition. (The basic "lockup cycle" is as discussed later in Section 3.2.2.) In addition to the "new tire" data, a set of measurements were made under identical conditions, but with a tire whose initial state was that which followed preparation by an ASTM-recommended break-in procedure (free rolling for 100 miles at highway speeds). As shown in Figure 5, the free-rolling break-in procedure clearly did not serve to establish a steady-state or asymptotic performance with this tire. Further, it was clear that a preconditioning practice involving 20 lockup cycles would be required to assure achievement of a steady performance. The preconditioning work history was found to impose a rather insignificant tread surface adjustment, with less than 1/32 in. tread depth loss typically observed.

In a duplicate experiment conducted with the ASTM G78-15 tire (designation E501-73), the data shown in Figure 6 was obtained, indicating a much "quicker" achievement of steady-state performance. On the basis of these measurements it was determined that the burdensome 100-mile break-in practice would be avoided and, instead, a preconditioning involving 10 lockup cycles would be conducted on the ASTM tire.

Following the specified preparation procedure, then, a set of data was gathered using both of the subject tires, under each of 12 conditions of surface and velocity. On the basis of data shown in Figure 7, the ASTM E501-73 tire was judged to possess a traction potential which was sufficiently close to that of the "representative" Goodyear Polyglas tire that the ASTM selection could be applied as the reference tire in this study. This judgment was based upon the magnitude of the differences in performance of these two tires as compared to the range of differences which were observed among the eleven-tire sample. As can be noted in Figure 7, the broadest departure of the ASTM tire from the Goodyear's

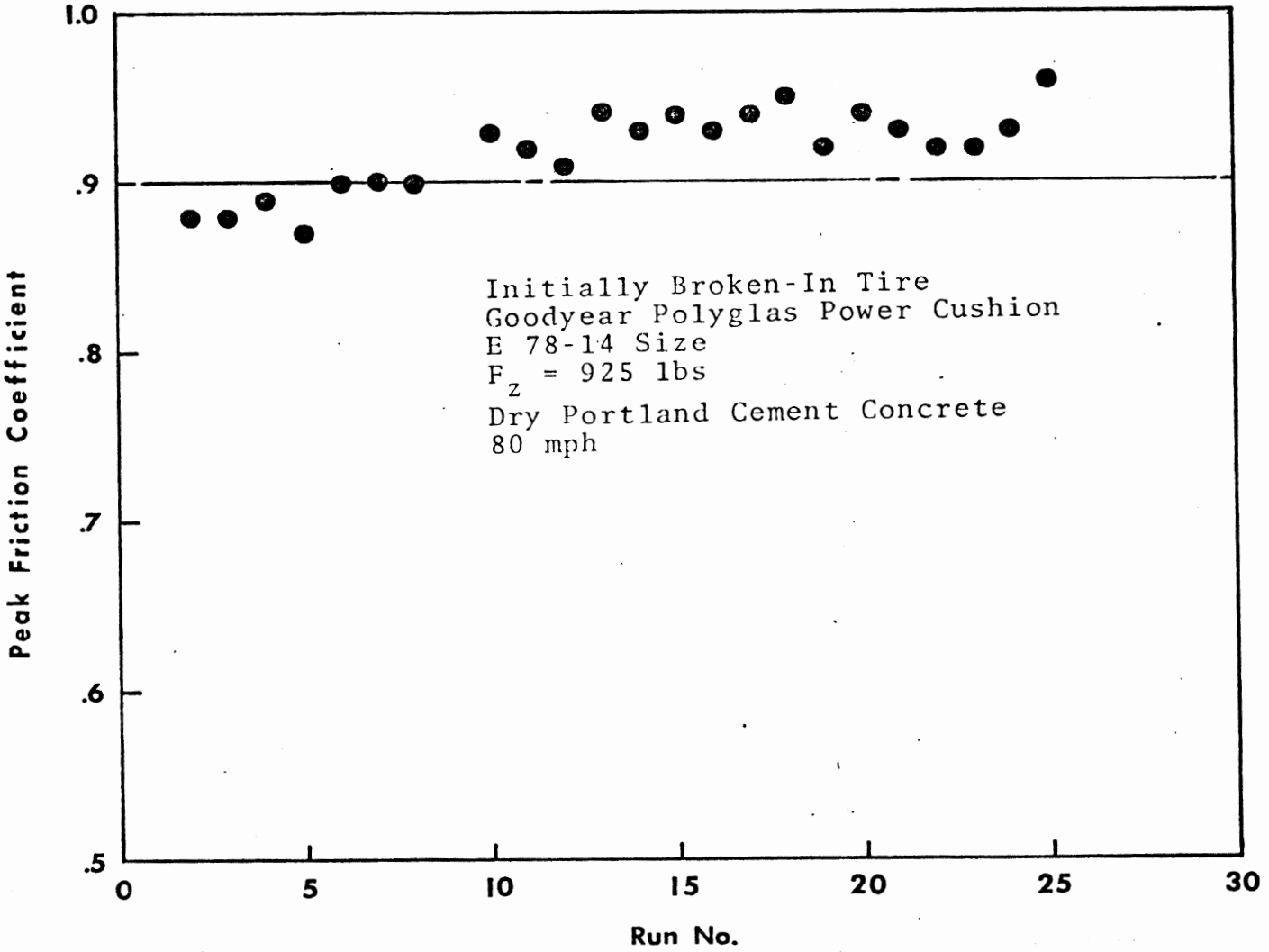

Figure 5. Sensitivity of peak F_x/F_z performance of the Polyglas tire to cumulative work history—beginning with tire in its "100-mile worn-in" condition.

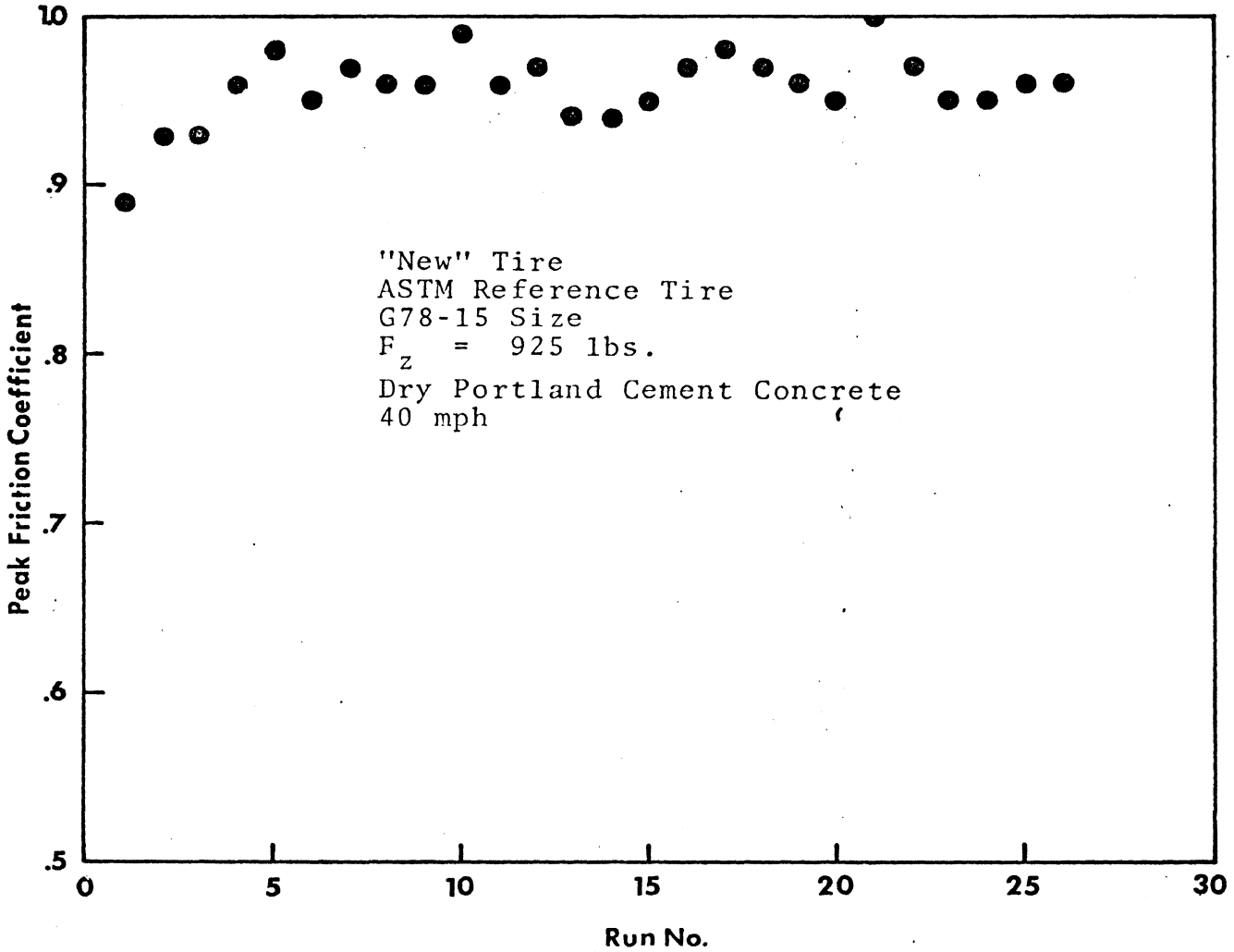

Figure 6. Sensitivity of peak F_x/F_z performance of the ASTM tire to cumulative work history—beginning with tire in its new condition.

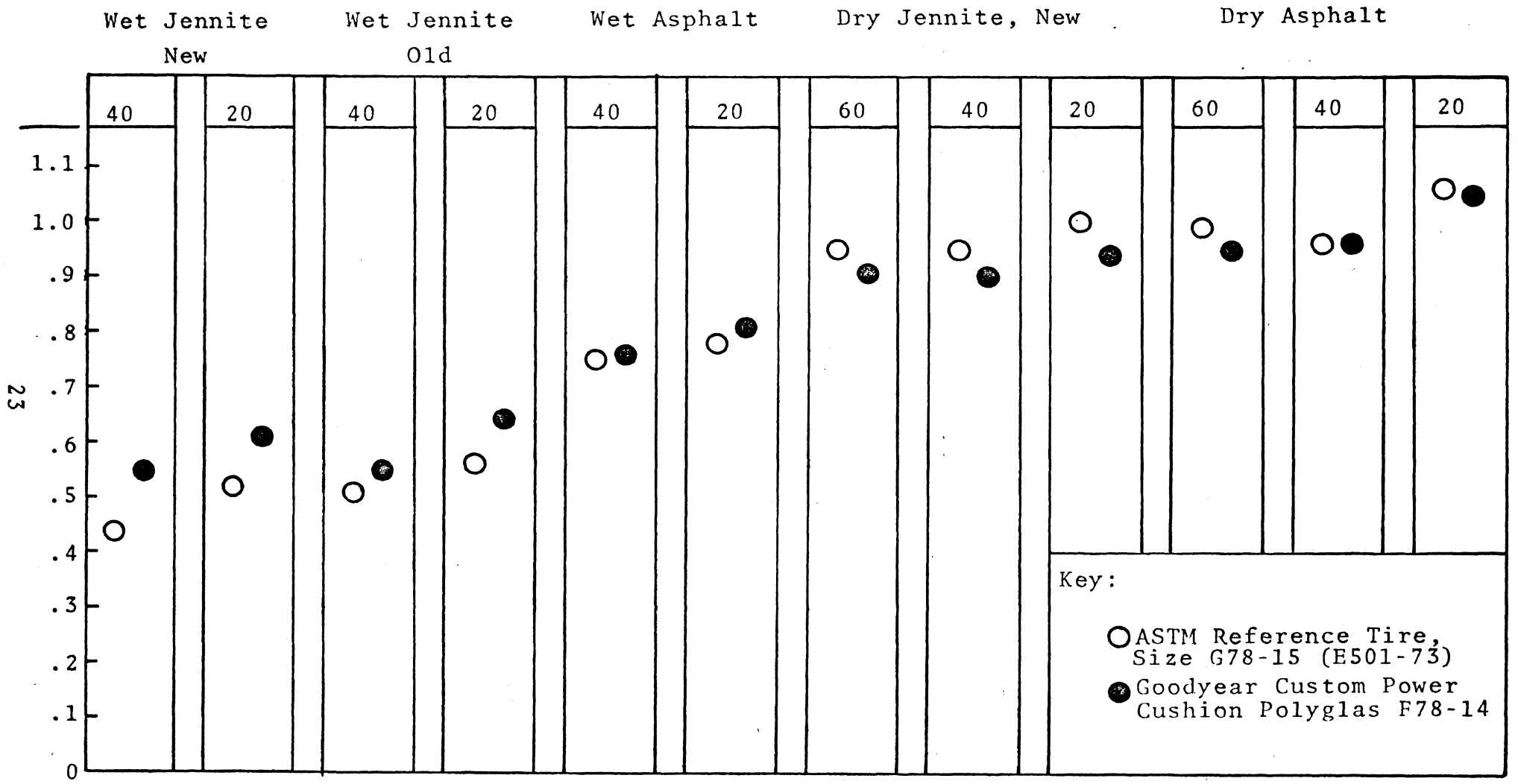

Figure 7. Polyglas tire-ASTM tire comparison data.

traction performance occurs on wet coated-asphalt surfaces—an observation which has been made by other organizations capable of such measurements.

3.2 COMPUTATION OF IDEAL STOPPING DISTANCE

The Braking Efficiency Test Technique provides a measure of the test vehicle's braking efficiency as defined by the equation:

$$\text{Eff} = \frac{\text{Ideal Stopping Dist.}}{\text{Measured Stopping Dist.}} \times 100\% \qquad (3.1)$$

where the "measured stopping distance" is the minimum stopping distance of the test vehicle and the "ideal stopping distance" is the minimum stopping distance which the reference passenger vehicle could ideally obtain, given the friction properties of the reference tire/test-surface combination.

The use of the term "ideal" implies several arbitrary, but supportable, assumptions with regard to the reference vehicle's performance during the stopping process. In general, these assumptions are made to yield a determination of the minimum stopping distance imaginable, while accounting for the interfacial shear force potential of the reference tire/test surface combination as this potential is influenced by the reference vehicle parameters. Additionally, the assumptions serve to maintain a practical level of simplicity in problem solution.

The basic assumptions which underly the derivation of the ideal stopping distance are listed below in what might be considered "order of importance."

1) The reference vehicle's braking system is such as to maintain the generation of peak available brake force at each tire during the entire stopping process. Implicit in this statement

is the fact that brake system response is instantaneous, not only during the stop, but at its onset.

2) Reference tire/test-surface peak longitudinal friction performance may be described by the equations:

$$\mu_{PF} = A_F V^2 + B_F V + C_F \tag{3.2a}$$

$$\mu_{PR} = A_R V^2 + B_R V + C_R \tag{3.2b}$$

where V is vehicle velocity, μ_p is peak normalized longitudinal shear force (F_x/F_z), A, B, and C are parametric constants, and the subscripts F and R denote front and rear tires, respectively.

3) The pitch response of the reference vehicle is instantaneous, i.e., fore/aft load transfer is quasi-static.

Given the acceptance of the premise that ideal stopping distance is the proper reference, or normalizer, for the braking efficiency measure, then assumption (1) is justified in that it embodies the essential meaning of ideal. Minimum (or ideal) stopping distance will result from continuous usage of the peak available traction force at each of the reference vehicle's tires. However, the argument has been encountered that suggests, while peak friction utilization is reasonable, the assumption of an instantaneous brake application rate is not. After all, such performance is impossible in the real world and must be accounted for in the technique.

Indeed, this is true, but continuous peak friction utilization is equally impossible. The list of "impossibilities" in any simple notion of "ideal" is fundamentally unlimited. For instance, given the state-of-the-art, the use of truck tires whose friction capability is as high as the

reference tire may be equally impossible. The point is merely that each of these impossibilities represents a safety degrading penalty which results in a real-world stopping performance which is somewhat less than ideal. Each source from which less than ideal performance derives is no more conceptually confounding than any other. Each source adds feet to stopping distance performance; each foot just as likely to result in accidents as any other.

This is not to say that such real-world considerations may go unaccounted for. On the contrary, they may all be accounted for together, none receiving special significance over the other, by establishing a realistic level of required braking efficiency. The general question of performance level selection is addressed more fully in Section 5.0, "Application of the Braking Efficiency Test Technique to Rulemaking."

Assumption (2), above, derives its support from a more technical basis. The reference tire, operating on a given surface, will show peak longitudinal friction capability which varies as a function of both vertical load and velocity. During a stop, the velocity of the reference vehicle will vary from the initial test velocity down to zero. The vertical load, however, which is experienced at each of the vehicle's tires will be more nearly constant, although loading of front tires may be very different from loading of rear tires. Accordingly, we have chosen to define front tire and rear tire traction capability as separate functions of velocity, without specifically describing a load sensitivity function. This definition is rationalized by way of the following discussion.

Consider that each reference tire/test-surface combination will exhibit what might be called a nominal peak friction capability. Given the ideal nature of the reference vehicle's braking system, this friction level, μ_{nom}, will be equal,

in g-units, to the nominal deceleration of the reference vehicle and will, in combination with the reference vehicle parameters, establish a nominal load level for the front (F_{zF}) and rear (F_{zR}) tires, respectively, according to the following formula:

$$F_{zF_{nom}} = 994 + 370\ \mu_{nom} \quad \text{lb.} \tag{3.3a}$$

$$F_{zR_{nom}} = 859 - 370\ \mu_{nom} \quad \text{lb.} \tag{3.3b}$$

The time history of reference tire loadings during a stop will vary only slightly about these nominal values due to velocity and load sensitivities. Consider, for example, the reference tire data gathered during this study's demonstration test program and presented in Figure 8. For a given surface, the maximum span in peak longitudinal friction across velocity and load variations (load variations much larger than the load range over which a front or rear tire of the reference vehicle would be operated) is 0.16. By Equations (3.3) an equal variation in vehicle deceleration implies a tire load variation of approximately 59 pounds. With this result, two points become significant:

1) The reference tire, having been identified as a representative passenger car tire, will exhibit very small variations in longitudinal traction performance due to load variations of the order of 60 lbs.

2) It is unreasonable to expect an over-the-road tire tester to have sufficient force measurement fidelity to identify such small variations in longitudinal traction performance.

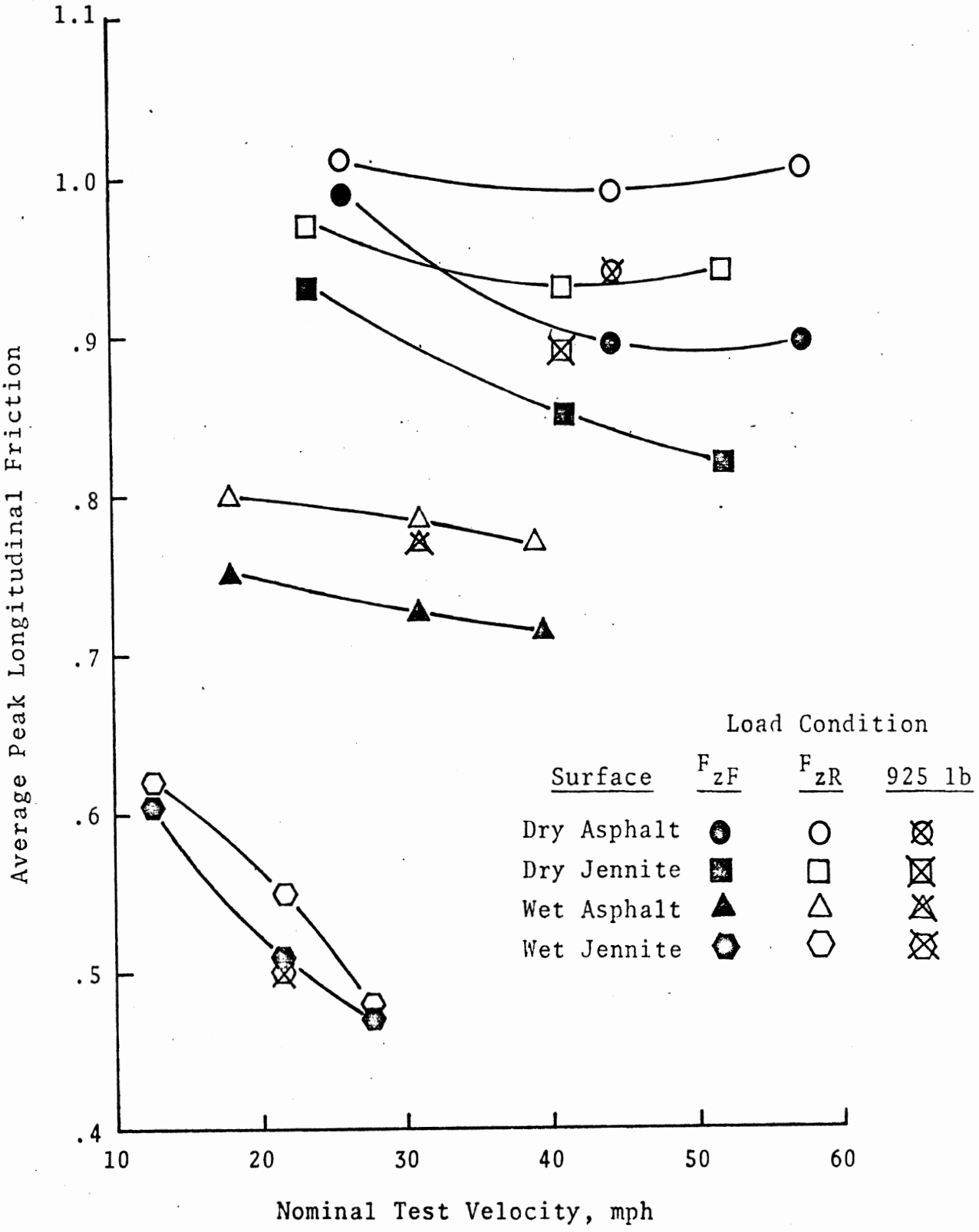

Figure 8. Reference tire data review.

It therefore is reasonable to represent the reference tire traction performance, as required for the calculation of ideal stopping distance, as two independent functions, representing front and rear tire performance, respectively, Each function is independent of load, thus ignoring small load variations occurring at each axle, but each function is unique such that their differences encompass performance variations resulting from the large tire load differences, front to rear.

The actual functions used as tire performance descriptors are those of Equation (3.2) . Each function is sensitive to velocity in both the first and second power. Thereby, a reasonable representation of the velocity sensitivity of peak longitudinal friction performance obtains.

The basis for assumption (3) lies primarily in pragmatism. The assumption of quasi-static load transfer greatly reduces the complexity of the ideal stopping distance calculation (to say nothing of avoiding the need for determining mean passenger car spring rates and pitch moments of inertia) while not damaging the conceptual foundation of the calculation.

Having established the basis for the ideal stopping distance (D_I) problem, the mechanics of its solution are rather straightforward. Details of the derivation of a closed-form expression for D_I are given in Appendix C, Section C.3.1.1.

Several sample calculations have been made to establish the validity of this closed-form solution. Sample results from the algebraic, closed-form solution were compared with ideal stopping distances calculated using a numerical integration solution. These results agreed to within 0.1 foot. (Stopping distances for these examples ranged from 132 to 297 feet.)

3.3 THE MEASUREMENT OF THE REFERENCE TIRE'S TRACTION PERFORMANCE

Measurement of the peak longitudinal traction capability of the reference tire, over the range of velocities and loads of interest, is necessary in order to implement the calculation of the ideal stopping distance. As indicated in Section 3.2, the mathematical expressions used to model the reference tire's peak traction performance provide for the effects of loading differences, front to rear, as well as for a quadratic velocity effect.

Thus the braking efficiency method requires that tire tests be conducted in order to provide sufficient data to establish the values of the parametric constants of Equations (3.2a) and (3.2b). The accomplishment of this task implies the solution of three problems, namely:

1) Establishment of a well designed tire test matrix encompassing appropriate values of test velocity and tire loading.

2) Employment of an appropriate tire test device.

3) Effective implementation of the resulting data.

The following three sections address each of these problems respectively.

3.3.1 DESIGN OF A TIRE TEST MATRIX. In general, the tire test matrix must provide sufficient data points to establish the peak longitudinal friction performance over the range of loads and velocities to which the tire would be subjected during a minimum distance stop of the reference vehicle on the test surface of interest. Specifically, the matrix must provide sufficient data points to permit the fitting of quadratic expressions to the front and rear tire traction equations.

Given the parametric description of the reference vehicle, and the assumption of quasi-static pitch behavior, the vertical load imposed upon the reference vehicle's front and rear tires may be expressed as a function of vehicle deceleration, as follows:

$$F_{zF'} = 994 + 370\ a_x \quad \text{lb.} \tag{3.4a}$$

$$F_{zR'} = 859 - 370\ a_x \quad \text{lb.} \tag{3.4b}$$

where

$F_{zF'}$ = vertical load on each front tire

$F_{zR'}$ = vertical load on each rear tire

a_x = longitudinal deceleration in g units

Given the ideal nature of the reference vehicle's braking system, a_x in Equations (3.4) is simply a function of the peak longitudinal friction properties of the reference tire/test-surface combination. Therefore, vertical loading appropriate for the tire test activity is dependent on tire-surface friction properties.

In the context of a vehicle test program, appropriate tire test velocities also became dependent on tire-surface friction. Velocities of interest range from V_o, the initial velocity of the stop, down to zero. Although the reference vehicle "stop" is a calculation activity, the test vehicle must be subject to real-world stopping distance tests from the same velocity. Particularly for reasons of test safety, V_o must be chosen according to the friction characteristic of the test surface.

A dilemma thus arises in which the tire test conditions of load and velocity should be chosen according to friction

properties of the tire/surface combination; properties which are unknown until tests are conducted.

To solve this dilemma, the tire test matrix condition and the initial velocity of the stopping distance test are determined according to the results of an initial set of tire tests which establish the nominal peak friction level, μ_{nom}, of the reference tire/test surface combination. These tests are conducted with the test tire experiencing a load, F_{zt}, of 925 lb. (which is one-quarter of the weight of the reference vehicle or the average tire load imposed by the reference vehicle) and at a test velocity, V_t, within the range

$$.707\ V_o - 5 \leq V_t \leq .707\ V_o + 5 \qquad (3.5)$$

where V_o and V_t are in miles per hour. The velocity, V_o, is the initial velocity from which vehicle stopping performance is measured. V_o is determined, as a function of μ_{nom}, according to the relationship described in Figure 9. The value of μ_{nom} is defined as the average peak value of longitudinal friction measured in five tests conducted at F_{zt} and V_t.

The relationship described in Figure 9 derives primarily from experience gathered in the demonstration test program regarding test site safety. Particularly in the middle range of μ_{nom}, V_o values are lower than those originally envisioned and may appear to the reader as somewhat lower than necessary. This results from the fact that μ_{nom} is a peak friction measure, while test site safety is more closely related to slide friction values. (Test safety becomes a serious issue when vehicle control is lost due to wheel lock and, consequently, slide friction levels prevail.) The relationship described by Figure 9 has the further advantage of containing no discontinuities in the initial velocity prescription. (That is, the conduct of compliance testing on marginally

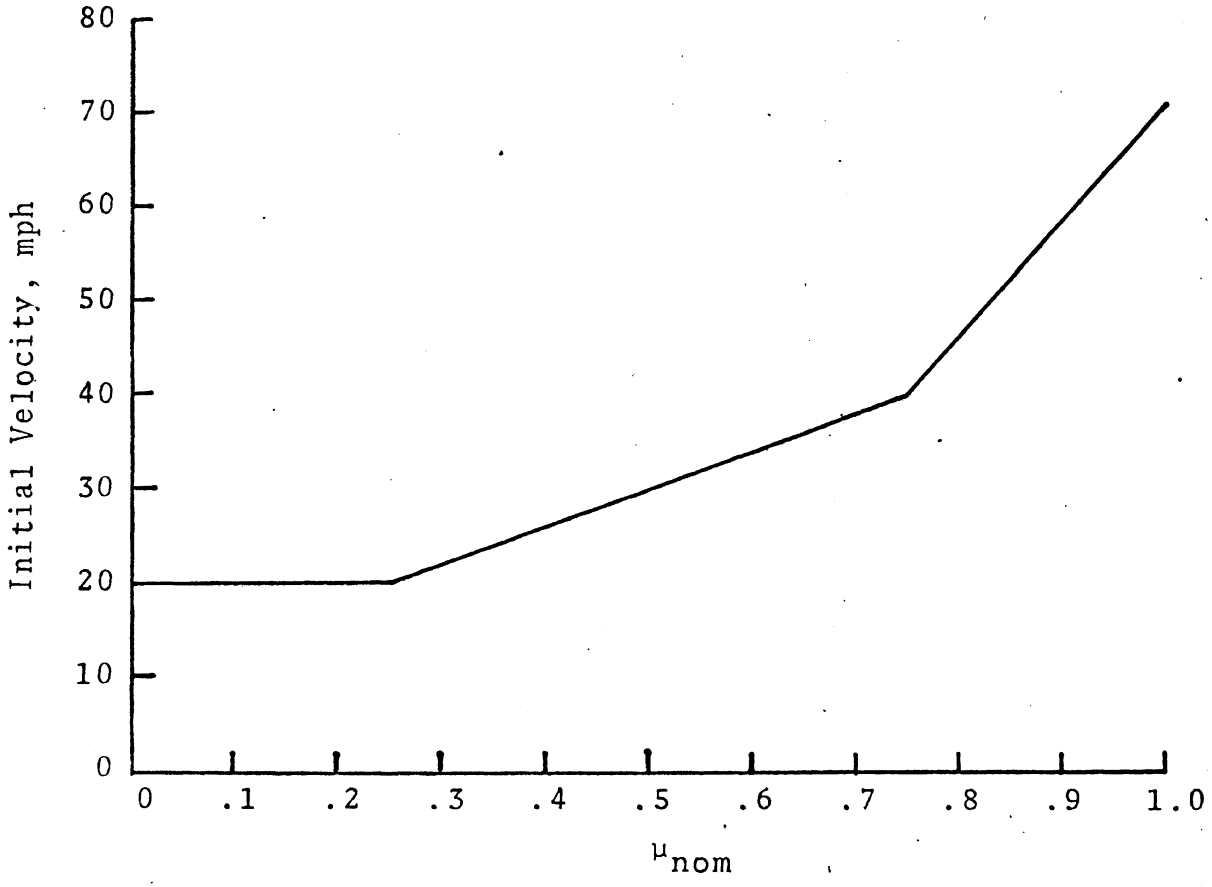

Figure 9. Initial velocity as a function of μ_{nom}.

"different" surfaces cannot require major differences in the testing program or in vehicle performance.)

Since the permissible range of velocity (V_t) at which this initial tire test is run (.707 V_o ± 5 mph) is dependent on μ_{nom}, whose value is not known until the test is complete, an iterative test process is required. However, the ± 5 mph tolerance in V_t is large enough that, given a reasonable initial judgment regarding the value of μ_{nom}, a qualifying set of five tire tests may be easily arrived at after conducting only a very few initial trial tests.

With the values of V_o and μ_{nom} established, the tire test matrix appropriate for the particular test surface may be established. The tire test matrix is a six-point, two-dimensional matrix derived from three velocity and two normal load conditions. The three test velocities are:

$$V_1 = .913\ V_o \tag{3.7a}$$

$$V_2 = .707\ V_o \tag{3.7b}$$

$$V_3 = .408\ V_o \tag{3.7c}$$

These three velocities were chosen according to the following rationale. Assuming constant deceleration, a_x, the relationship between instantaneous velocity and distance traversed is shown in Figure 10. Test velocity points are chosen for the tire data matrix based upon an equal contribution to stopping distance. Thus the stopping distance (d_t) of Figure 10 is partitioned into three equal segments and the velocity accruing at the median distance of each partition is designated as one of the test velocities.*

*It will be noted in Section 4.4.1 that the choice of these three velocities resulted in certain difficulties in fitting tire data to Equations (3.3). Consequently, in Appendix D, four velocities have been suggested for use in future applications of the technique.

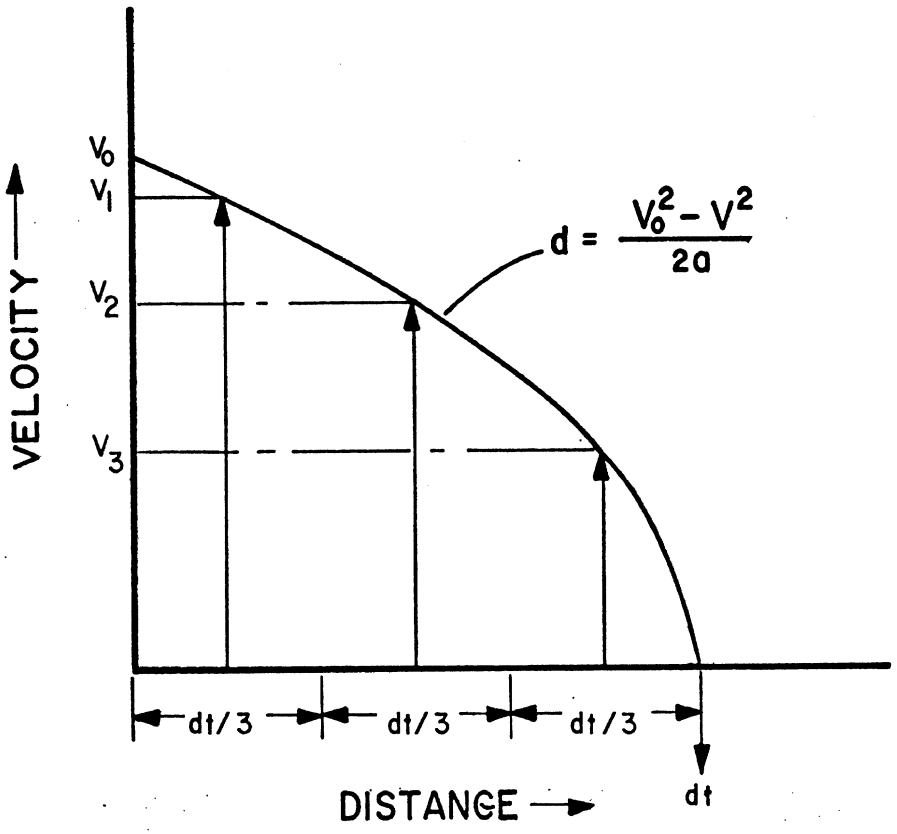

Figure 10. Velocity vs. distance for a constant deceleration stop.

Note that vehicle velocity which occurs at 1/2 the stopping distance is .707 V_o. It is this "median distance velocity" which was employed in Equation (3.6) as the most representative velocity about which to define the acceptable range for the initial tire test velocity, V_t.

The two conditions of normal load (F_z) at which tire tests are conducted are defined as indicated earlier by the relations:

$$F_{zF} = 994 + 370\ \mu_{nom} \tag{3.7a}$$

$$F_{zR} = 859 - 370\ \mu_{nom} \tag{3.7b}$$

By way of review, all test velocities and test tire loads, as they relate to μ_{nom}, appear in Figures 11 and 12.

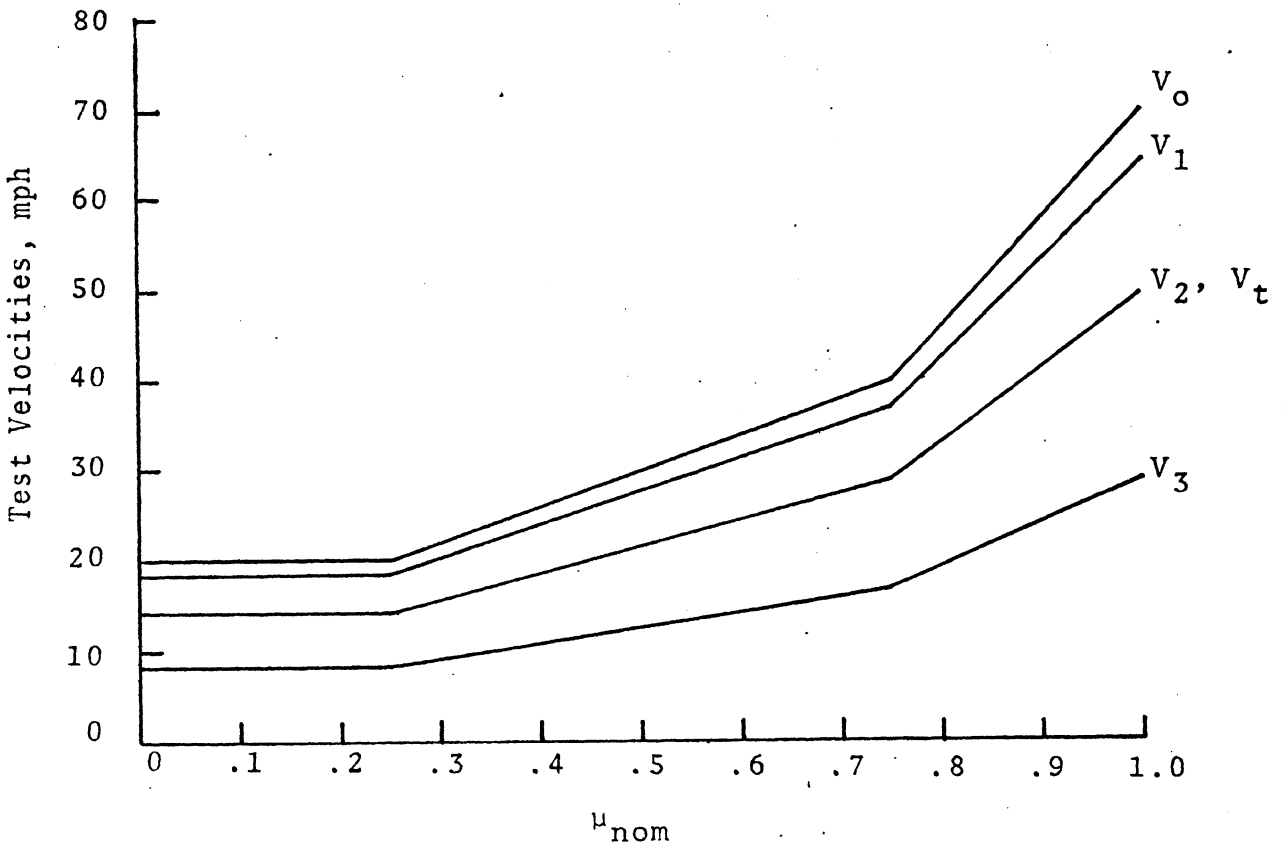

Figure 11. Test velocities as a function of μ_{nom}

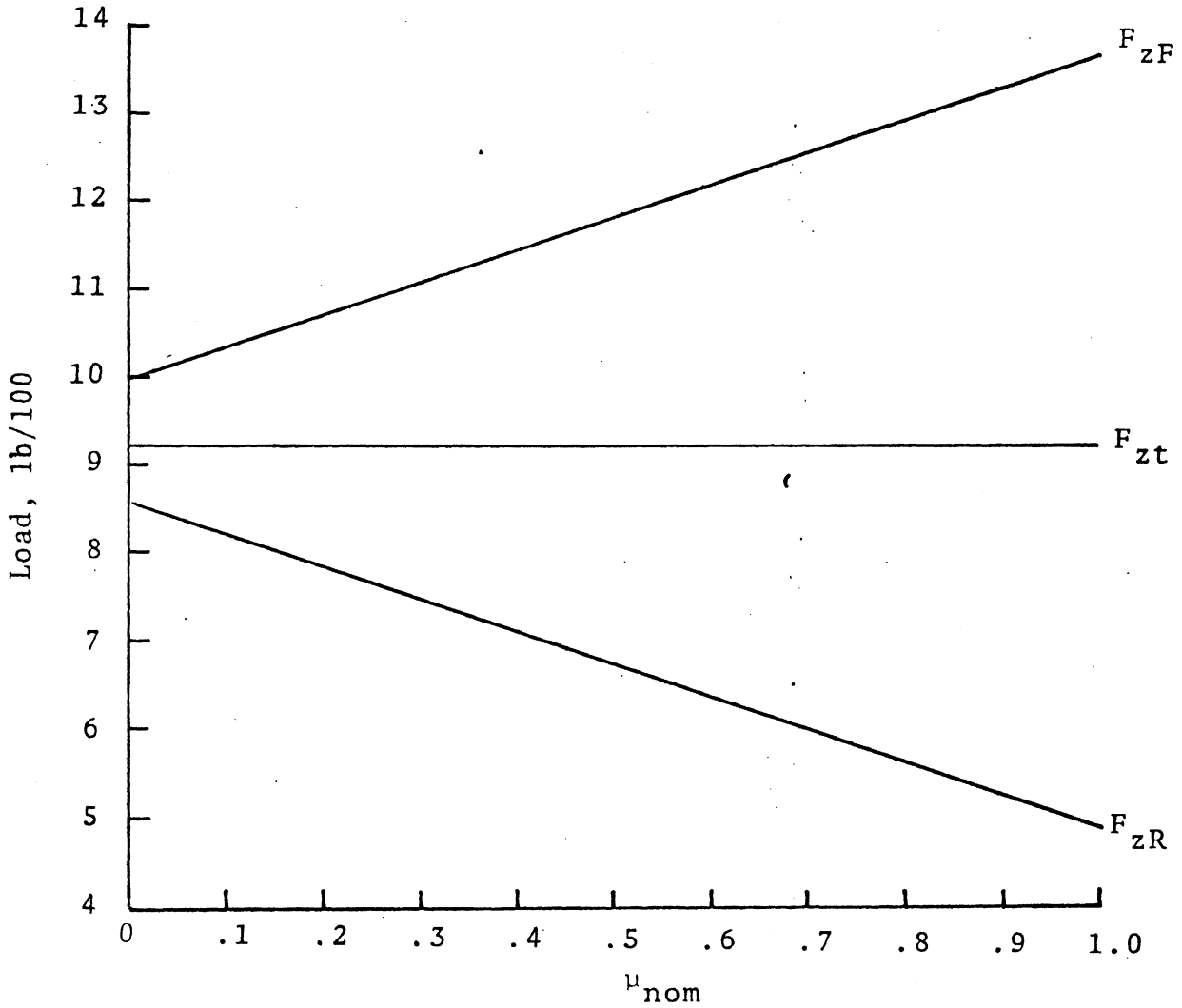

Figure 12. Tire test loads as a function of μ_{nom}

Thus is described a six-point tire test matrix. A minimum of five valid tire tests must be conducted for each of the six matrix points (i.e., a minimum of 30 tire tests are needed to describe the test surface). A tire test is considered valid when it produces an F_z* measure within ± 50 lb. of the prescribed vertical load and a V_5* condition within ± 2 mph of the prescribed test velocity.

3.3.2 DEVELOPMENT OF THE SURFACE FRICTION DYNAMOMETER. The braking efficiency test technique, by requiring the calculation of an ideal stopping distance of the reference passenger vehicle on the test surface of interest, demands the gathering of reference tire/test surface peak longitudinal friction data. This data must be gathered at a variety of loads and velocities, in accordance with the above defined test matrix.

A review of the available tire test devices showed that very few of them are suitably designed to facilitate the required measurements. For example, the so-called "skid trailer," which does exist in large numbers, has limited applicability to the braking efficiency tire test problem for two reasons. Firstly, skid trailers are not designed specifically for tire testing at a variety of vertical loads. Although test tire loading is variable by changing trailer loading, it is a cumbersome procedure.

Of greater interest, however, is a problem implied by the need to determine peak, rather than sliding friction. The great majority of trailer-type devices have been ineffective in suppressing the undulation in vertical load on the test wheel(s) which results from operation on surfaces which are not perfectly smooth. This variation in load, combined with the very low time constant exhibited by the wheel spin-down system results in marked variation in peak

---

*Detailed definitions of F_z and V_5 values as derived from raw test data are given in Appendix C, Section C.2.

longitudinal force exhibited from run to run, plus a very short (difficult to interpret) recording of peak force.

One method for solving this problem involves closed-loop control of the longitudinal slip of the test tire. Indeed, there exist a small number of tire test devices which provide such control and which would be compatible with the tire test needs of the braking efficiency test technique. Unfortunately, such devices require elaborate control systems and consequently are rather expensive. Inasmuch as the brake efficiency test technique is considered for application in a safety standards context, it was not deemed reasonable to require the use of such an economically burdensome device.

Thus, a major portion of the effort of this program was directed toward the development of a tire test device, technically suited to the needs of the braking efficiency test technique, but whose cost would not exceed the market value of commercially-available ASTM skid trailers.

The Surface Friction Dynamometer (SFD) developed in this program is pictured in Figures 13 and 14. A pickup truck with a crew cab mounts a device capable of measuring longitudinal friction performance of passenger car tires on paved surfaces. The device will accept 14- and 15-inch passenger car tires and is designed to measure the longitudinal shear force characteristics of tires operated at vertical loads ranging from 400 to 2000 pounds.

The reference or test tire is located at the rear of the vehicle on the vehicle center line. The tire is suspended by a wheel carriage structure (WC) which is free to move vertically and is otherwise constrained by a pair of low friction, ball spline assemblies. A biaxial serial load cell joins the test wheel spindle assembly to the WC, and transduces vertical (F_z) and longitudinal (F_x) forces. Vertical tire forces are generated by a low rate air spring which bears upon the WC.

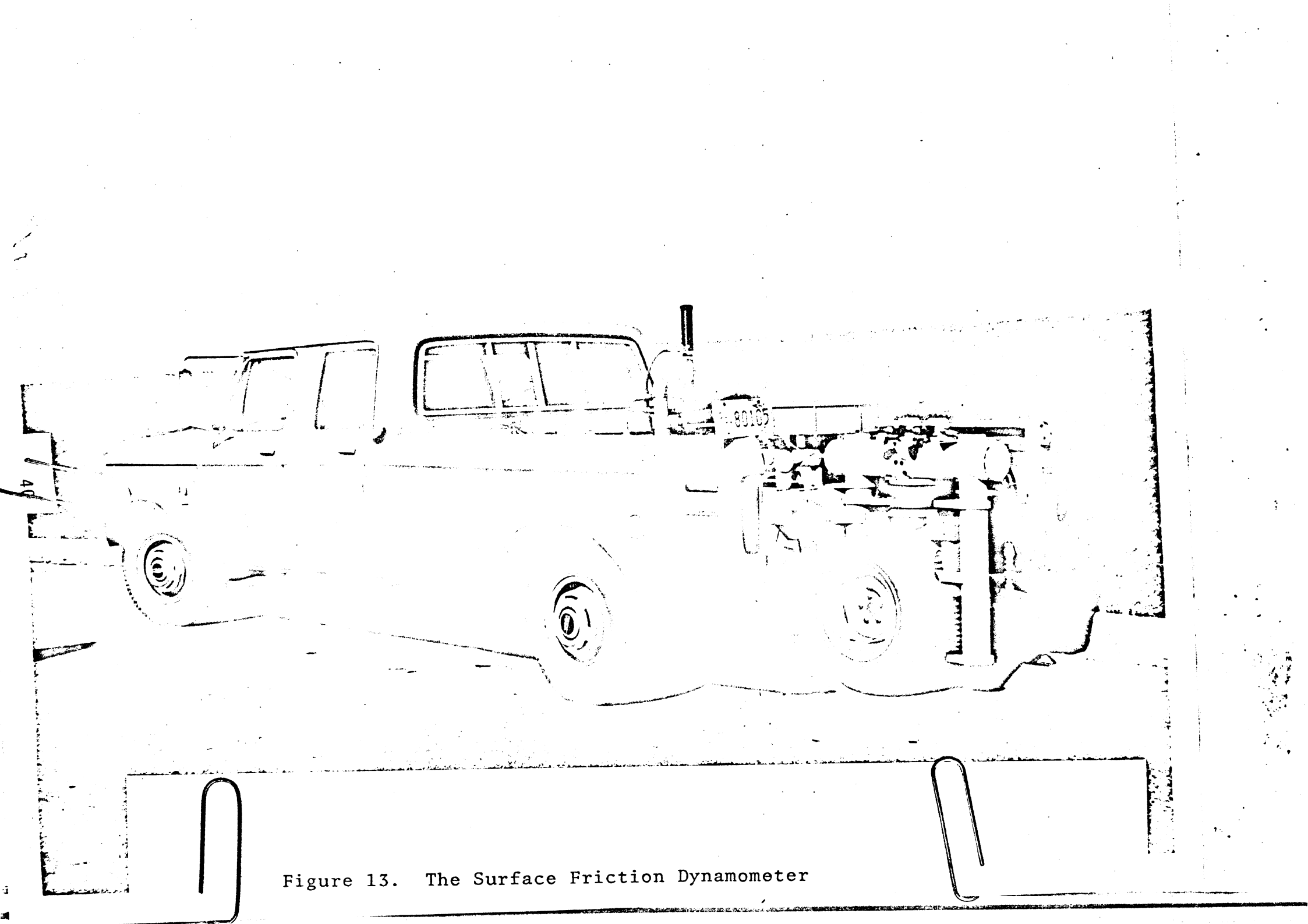

Figure 13. The Surface Friction Dynamometer

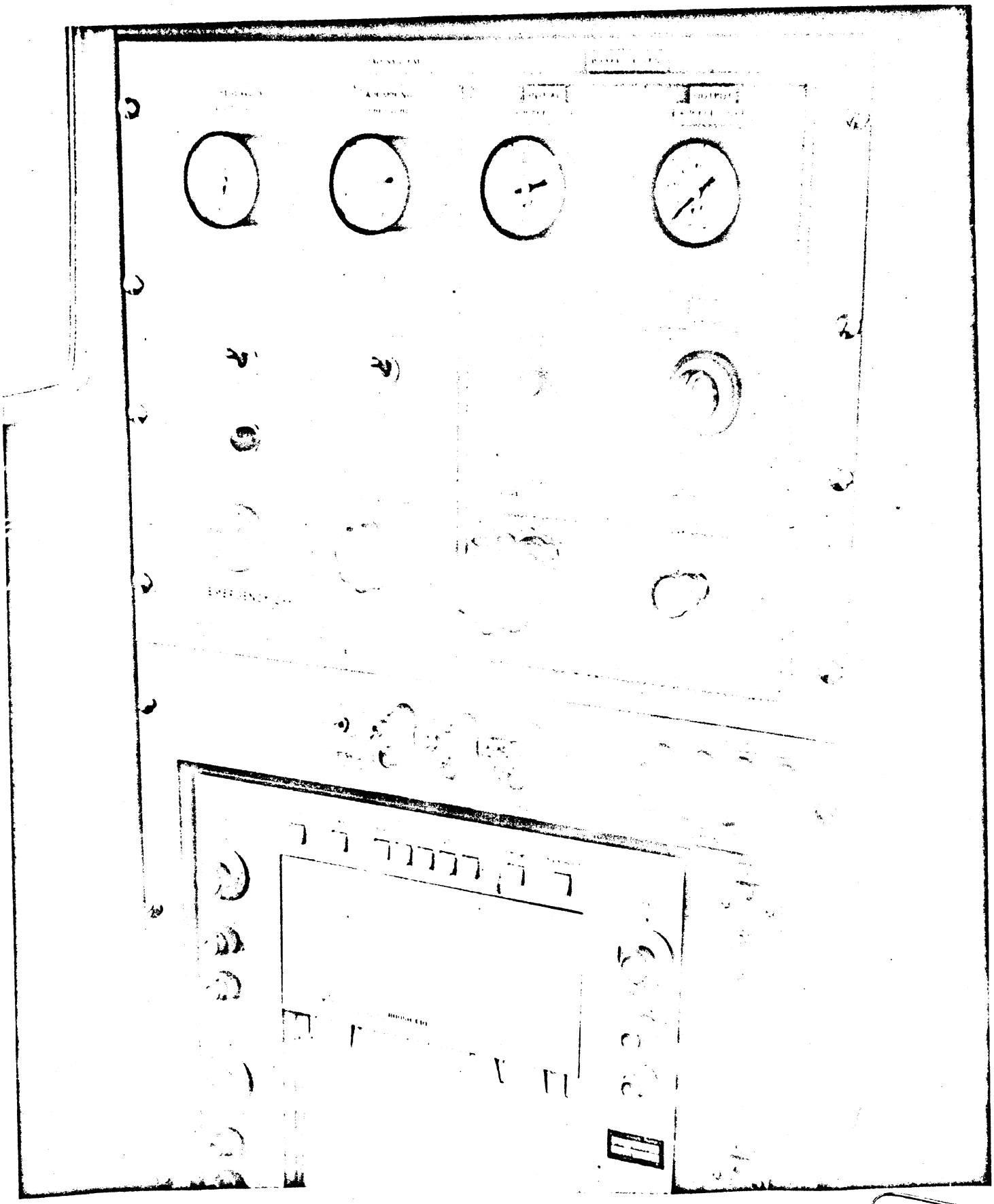

Figure 14. Instrumentation and control module of the Surface Friction Dynamometer.

The test wheel is braked by a single cylinder, floating caliper disc brake.

In order to elongate the spin-down transient of the test wheel for the purpose of recording peak traction performance, the rotational degree of freedom of the test wheel is hydraulically coupled to that of a chassis-mounted flywheel. The effective rotational moment of inertia of the test wheel system is thereby increased roughly tenfold, effecting a similar increase in the response time of this system, thereby facilitating improved accuracy in peak frictional performance measurement. An example of SFD-gathered data showing the sustained peak reading capability appears in Figure 15.

Instrumentation and control devices are located in the rear section of the cab. Continuous analog signals of F_x, F_z, F_x/F_z and vehicle velocity (V_5) are available for recording (any three concurrently) on a three-channel ink-pen recorder. Galvanometer read-out of test wheel brake temperature is also provided.

A detailed description of the design of this device is presented in Appendix B, together with operating procedures which are recommended for its use.

3.4 THE CONDUCT OF LIMIT BRAKING MEASUREMENTS ON A TEST VEHICLE

Since the measurement of limit braking performance involves a stopping distance characterization, this study clearly benefitted from the existence of established test methodologies. In the interests of achieving greater test objectivity, however, certain developments were pursued. They involved the achievement of an open-loop brake pedal application procedure, as well as an objective monitoring of the occurrence of wheel lockup. While the open-loop pedal application constitutes a conceptually significant

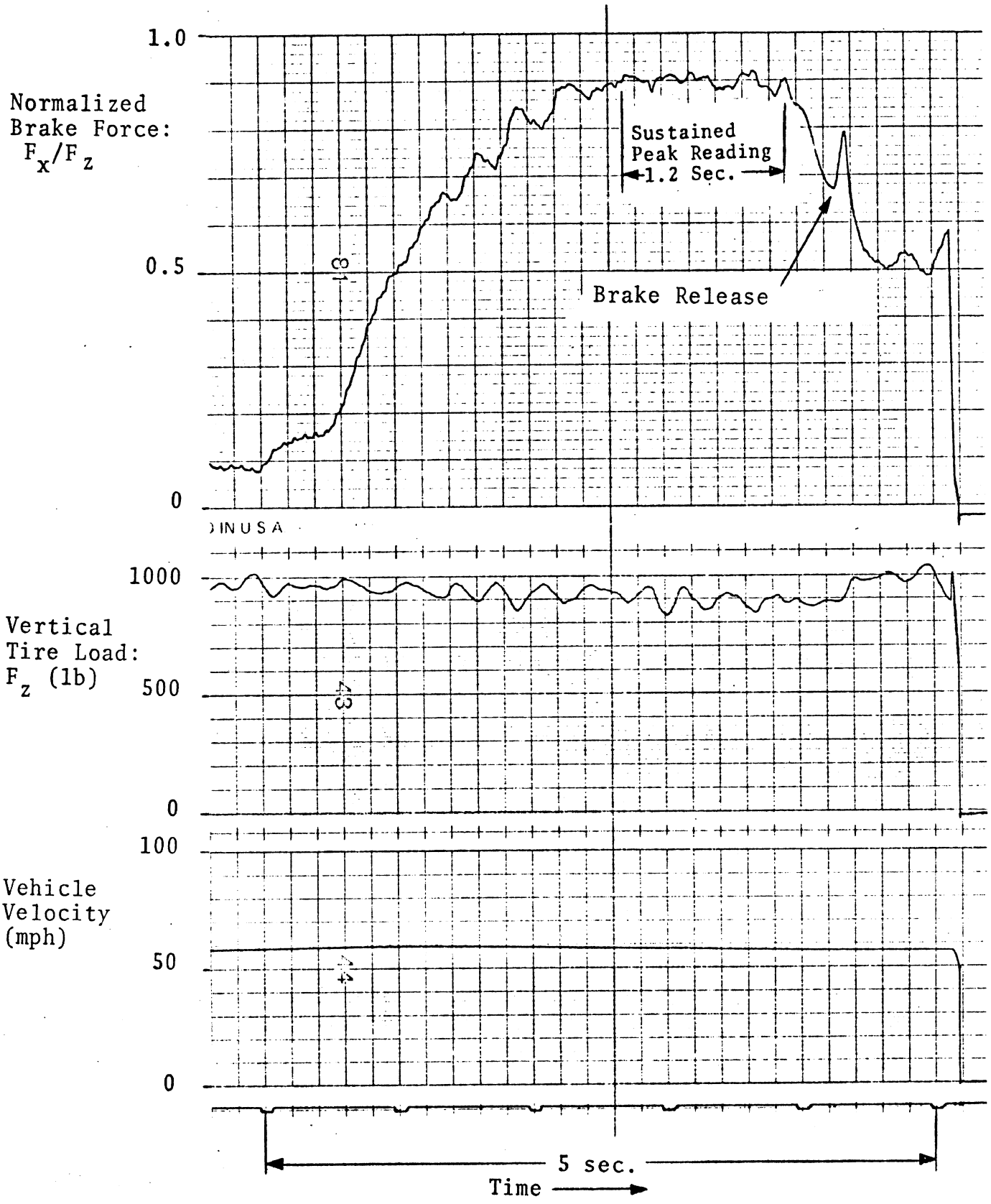

Figure 15. Surface Friction Dynamometer: Example data.

departure from current stopping distance measurement practice, per FMVSS 121 and 105-75, the wheel lockup monitor is merely a hardware development.

The development of a pedal-actuation device was undertaken to provide a constant force application of adjustable magnitude, similar in fidelity to the force feedback operation of a "brake machine" (such as is currently marketed, for example, under a General Motors patent). The lockup-monitor hardware was designed to provide an indication of wheel lockup to the driver of the test vehicle, eliminating the interpretive judgment of lockup occurrence by an observer stationed external to the vehicle.

3.4.1 PEDAL FORCE LIMITER. The conduct of open-loop limit braking tests has been accomplished using pedal-displacement and force-limiting devices as well as closed-loop force servos and brake-line-pressure limiting systems. While pedal force is the input variable whose control is desired (per arguments presented in Section 2.0), difficulty in achieving this control has fostered the pedal-displacement and line-pressure constraint methods. Control of pedal displacement has been found to be unacceptable in measuring the limit stopping performance of vehicles with hydraulic brake systems. The thermal expansion of brake drums in such systems causes a decreasing pedal force at constant displacement, thereby rendering a faulty analogue of the desired constant-force condition.

Line-pressure limiting schemes have been demonstrated as adequate for measuring the limit braking performance of vehicles with hydraulic brake systems. For certain hydraulic systems, however, proportioning is achieved through differential pressures at the master cylinder, such that line-pressure limiting becomes very difficult. Thus the general solution to the problem lies in the limiting of pedal force itself.

The pedal force limiting device developed in this study and demonstrated in full-scale tests is shown in Figures 16 and 17. Note that it is mounted on the brake pedal as a serial bellows-type actuator whose application force is reacted by a foot-constrained backstop. The bellows component provides a virtually frictionless mechanism for application of an adjustable level force. The bellows is inflated through the valving of a stored volume of pre-regulated air (see Figure 18). The equilibrium pressure provides a static pedal force which varies slightly during a stop as the pedal force/displacement relationship of the brake system changes.

The design of the limter device provided for emergency pedal release, merely by removal of foot pressure from the hinged "backstop" plate. Emergency application of greater pedal effort required manual disengagement of a locking tab at the base of the backstop, permitting a follow-through pedal motion.

3.4.2 PEDAL DISPLACEMENT LIMITER. As discussed in Section 2.0, brake pedal displacement is the input variable to be controlled in performing open-loop measurements of the braking performance of air-braked vehicles. Hardware for accomplishing constant pedal displacement is usually configured to limit the downward travel of the brake pedal. In use, the driver applies sufficient pedal force to contact the stop and maintain pedal displacement.

Due to the high gain of most air brake treadle valves, pedal stops must be very rigid to maintain an effectively constant pedal displacement against the variations in pedal force which the driver invariably applies during the stop. The flexibility of the floor structure in the vicinity of the brake pedal can, however, make this a difficult task.

Figure 16. Constant pedal force device.

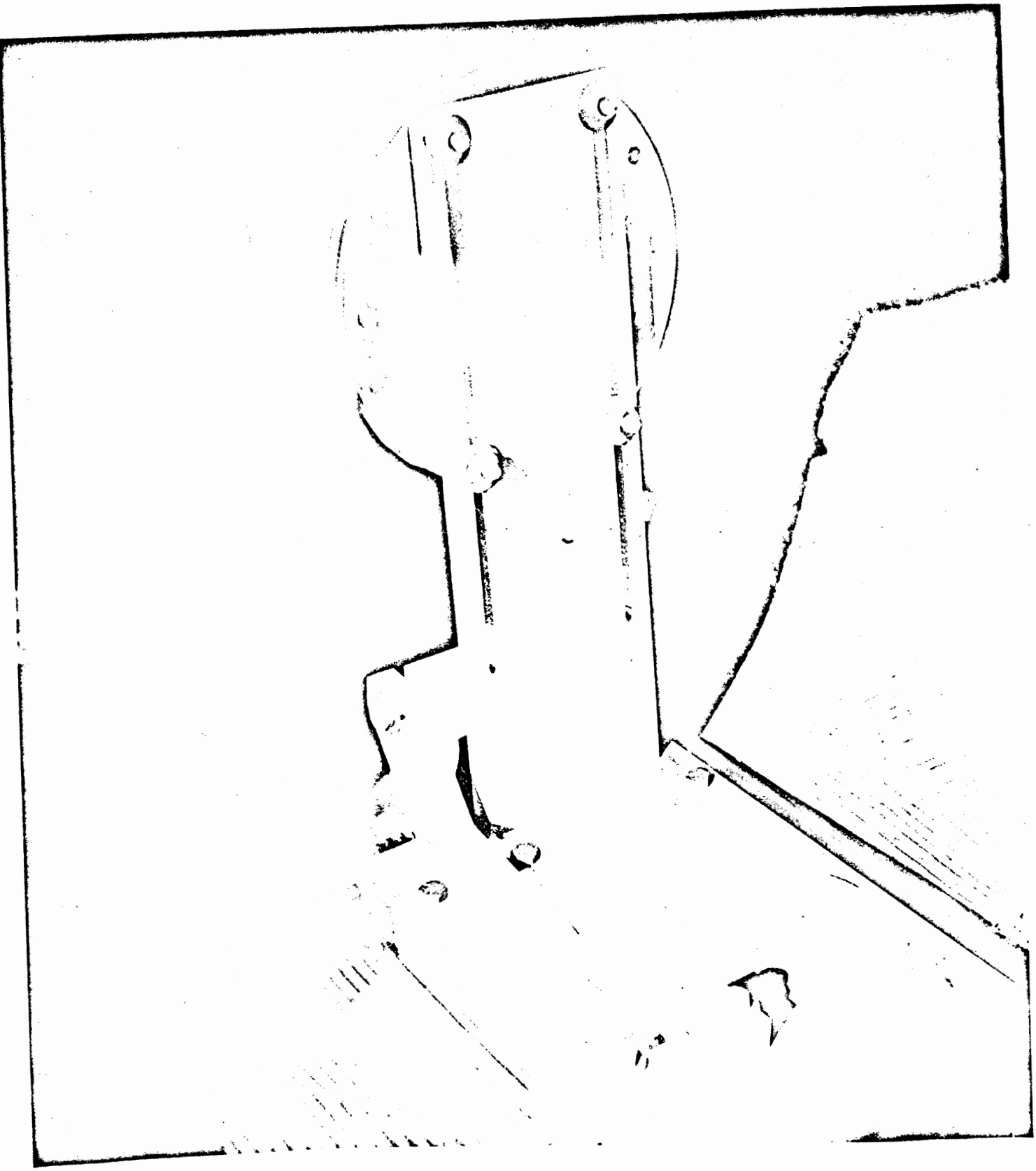

Figure 17. Constant pedal force device installed in vehicle.

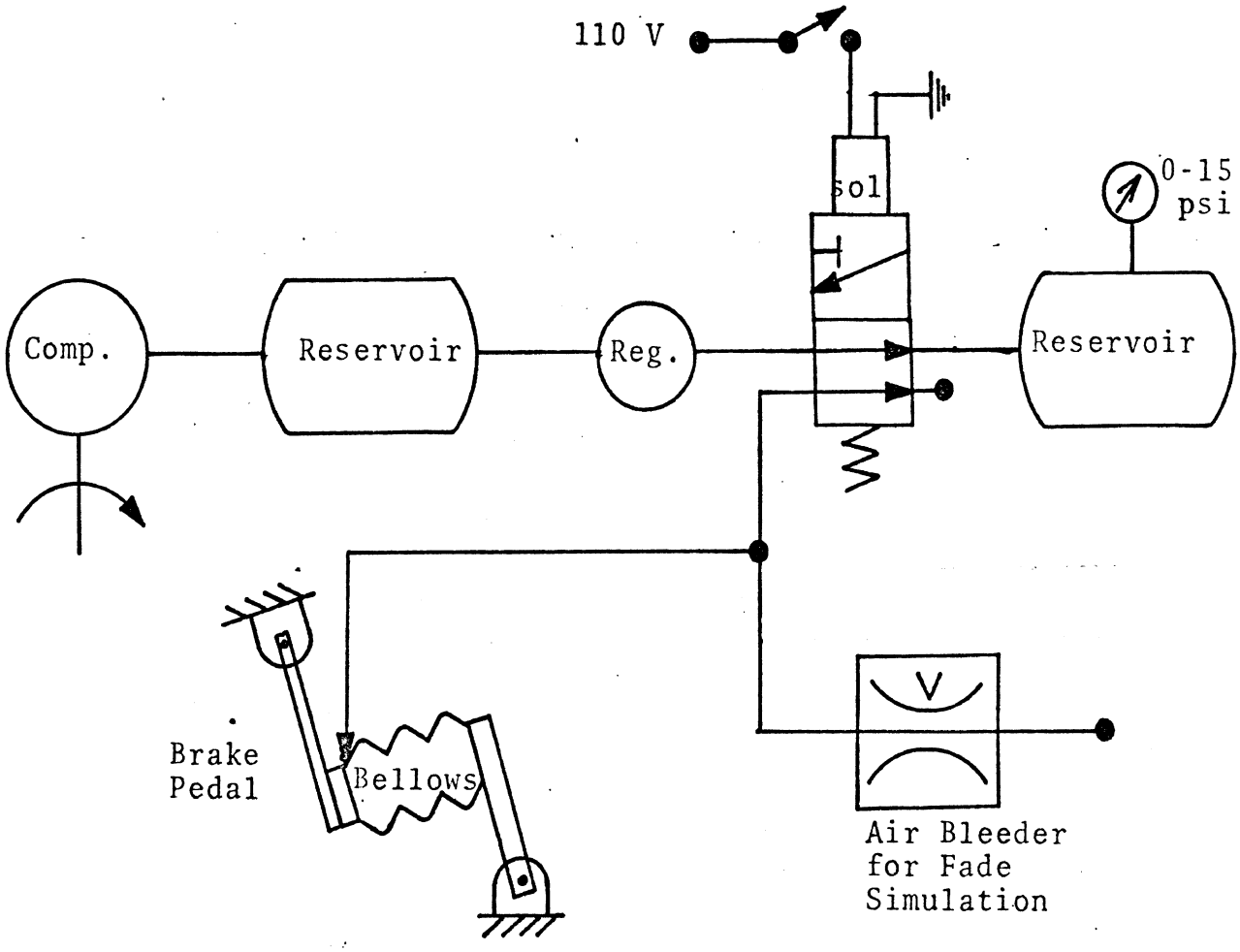

Figure 18. Schematic diagram: Constant pedal force device.

To circumvent this difficulty, the pedal stop pictured in Figure 19 was developed in this study. This device limits the upward travel of the brake pedal. Thus, at the onset of brake application the driver needs only to activate the brake pedal sufficiently for the catch-pin to latch in the restraining mechanism. Thereafter, no driver contact with the brake pedal is required. A catch-pin retractor mechanism is provided for emergency brake release or application. Activation of this mechanism by the driver retracts the catch-pin and allows for free use of the brake pedal.

Unfortunately, test drivers at the facility at which the demonstration test program was conducted were wary of this new device. Concern for the ability to quickly release the brake in difficult situations was so severe that the new device was judged unacceptable by the driver. Consequently, a more conventional design, preventing downward motion, was employed in testing. The anticipated flexibility problems were encountered. Thus an air pressure gauge showing treadle valve output pressure was displayed to the driver. Driver feedback, plus the pedal stop, was employed to maintain constant brake line pressure during a stop.

3.4.3 DEVELOPMENT OF A WHEEL LOCKUP MONITOR. Vehicle braking performance testing, as defined in FMVSS 105-75 and 121, and as required by the braking efficiency test method prescribed herein, demand the performance of stopping distance tests without the occurrence of wheel lock (or with only "momentary" wheel lock). However, the condition known as "wheel lock" has not, heretofore, been objectively defined in the applicable safety standards. Indeed, the occurrence of wheel lock is frequently determined by the subjective judgment of observers at the test site.

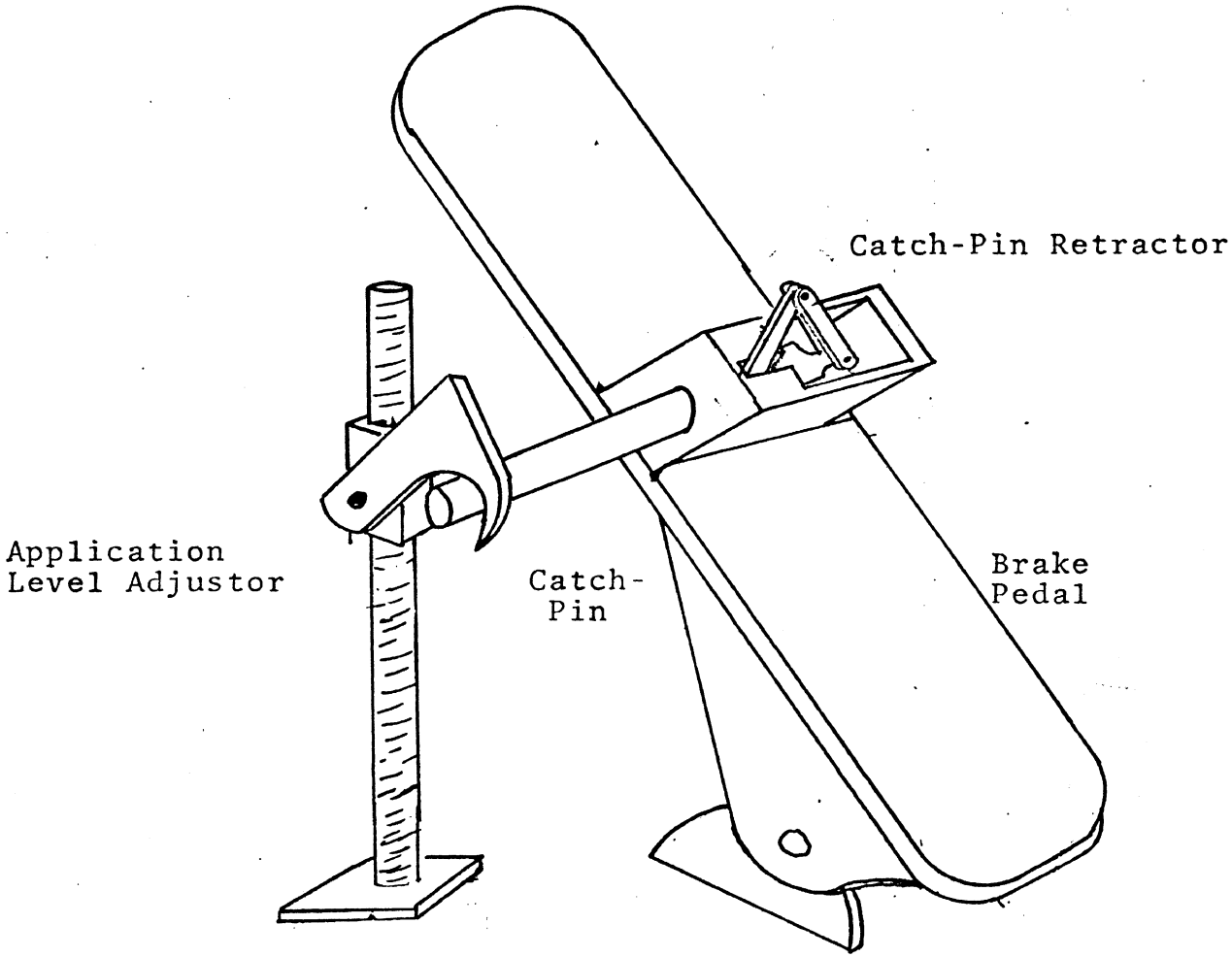

Figure 19. Pedal stop device.

In order to upgrade the objectivity of both the definition and determination of wheel lock, the development of an automatic wheel lock monitoring system was undertaken in this project.

Major considerations in the development of this system were:

(1) applicability to a broad range of vehicles

(2) ease of installation

(3) simplicity in operation and data presentation

(4) objectivity of wheel lock determination.

The resulting system is composed of three basic elements:

(1) wheel rotation transducer

(2) fifth wheel with digital tachometer

(3) electronic logic module.

The wheel rotation transducer is illustrated in Figure 20. It consists of a compression strut for attachment to the road wheel, and a pulse signal generator (Fig. 21) which mounts on the vehicle body. These two units are interconnected via a flexible drive cable which drives the pulse generator. The compression strut mounting unit is essentially a compression turnbuckle. Its length is adjustable such that it may be mounted on wheels ranging from the 13-inch diameter passenger car wheel to the 22 1/2-inch diameter truck wheel.

The output signals of as many as ten wheel rotation transducers are input to the electronic logic module shown in Figure 22. These signals, along with the digital output of a fifth wheel measuring vehicle velocity, are operated upon to determine the occurrence of wheel lock according to the following definition:

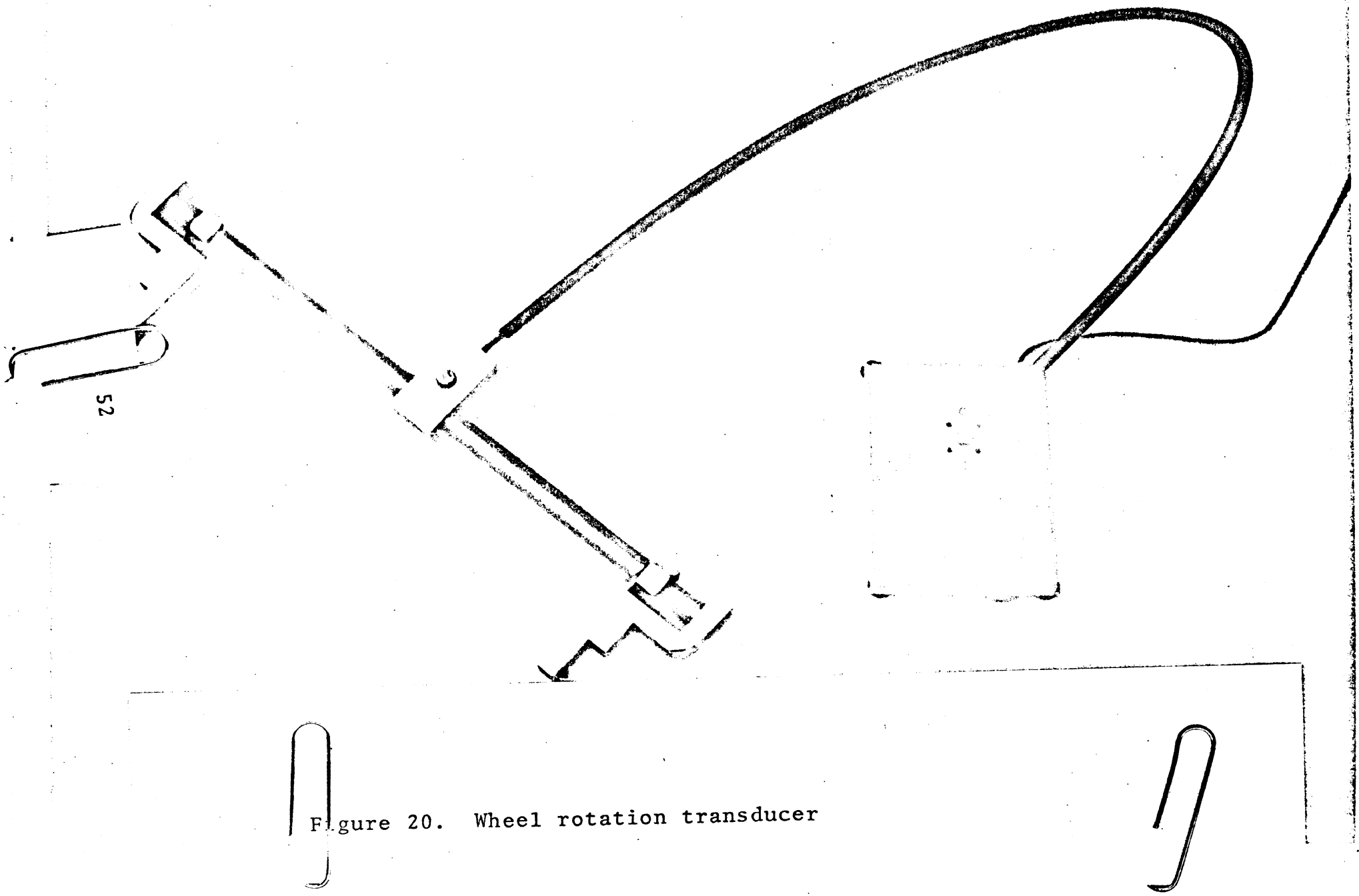

Figure 20. Wheel rotation transducer

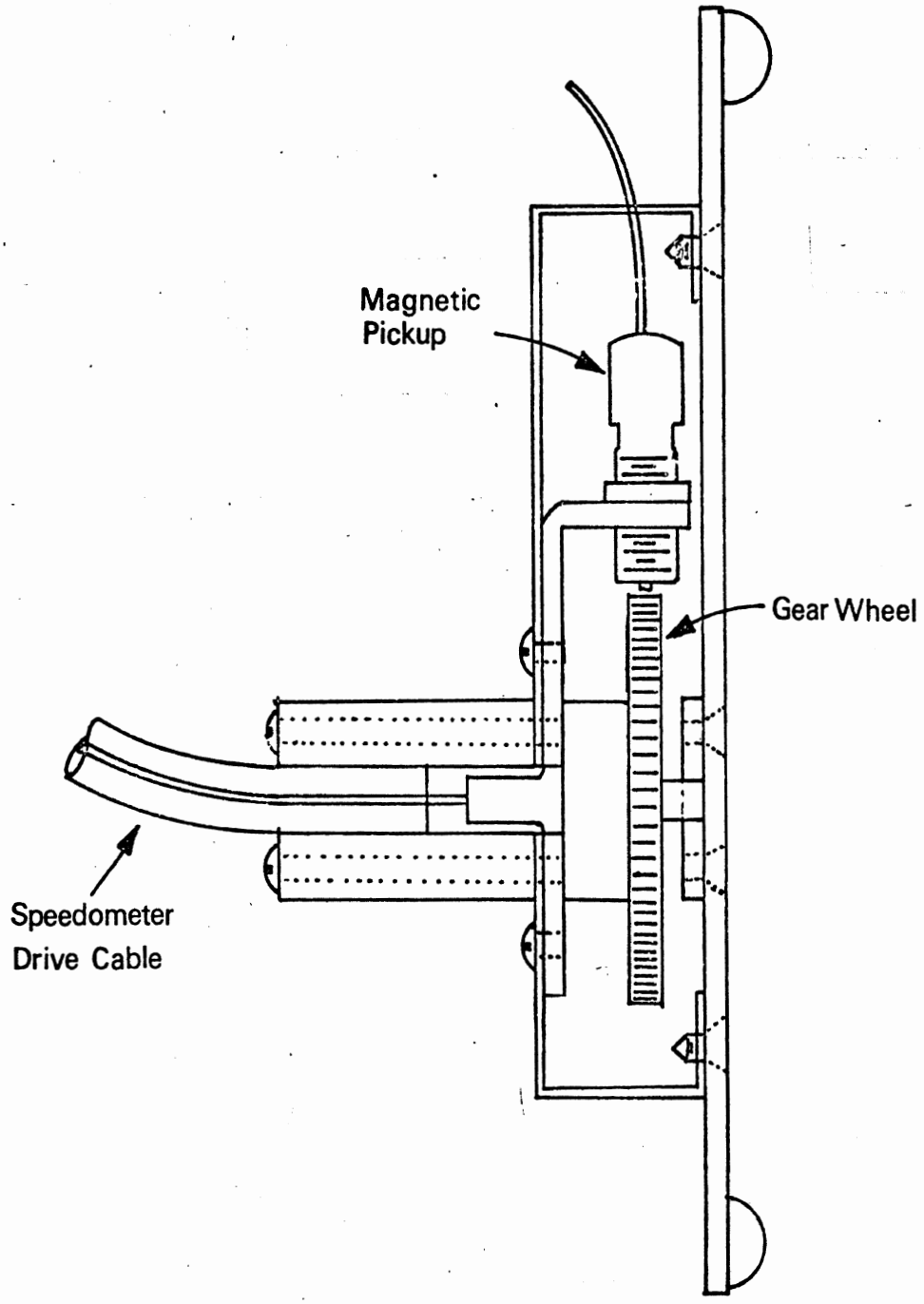

Figure 21. Wheel rotation transducer pulse generator.

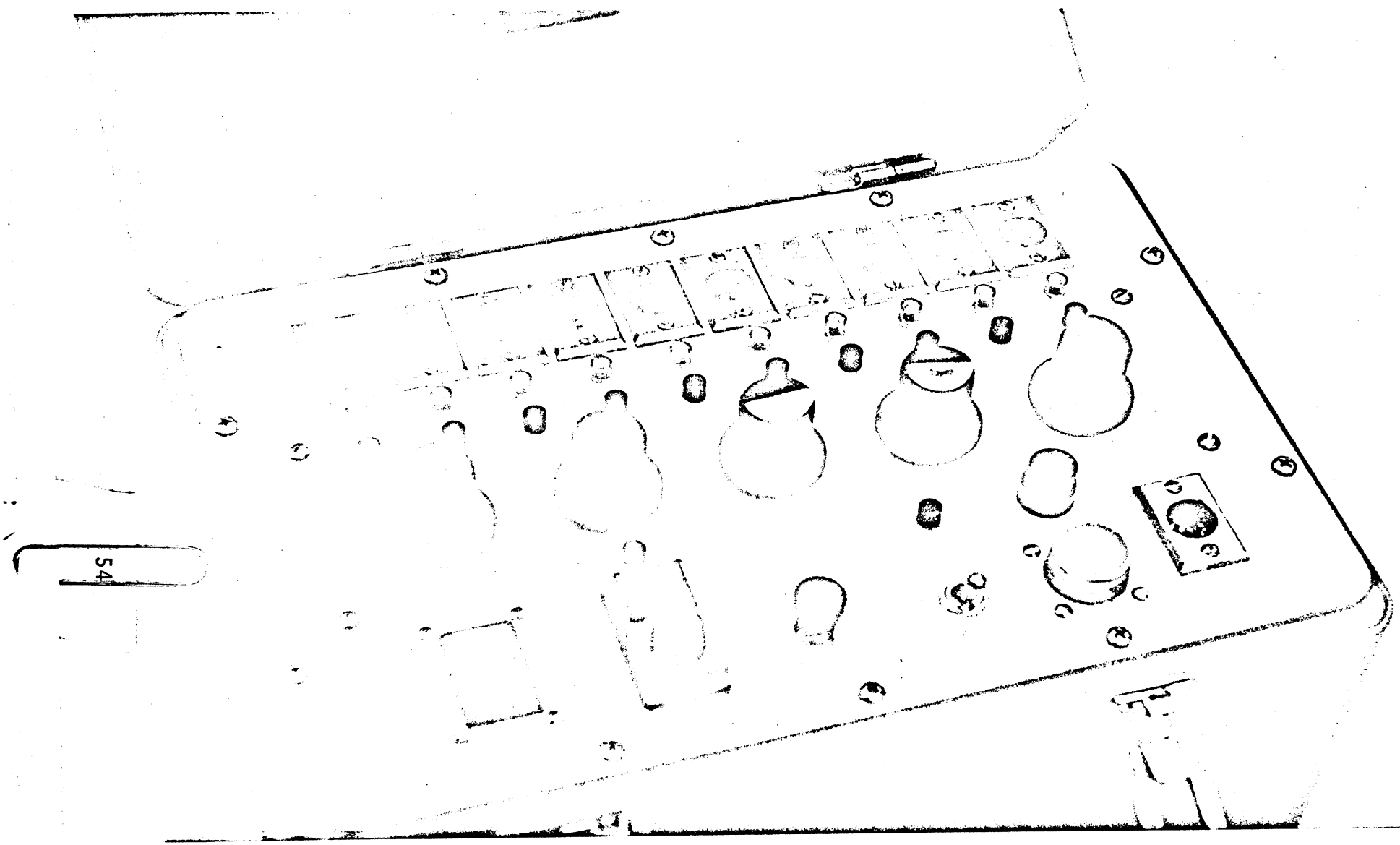

Figure 22. Wheel lock logic module.

Wheel lock has occurred if a wheel sustains a rotational velocity of less than ω for a time period of x while vehicle velocity (V_5) is greater than V.

A schematic diagram of the computing module logic scheme appears in Figure 23. The quantities ω, x, and V are programmable inputs to the computing module. The system output is displayed by way of signal lights which are located on the control panel of the logic module.

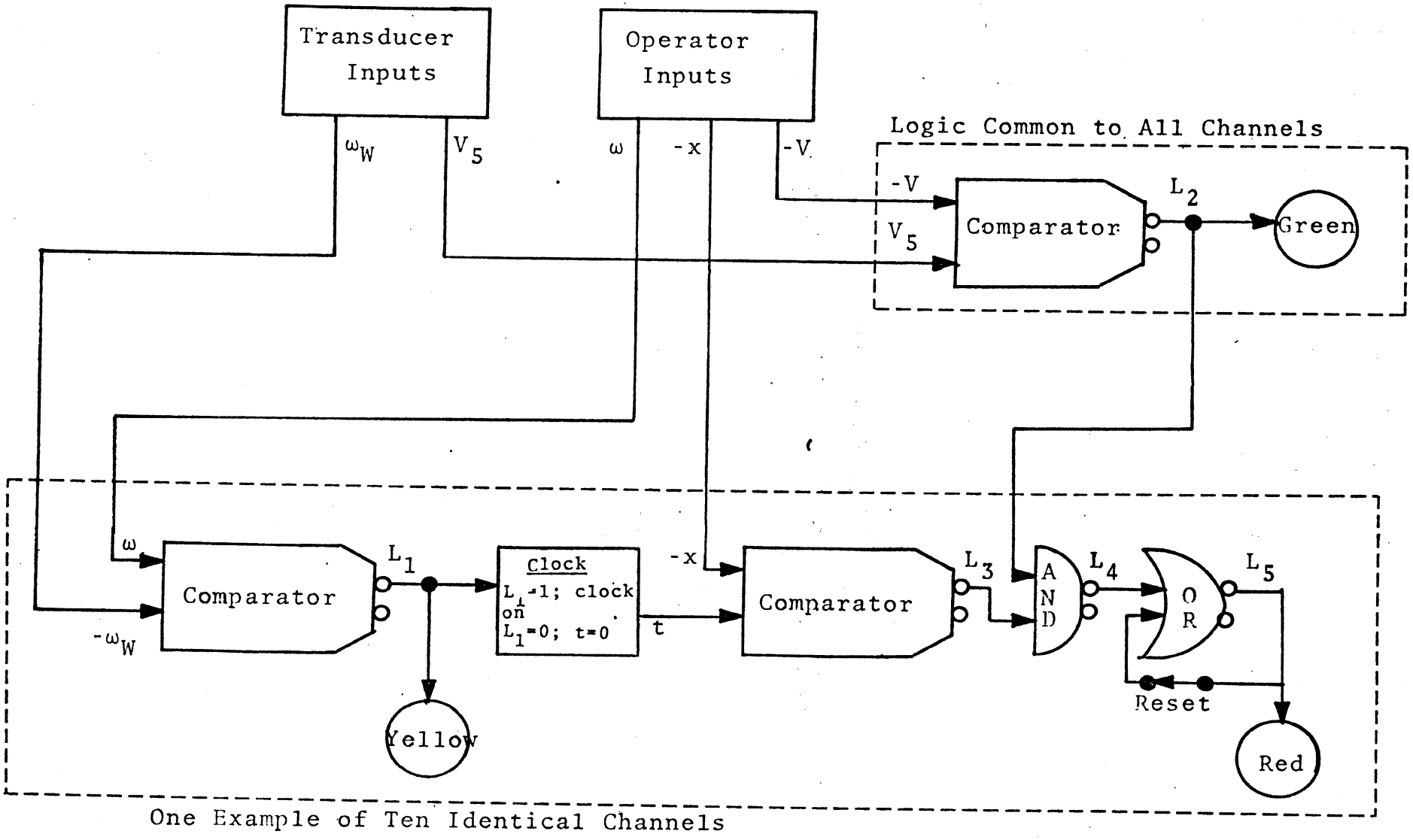

Figure 23. Schematic diagram: Wheel lock logic module.

4.0 CONDUCT AND RESULTS OF THE DEMONSTRATION TEST PROGRAM

This section is concerned with presenting the experimental findings produced by a program of demonstration tests which were conducted within this study. The objectives of the test program were twofold: (1) to evaluate the practicality of the brake efficiency test technique, as presented in the preceding sections, and (2) to evaluate the specific set of test-related hardware developed under this study. The section will present both the conduct and results of the test program through discussions of

1) the test vehicles
2) the test matrix
3) test procedure
4) test program results.

4.1 THE TEST VEHICLES

The vehicle stopping distance test portion of the braking efficiency test technique addresses two generic classes of vehicles, namely, vehicles with hydraulic brake systems and those with air brake systems. (The germane difference in these two systems is the mechanical nature of the brake control input device. Hydraulic systems use master cylinders which are essentially force input devices, while the treadle valve of air systems is essentially a displacement input device.) Consequently, two vehicles, one of each classification, were employed in the demonstration test program. These vehicles were:

(1) 1969 Chevrolet Townsman Station Wagon

(2) 1974 Diamond Reo COE 6x4.

4.1.1 THE HYDRAULIC BRAKE VEHICLE. The Chevrolet station wagon used in the demonstration test program was an HSRI-developed test vehicle known as the Variable Braking Vehicle (VBV). (For a description of the VBV, see Appendix E.) This

vehicle was seen as providing a major advantage to this study in that its programmable, servo-controlled braking system could be configured to provide an objectively definable set of brake system properties.

The use of the VBV essentially provided four "different" hydraulically-braked test vehicles for the study. By adjusting pedal force/line pressure gain for the rear axle brake system, three levels of brake proportioning were attained. The fourth condition of the vehicle involved alteration of the nominal fade characteristics of the vehicle. A peak reading circuit was employed to maintain constant rear brake line pressure, while accelerated front brake fade was simulated by slowly bleeding air from the brake pedal actuator, thus reducing brake pedal force (and front brake effectiveness) during the stop.

Prior to testing, the VBV brake system was overhauled, although the installation of new brake pads was not necessary. Consequently, no burnishing activity was undertaken.

Instrumentation items on this vehicle (exclusive of instrumentation resident on the VBV and not used for data gathering purposes) included:

1) Wheel rotation transducers on all wheels and associated logic circuitry (see Section 3.4.3).
2) Fifth wheel for sensing velocity and associated circuitry.
3) Thermocouples in one pad of all four brakes.
4) Pedal force transducer.

In addition to the above items, the pedal-force device described in Section 3.4.1 was installed in this vehicle.

The fifth wheel (and associated circuitry) was used to sense the initial test velocity and to measure stopping distance. The circuitry, which memorizes initial velocity

and initiates the distance measure, was activated by the same driver-operated switch which activated the pedal-force device.

A pedal-force transducer was used to examine the performance of the constant pedal-force device. However, this measurement is not necessary to the braking efficiency method. (A maximum pedal force boundary could be established by limiting the air pressure available to operate the device.)

4.1.2 THE AIR-BRAKE VEHICLE. The 1974 Diamond Reo tractor had a 142" wheelbase and was equipped with suspensions rated at 12,000 lb. (front) and 34,000 lb. (rear). Tests were conducted with the vehicle in the "bobtail" condition and "loaded" (equipped with flatbed body and iron weights bringing the vehicle to a load condition of 11,000 lb. front and 34,000 lb. rear).

Instrumentation employed on this vehicle included:

1) Wheel rotation transducers on each wheel and associated logic circuitry.
2) Fifth wheel and associated circuitry.
3) Thermocouples in one shoe of each brake.
4) Pressure gauge at the output of the treadle valve.

In addition to the above items, this vehicle was equipped with the conventional pedal-stop device discussed in Section 3.4.2.

As was the case with the passenger car, the fifth wheel and associated circuitry were used to determine both initial velocity and stopping distance. In the case of the air-braked vehicle, activation of the fifth-wheel circuitry was triggered via the brake light signal. The air-pressure gauge was intended

for evaluating the performance of the pedal-stop device and is not seen as essential to the brake efficiency test technique.

Since this vehicle was new (less than 100 miles on the odometer) prior to testing, little vehicle preparation, other than the installation of instrumentation, was required. A burnishing program, as per FMVSS 121, was conducted. The program was terminated at 350 snubs, at which time the brake effectiveness of the vehicle had stabilized.

4.2 THE TEST MATRIX

In order to demonstrate the viability of the braking efficiency test technique, the straight-line limit braking performance of both the hydraulic and air-braked test vehicles was measured on four surfaces and for a variety of vehicle conditions, as outlined in the following two sections.

A full matrix of tire tests was also conducted with the SFD on each of four test surfaces, providing data for the calculation of ideal stopping distance for each surface. Certain developmental problems associated with the SFD (see Section 4.4) made it impossible to conduct a full tire test matrix with each individual vehicle test condition as originally intended. However, periodic tests were conducted in accompaniment with each vehicle test to insure consistency of the surface condition.

In addition to straight-line braking efficiency measures, braking-in-a-turn efficiency measures were conducted on each of the test vehicles under a variety of conditions, as described in Section 4.2.3.

4.2.1 THE HYDRAULIC BRAKE VEHICLE. In addition to variations in brake proportioning and fade, as outlined in Section 4.1.1, the test matrix for the hydraulically-braked vehicle was compounded by using three different sets of tires and by testing on four surfaces. The entire test matrix for this vehicle is described in Table 4.1.

TABLE 4.1. THE HYDRAULIC BRAKE VEHICLE TEST MATRIX

Condition Number	Surface	Tire	Brake Proportioning	Differential Fade
1	D_1	T_A	P_A	F_A
2	D_1	T_A	P_B	F_A
3	D_1	T_A	P_C	F_A
4	D_1	T_A	P_A	F_B
5	D_2	T_A	P_A	F_A
6	D_1	T_B	P_A	F_A
7	D_1	T_B	P_C	F_A
8	D_1	T_C	P_A	F_A
9	D_1	T_C	P_C	F_A
10	W_1	T_A	P_A	F_A
11	W_2	T_A	P_A	F_A
12	W_2	T_A	P_B	F_A
13	W_2	T_A	P_C	F_A
14	W_2	T_B	P_A	F_A
15	W_2	T_C	P_A	F_A

DEFINITION OF MATRIX CONDITIONS

D_1	high friction dry asphalt surface
D_2	lower friction dry jennite surface
W_1	higher friction wet asphalt surface
W_2	low friction wet jennite surface
T_A	baseline tire selection - Goodyear Polyglas Custom Power Cushion L78-15
T_B	second tire selection - Uniroyal Tiger Paw Polyester L78-15
T_C	third tire selection - Uniroyal Fastrak L78-15
P_A	baseline proportioning setting, 56% front, 44% rear (design value for this vehicle)
P_B	second proportioning setting, 62% front, 38% rear
P_C	Third proportioning setting, 50% front, 50% rear
F_A	baseline differential fade condition
F_B	second differential fade condition (nominal 20% reduction in front brake effectiveness over the course of a stop)

The matrix shown in Table 4.1 provides tests of the baseline condition vehicle on four different surfaces (Tests #1, 5, 10, and 11). In addition, the vehicle was tested in seven different variations from the baseline condition on the higher friction dry surface (Tests #2, 3, 4, 6, 7, 8, and 9). On the lowest friction wet surface, four variations from the baseline condition were examined (Tests #12, 13, 14, and 15). One condition variation which was not examined on both the dry

and wet surface is the F_B differential fade selection. The wet surface F_B condition was omitted because the low velocity of that reduced friction test would not stimulate a significant degree of brake fade.

4.2.2 THE AIR-BRAKED VEHICLE. The air-braked heavy truck was subjected to the braking efficiency test matrix indicated in Table 4.2. (Surface designations refer to those given in Table 4.1.) As indicated in the table, the vehicle was tested for limit braking performance on four surfaces and in both the bobtail and loaded conditions.

TABLE 4.2 THE AIR BRAKE VEHICLE TEST MATRIX

Condition No.	Surface	Loading
1	D_1	Bobtail
2	D_2	Bobtail
3	W_1	Bobtail
4	W_2	Bobtail
5	D_1	Loaded
6	W_2	Loaded

4.2.3 BRAKING-IN-A-TURN TESTS. The limit braking-in-a-turn performance of both the hydraulic- and air-braked vehicles was measured. Since the braking-in-a-turn efficiency test is viewed primarily as a brake performance measure compounded by lateral load transfer deriving from the turning maneuvers, these tests were conducted at relatively low levels of lateral accelerations.

During a turn, the inside wheels are relatively lightly loaded and therefore provided relatively little tire side

force contributing to vehicle stability. Consequently, lock-up of inside wheels was allowed during braking-in-a-turn tests.

A measure of minimum no-outside-wheels-locked stopping distance was obtained for each of the test conditions described in Table 4.3. It had originally been planned that the initial velocity of the braking-in-a-turn tests would be equal to V_o as determined by the μ_{nom} of the test surface (the same as for straight-line braking efficiency testing) and that the turn radius would be established such that the passenger car would experience an initial lateral acceleration of .3 g and the truck, .2 g. That is

$$R = .0668 \frac{V_o^2}{a_y}$$

where R is the turn radius in feet, V_o is in mph and

$$a_y = \begin{cases} .3 \text{ for the passenger car} \\ .2 \text{ for the truck} \end{cases}$$

On the wet jennite surface, this scheme established a satisfactory turning radius of 200 ft. for the passenger car and 300 ft. for the truck. However, on the dry jennite, the scheme resulted in radii which were too large for the available facility.

Consequently, the tests conducted on the dry jennite employed the same radius turns as used on the wet jennite. The initial velocities were then chosen to produce nominal .3 g and .2 g turns for the passenger car and truck, respectively.

TABLE 4.3. BRAKING-IN-A-TURN TEST MATRIX

Surface	Vehicle	Vehicle Condition	Nominal Initial Velocity	Turn Radius	Nominal Initial Lateral Accel.
D_2	Station Wagon	Tire: T_A Proportioning: P_C Fade: F_A	30 mph	200 ft.	.3g
W_2	Station Wagon	Tire: T_A Proportioning: P_A Fade: F_A	30 mph	200 ft.	.3g
D_2	Truck	Bobtail	30 mph	300 ft.	.2g
W_2	Truck	Bobtail	25 mph	300 ft.	.14g

In the truck tests which were run at 0.2 g a_y on the wet jennite surface, it was found that vehicle directional control was lost at a level of braking substantially below that required to achieve lockup of outside wheels. Consequently, tests were conducted at the reduced level of V_o shown in Table 4.4, resulting in a .14 g initial lateral velocity.

4.3 TEST PROCEDURE

4.3.1 SURFACE FRICTION DYNAMOMETER TEST PROCEDURE. The operation of the Surface Friction Dynamometer involves the conduct of numerous checkout and calibration steps which are done prior to each day's data taking. These details are described in Appendix B. For the gathering of a specific set of data, however, a standard set of procedures was followed as outlined below.

The reference test tire was mounted on the Tire and Rim Association approved rim and statically balanced.

The inflation pressure of the test tire was maintained at a selected "warm" value of 27 psi throughout the entire test operation. This warm pressure was determined by first setting the inflation pressure at the Tire and Rim Association recommended 24 psi with the tire in its "cold" (ambient temperature) condition, and then running the tire for ten miles at a nominal 925 lb. loading. "Warm" pressure was maintained by the following procedure:

1) At the beginning of a tire test series, tire pressure was set at 24 psi "cold," and the tire was run ten miles at 925 lb. load to obtain a warm operating condition. Inflation pressure was then adjusted to 27 psi, if necessary.

2) For the first several tire tests, inflation pressure was checked and adjusted to 27 psi after each pass over the subject surface.

3) When it became apparent that (2) had established a stable condition, tire pressure was checked and adjusted if necessary on every third pass over the subject surface.

On the basis of the data presented in Figure 5, ASTM test tires were "preconditioned" prior to testing by conducting at least ten lockup cycles on a dry surface at a load of 925 lb. This preparation practice was conducted to stabilize the shear force behavior of the tire sample. Applying the scheme which was presented in Section 3.3.1, tire testing on each test surface was initiated with a series of μ_{nom} tests, followed by the conduct of 30 test runs covering the six-point load and velocity matrix.

When testing on wet surfaces, external watering via a tanker truck was used. Prior to testing, the surface was wetted several times to insure a stable water depth. Thereafter, the SFD would traverse the test surface to perform tire tests immediately after the water tanker had completed a wetting pass.

In all tire testing, an effort was made to perform tests only over the estimated length of test surface on which the vehicle under test would actually perform its stop. This procedure generally allowed one test per pass at velocity V_1, two at V_2, and three at V_3.

It had originally been planned to perform one complete tire test matrix on a surface for each day on which vehicle testing was performed on that surface. Developmental difficulties with the SFD precluded this mode of operation. (See Section 4.4.1.) Consequently, one complete matrix was

performed on each surface. Thereafter, a μ_{nom} check was performed concurrently with vehicle testing. In all cases, this check fell within a ± .04 range of μ_{nom}.

4.2.3 TEST PROCEDURE FOR THE HYDRAULICALLY-BRAKED VEHICLE. Limit stopping distance measures were made on each of the four test surfaces from the initial velocity, V_o, as determined by the μ_{nom} value for the surface.

Prior to testing, tires were inflated to the manufacturer's recommended pressure. Brake lining temperature was not permitted to be above 200°F at the initiation of each test run.

In conducting the test stop sequence, the vehicle was driven at an initial velocity slightly above V_o, at which time the driver released the accelerator and coasted down to V_o (with the automatic transmission remaining in "Drive"). On observing the fifth wheel speedometer, the driver activated the pedal force device as the vehicle passed through V_o.

By means of a sequential test procedure, the maximum pedal force for a no-wheel-lock-stop was determined. A minimum of five stops were then conducted at a value of pedal force which was just below the level required for wheel lock.

On dry surfaces, with the brake proportioning adjusted to the nominal or to the forward bias condition, wheel lock could sometimes not be attained due to the force limitation of the pedal force device. In such cases, five stops were conducted at the maximum pedal force.

4.3.3 THE AIR-BRAKED VEHICLE TEST PROCEDURE. The procedure for testing the air-braked truck was identical to that used for the passenger car with two exceptions.

Firstly, the manual transmission required that the clutch be depressed during braking, and secondly, the pedal displacement limiter was employed to obtain a constant air pressure braking level.

The same iterative procedure was employed for locating the brake input at which performance was measured. At least five repeats of the "limit proximity" stop were performed.

4.3.4 BRAKING-IN-A-TURN TEST PROCEDURE. A 12-foot wide lane at the proper radius, as called for in Table 4.4, was laid out on the test surface using traffic cones as lane markers. Braking-in-a-turn tests were then conducted with each of the test vehicles as described in the previous sections with the additional constraints that: (a) the entire stopping procedure be conducted within the prescribed lane without disturbing any of the traffic cones, and that (b) the outside wheel-lock criterion (see Section 4.2.3) be observed.

The same iterative procedure was employed for locating the limit performance braking input. A minimum of five repeats of the "limit proximity" stop were performed.

4.4 TEST PROGRAM RESULTS

4.4.1 TIRE TEST RESULTS. Early in the tire test activity a problem was encountered in the SFD force measurement system. Measurement errors were observed which indicated a sensitivity of the transduced forces, F_x and F_z, to the torque which is transmitted through the connection of the test wheel to the hydraulic motor (see Appendix B). The force measurement errors were on the order of 10 lbs., such that they became apparent only when measuring small forces such as derive on wet surfaces and/or at low values of vertical load.

To avoid the problem* in an expedient manner, the SFD was operated throughout the demonstration testing with the flywheel system disconnected.

The tire data obtained with the SFD on each of the four test surfaces appears in Figures 24 through 27. Each graph contains plots of the experimental data points gathered on a surface plus a plot of the tire descriptor equation which results when the data are fitted to equations of the form:

$$\mu_{PF} = A_F V^2 + B_F V + C_F$$

$$\mu_{PR} = A_R V^2 + B_R V + C_R$$

Table 4.4 presents values of μ_{nom} and V_o, together with the tire descriptor equations, and the ideal stopping distances (assuming an initial velocity of V_o) which derive from these tire data.

Upon examination of the dry surface data (Figures 24 and 25) it is apparent that the SFD provides peak longitudinal traction measurements with a rather high degree of repeatability. The wet surface measurements (Figures 26 and 27) show considerably more scatter than the dry surface data. This result is to be expected due to the difficulty of maintaining constant water depth, both spatially and temporally, and the sensitivity of traction performance to this parameter. The repeatability of the tire data is quantified in Table 4.5. The table presents the standard deviation of the tire traction measurements relative to the fitted second order curves for each set of data points, i.e., data at the same nominal values of load and velocity. The maximum standard deviation on peak longitudinal traction for data gathered on a dry surface was

*Efforts to deal with this developmental problem continue at the time of the writing of this report.

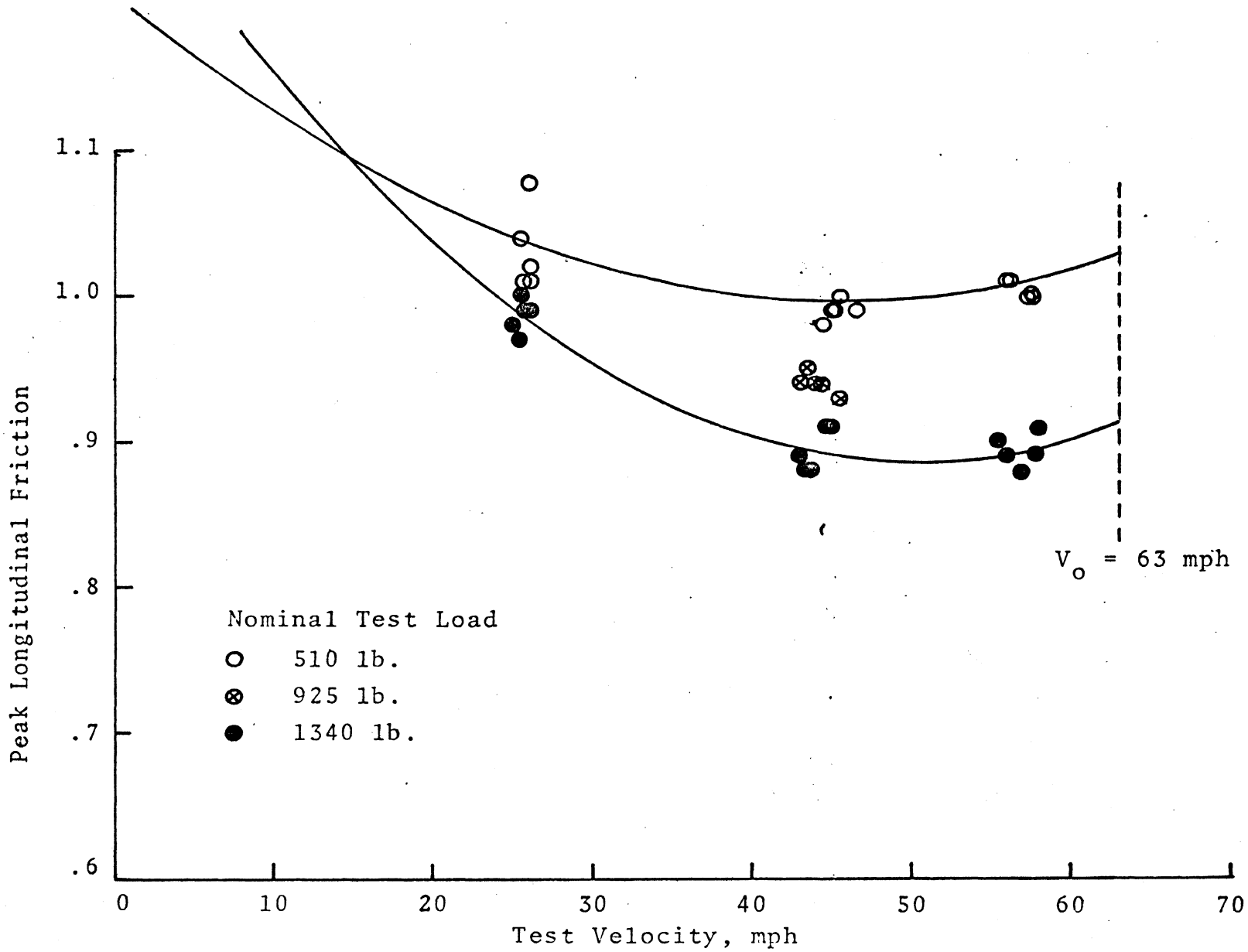

Figure 24. Reference tire data: Dry asphalt surface.

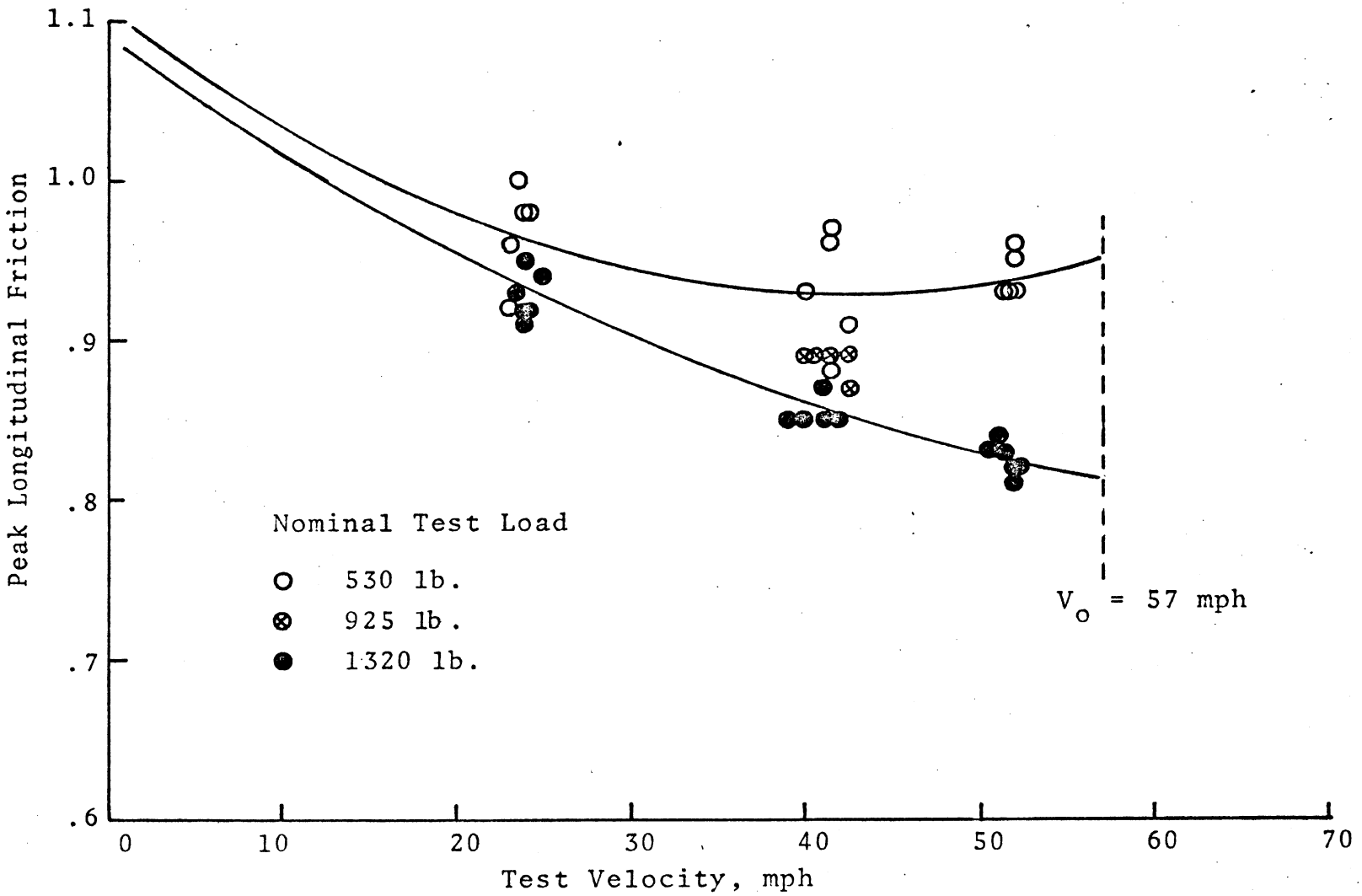

Figure 25. Reference tire data: Dry jennite surface.

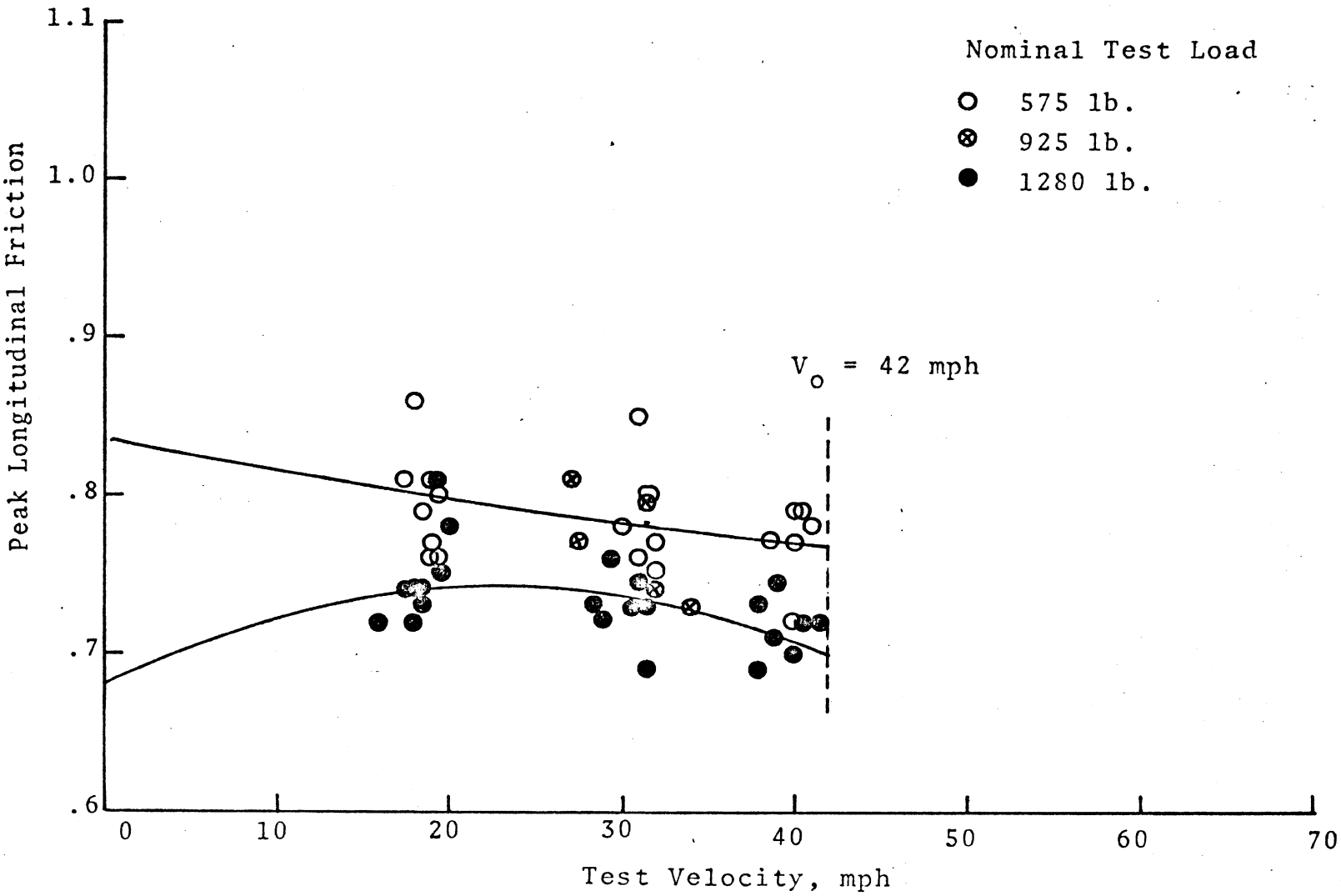

Figure 26. Reference tire data: Wet asphalt surface.

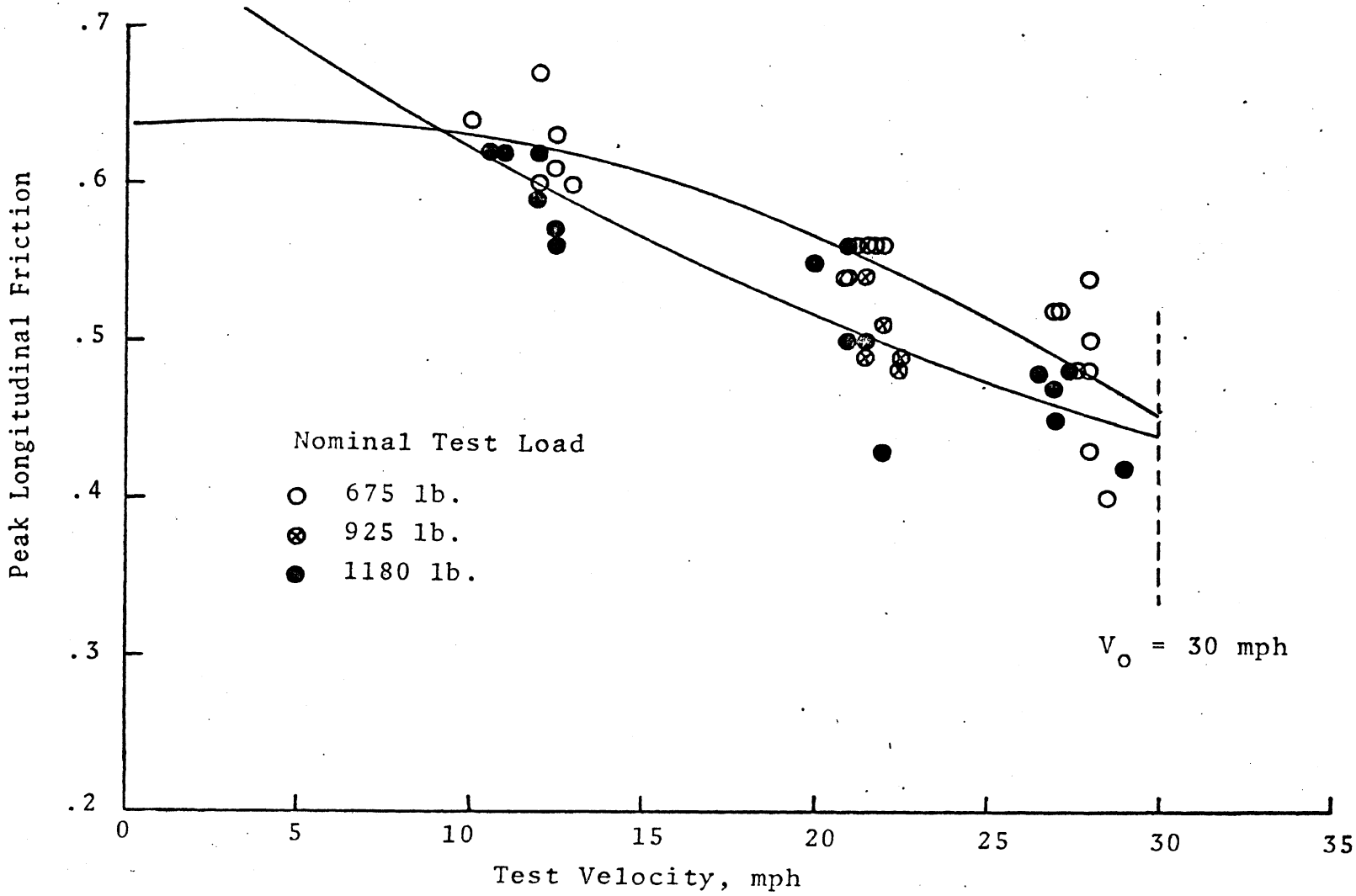

Figure 27. Reference tire data: Wet jennite surface.

TABLE 4.4

TEST SURFACE DESCRIPTIONS

Surface	μ_{nom}	Tire Equations	V_o	D_I
Dry Asphalt	.94	$\mu_{PF} = (.162 \times 10^{-3})V^2 - (.164 \times 10^{-1})V + 1.30$ $\mu_{PR} = (.103 \times 10^{-3})V^2 - (.940 \times 10^{-2})V + 1.21$	63.0 mph	139.2 ft.
Dry Jennite	.89	$\mu_{PF} = (.521 \times 10^{-4})V^2 - (.778 \times 10^{-2})V + 1.09$ $\mu_{PR} = (.996 \times 10^{-4})V^2 - (.848 \times 10^{-2})V + 1.11$	57.0 mph	121.5 ft.
Wet Asphalt	.77	$\mu_{PF} = -(.118 \times 10^{-3})V^2 + (.542 \times 10^{-2})V + .682$ $\mu_{PR} = (.146 \times 10^{-4})V^2 - (.230 \times 10^{-2})V + .837$	42.5 mph	80.9 ft.
Wet Jennite	.50	$\mu_{PF} = (.153 \times 10^{-3})V^2 - (.153 \times 10^{-1})V + .760$ $\mu_{PR} = -(.281 \times 10^{-3})V^2 + (.220 \times 10^{-2})V + .637$	30 mph	57.0 ft.

TABLE 4.5

TIRE DATA: STANDARD DEVIATION ON μ_p

Dry Asphalt

Velocity	Load 1340 lb.	510 lb.
57.5 mph	.005	.004
44.5 mph	.007	.004
25 mph	.005	.012

Dry Jennite

Velocity	Load 1320 lb.	530 lb.
52.0 mph	.004	.006
40.3 mph	.005	.015
23.3 mph	.006	.013

Wet Asphalt

Velocity	Load 1280 lb.	575 lb.
38.8 mph	.007	.010
30.0 mph	.006	.014
17.3 mph	.009	.009

Wet Jennite

Velocity	Load 1180 lb.	675 lb.
27.4 mph	.008	.014
21.2 mph	.016	.005
12.2 mph	.007	.010

.015 while the average was .007. For wet surface data, the maximum was .016 while the average was .010.

In order to examine the effect of these variabilities on the braking efficiency measure, ideal stopping distances for each surface were calculated using two alternate tire equations, representing plus and minus "one standard deviation" in the μ_p values which were shown in Figures 24 through 27. Each new tire equation was determined on the basis of three data points:

$$V_i \ , \ [\mu_p(V_i) + \sigma_i] \qquad i = 1,2,3$$

or

$$V_i \ , \ [\mu_p(V_i) - \sigma_i] \qquad i = 1,2,3$$

where

V_i ; i = 1,2,3 are the three tire test velocities

$\mu_p(V_i)$; i = 1,2,3 are the associated three μ_p values calculated from the original tire equation

σ_i ; i = 1,2,3 are the associated standard deviations as given in Table 4.5.

The "plus and minus σ" equations yielded results as shown in Table 4.6, with the maximum effect on ideal stopping distance seen as a change of 1.2 ft. (2.1%) on the wet jennite surface.

The tire data, particularly that of Figures 26 and 27, indicate a shortcoming in the three-velocity test matrix scheme. As can be seen in these figures, certain of the tire equations indicate a pronounced curvature which results in unrealistic intercept values. This, of course, is due to the absence of tire data in the low velocity region (below V_3), which permits somewhat excessive influence of the V^2 term in

TABLE 4.6

EFFECT OF TIRE DATA VARIANCE ON IDEAL STOPPING DISTANCE

Surface	Ideal Stopping Distances (ft.) Calculated From: Base Tire Equations	"$\mu_p+\sigma$" Equations	"$\mu_p-\sigma$" Equations
Dry Asphalt	139.1	138.4	140.0
Dry Jennite	121.5	120.4	122.1
Wet Asphalt	80.9	80.1	81.9
Wet Jennite	57.0	56.1	58.2

the curve fit equations. While this region has relatively little effect on stopping distance, it was concluded from these poorly fitted expressions that additional tire data should be taken in the vicinity of .2 V_o*.

Finally, the tire test data of Figures 24 through 27 indicate the importance of both tire load and velocity in the characterization of the traction potential of the reference tire. In particular, the dry surface data of Figures 24 and 25 indicate that the sensitivity of peak traction to tire load level at high velocities is as large, if not larger, than the sensitivity to velocity at a constant load. Further, the data indicate that sensitivities of tire traction to either load or velocity can be on the order of 10% over the full range of conditions imposed by the reference vehicle.

*Appendix D includes a description of the resulting altered tire test matrix.

4.4.2 VEHICLE TEST PROGRAM RESULTS: HYDRAULICALLY-BRAKED VEHICLE. The results of the braking efficiency tests conducted on the hydraulically-braked vehicle appear in Table 4.7. Data are presented for all fifteen test conditions which were described in Table 4.1. For each condition, the average values of initial velocity, stopping distance, and the resulting braking efficiency measures are presented. In addition, the maximum and minimum values, and the maximum variations (maximum minus minimum) for each of these variables are given as an indicator of the repeatability of the vehicle testing method. Of most significance is the maximum variation of the braking efficiency numeric. On dry surfaces, the average of this figure is 4.7%, and on wet surfaces, 5.6%.

It should be noted that, in relative terms, the variation in stopping distance is somewhat larger than the variation in the efficiency numeric. In calculating efficiency, the measured stopping distance of a single run is normalized using the ideal stopping distance of that same run. Since the ideal stopping distance is calculated using the measured initial velocity of the run, the method removes the effects of variation in initial velocity from the resulting efficiency numeric.

The variation of the efficiency numeric, then, results from the inherent variability of the braking process, plus variations in the input pedal force, run to run. Testing experience indicated that the pedal force device used in this program was generally repeatable to within the nearest pound, run to run.

4.4.3 VEHICLE TEST PROGRAM RESULTS: AIR-BRAKED VEHICLE. The results of the braking efficiency tests conducted on the air-braked vehicle are given in Table 4.8. The table contains the average, the maximum and minimum, and the maximum variation of initial velocity, stopping distance and braking efficiency for tests conducted at each of the six test conditions (as were defined in Table 4.2).

TABLE 4.7

HYDRAULIC BRAKE VEHICLE TEST RESULTS

Condition Number	Initial Velocity (mph)				Stopping Distance (ft)				Braking Efficiency (%)				Impending Wheel Lock	
	Avg.	Max.	Min.	Maximum Variation	Avg.	Max.	Min.	Maximum Variation	Avg.	Max.	Min.	Maximum Variation	Front	Rear
1	63.4	63.8	62.8	1.0	187.2	195.0	181.7	13.3	75.2	77.3	72.8	4.5	X	
2	63.4	63.9	62.7	1.2	219.3	223.8	212.3	11.5	64.2	64.9	63.4	1.5	*	
3	63.4	64.3	63.0	1.3	204.1	211.4	191.1	20.3	69.1	72.8	66.7	6.1		X
4	63.5	63.7	63.1	0.6	217.1	226.9	213.1	12.8	65.1	66.2	62.3	3.9	*	
5	56.9	58.0	56.5	1.5	188.6	195.2	186.	9.2	64.2	67.8	61.1	6.7	X	
6	63.1	64.1	62.2	1.9	223.0	234.0	215.5	18.5	62.6	64.3	61.6	2.7	*	
7	63.1	63.5	62.9	0.6	203.8	211.0	200.0	11.0	68.6	70.3	66.2	4.1		X
8	63.2	63.7	62.5	1.2	214.9	230.6	205.0	25.6	65.2	68.8	60.5	8.3	X	
9	62.6	62.9	62.1	0.8	202.6	212.9	194.6	18.3	67.9	69.5	65.2	4.3		X
10	48.4	48.8	47.7	1.1**	153.9	161.5	150.6	10.9	68.9	71.7	64.3	7.4	X	
11	31.2	31.5	30.9	0.6	87.4	92.5	81.6	10.9	72.0	75.0	68.9	6.1	X	
12	31.1	31.3	30.9	0.4	89.2	93.5	86.6	6.9	70.0	72.4	65.5	6.9	X	
13	31.1	31.2	31.0	0.2	73.1	75.6	69.9	5.7	85.4	88.3	83.9	5.4		X
14	31.8	32.0	31.5	0.5	86.7	91.3	84.0	7.3	75.7	78.1	73.0	5.1	X	
15	29.6	30.2	29.3	0.9	76.4	78.6	74.6	4.0	72.4	73.7	71.4	2.3	X	

*Stopping distance tests conducted at maximum pedal force. No "wheel-lock stops" attained.

**V_o of 48 rather than 42.3 mph mistakenly employed.

TABLE 4.8

AIR BRAKE VEHICLE TEST RESULTS

Condition Number	Initial Velocity (mph)				Stopping Distance (ft)				Braking Efficiency (%)				Impending Wheel Lock		
	Avg.	Max.	Min.	Maximum Variation	Avg.	Max.	Min.	Maximum Variation	Avg.	Max.	Min.	Maximum Variation	Front	Middle	Rear
1	62.6	63.7	61.4	2.3	483.5	520.5	456.8	63.7	28.4	30.0	26.3	3.7		X	X
2	57.3	57.9	56.4	1.5	450.1	483.3	438.0	45.3	27.3	28.5	25.3	3.2		X	X
3	40.2	40.7	40.0	0.7*	271.1	285.3	256.6	28.7	26.6	27.8	25.3	2.5		X	
4	30.0	30.8	29.5	1.3	318.8	353.0	296.2	56.8	17.9	18.5	17.2	1.3			X
5	62.4	62.7	61.7	1.0	365.8	374.4	361.7	12.7	37.3	38.1	36.7	1.4		X	
6	29.7	30.0	29.5	0.5	183.3	193.0	173.0	20.0	30.5	32.5	29.5	3.0			X

*V_o value of 40 rather than 42.5 mph mistakenly employed.

Although the average value of maximum variation in braking efficiency is seen to be lower for the air-braked vehicle than for the hydraulically-braked vehicle, the normalized level of this measure is somewhat greater for the air-braked vehicle. That is, the average normalized braking efficiency variation (ANV), as calculated by Equation (4.1), is 7.2% for the passenger car, but is 9.2% for the truck.

$$ANV = \frac{\sum_{\text{Test Conditions}} \left[\frac{\text{Maximum efficiency variation}}{\text{Avg. braking efficiency}} \right]}{\text{No. of Test Conditions}} \times 100 \qquad (4.1)$$

This high variability in the truck test results is likely the result of a somewhat less satisfactory brake application technique. As discussed in Section 3.4.2, the sensitivity of treadle valve application repeatability to the rigidity of the pedal stop device was recognized. A pedal stop device which circumvented this problem by not requiring continuous driver foot pressure throughout the stop was developed during this study, but was not employed by test driver personnel because of their concern over its non-traditional character.

Variability in stopping distance tests was therefore compounded by the driver variations in actuating a conventional pedal stop. Testing experience indicated that line pressure repeatability from run to run was approximately 10% of the nominal value (as reflected by the ANV of the truck test data).

4.4.4 VEHICLE TEST PROGRAM RESULTS: BRAKING-IN-A-TURN TESTS. The results of the braking-in-a-turn efficiency tests conducted on both test vehicles appears in Table 4.9.

TABLE 4.9

Vehicle	Vehicle Condition*	Test Surface	Initial Velocity (mph) Avg.	Max.	Min.	Max Variation	Stopping Distance (ft) Avg.	Max.	Min.	Max. Variation	Braking Efficiency (%) Avg.	Max.	Min.	Max. Variation	Impending Wheel Lock Outside Front	Middle	Rear
Hydraulic Brake	T_A, P_C, F_A	Dry Jennite	30.5	31.4	29.5	1.9	52.7	55.6	48.8	6.8	61.5	62.8	60.0	2.8			X
Hydraulic Brake	T_A, P_A, F_A	Wet Jennite	29.9	30.5	29.2	1.3	73.2	77.9	68.6	9.3	77.7	79.3	76.2	3.1	X		
Air Brake	Bobtail	Dry Jennite	30.0	30.3	29.9	0.4	112.5	118.3	107.2	11.1	22.9	29.0	27.0	2.0		X	X
Air Brake	Bobtail	Wet Jennite	24.9	25.8	24.5	1.3	194.6	209.8	187.8	22.0	19.1	19.4	18.9	0.5			X

*See page 62 for symbol definitions.

For each test vehicle on each surface, the braking-in-a-turn efficiencies measured are quite comparable with the straight-line braking efficiencies presented earlier. Although the lateral load transfer resulting from the turning maneuver would tend to decrease efficiency, the use of the outside-wheel-lock limit criterion apparently negates this tendency.

5.0 APPLICATION OF THE BRAKING EFFICIENCY TEST TECHNIQUE TO RULEMAKING

The concept developed in this study is founded upon the argument that the only generally applicable braking performance requirement which the highway traffic system imposes upon its constituent vehicles concerns their relative stopping capability, one to another; the traffic stream imposes no specific absolute braking level requirement (although in individual traffic conflicts, more braking capability is better than less). In implementation of a concept deriving from this argument, a measure of relative capability has been defined by which a vehicle's performance on any surface can be meaningfully characterized. It is in regard to this "universality" quality that the authors feel the braking efficiency measure to be most worthy of consideration for rulemaking. In contrast to various fragmented approaches toward braking performance specification, the braking efficiency method permits a homogeneous treatment of pavement friction level. Accordingly, the method accounts for all possible test surfaces uniformly—suggesting that the relative performances of vehicles in traffic is just as pertinent to safety on one pavement as it is on any other.

The homogeneity quality of the method would, of course, be foiled if one were to divide the friction range into discrete, non-adjacent segments, for purposes of limiting the test regimes within which a standard might apply. Such a sectionalizing approach has a tendency, in currently defined braking standards, to focus the compliance assessment efforts of the manufacturing community on the measurement of vehicle performance precisely at the conditions of the defined boundaries. Currently, the two boundaries defined in FMVSS 121, at skid numbers of 30 and 75, do serve to identify high (above SN = 75) and low (below SN = 30) friction ranges, but there arises a natural concern on the part of vehicle manufacturers for assurance of

compliance on surfaces exhibiting skid numbers very near those values. A major reason for this concern derives from the inability to normalize data taken on "non-boundary condition" surfaces. The net effect, however, is to foster an evolutionary design process which concentrates upon the performance obtained under narrow and specialized conditions.

In considering the applicability of the braking efficiency method to a performance standard, we advocate an undivided treatment of the pavement friction range. We do recognize, however, that some bounds must be placed upon this range such that lowest and highest friction level requirements can be defined. Unfortunately, even the definition of upper and lower friction limits will necessarily impose the discussed burden of compliance at the friction boundaries, but this situation is simply unavoidable.

It would appear that a reasonable value for the upper limit of the friction range, defined in terms of the μ_{nom} characterization, could be determined on the basis of a highway pavement survey. In such an approach, an SFD-type machine would be employed to gather μ_{nom} data on a representative sample of the nation's highway pavements (dry). The resulting measurements would be used as the basis for specifying a reasonable upper boundary for μ_{nom}.

The definition of a lower friction limit, as is presumably achievable in the highway traffic environment, seems to demand that a pragmatic stance be taken in recogniition of the absence of a pertinent test technology for ice- or snow-contaminated surfaces. Thus we would not advocate a survey of the nation's wintertime friction conditions, since it is clear that such a survey would identify μ_{nom} values which are well below those levels which could be specified for compliance testing. Accordingly, the lower μ_{nom} boundary for a rule might be based upon measurements taken on wet, coated pavements such as are commonly used in vehicle test practice.

Regardless of the location on the μ_{nom} scale of the upper and lower boundary conditions, performance would be defineable for any surface whose μ_{nom} is within the described range. Thus one could evaluate performance on whatever surface pavement as might be available—although some attention should be given to surface profile irregularity. Clearly, the number of tests required to assure compliance over the entire friction range would be in direct relation to the vehicle development engineer's ability to analytically interpolate performance between measurements. Spot checking of a vehicle's braking efficiency at only two or three μ_{nom} levels, for example, will be adequate only if there exists a performance-predictive model which permits valid generalization over all values of μ_{nom}.

With regard to the setting of specifications of braking efficiency performance levels, certain considerations should be addressed.

Firstly, the ideal stopping distance computation has, by design, excluded a number of influences which, in an actual vehicle, tend to degrade minimum stopping distance capability. These influences, discussed in Section 3.2, included such items as brake system lag and the inability of mechanical friction brake systems to continuously sustain peak tire shear force utilization. Thus the vehicle population will, in general, exhibit limit stopping distances which exceed the ideal as was shown in the demonstration testing. (The only conceivable exception to this might be the case of a vehicle with very high traction tires, which vehicle could effectively utilize the high peak shear forces available to accrue a shorter than "ideal" stopping distance.) Aside from this remote conceptual possibility, the performance capability of vehicles will be sufficiently low that any reasonable specification of braking efficiency will involve efficiency values well below 100%.

Since the efficiency measure is based upon a representative passenger vehicle reference, a quantitative guide to scaling braking efficiency specifications can easily be established by

measuring the braking efficiencies of a representative sample of passenger cars on a selection of surface conditions. Such data would not only evaluate the nominal percentage efficiencies of modern passenger cars, but also indicate the extent to which the efficiency level of such vehicles varies over the surface friction range. Using these data as a practical reference, one could then evaluate the braking efficiency performances of other vehicle classes and determine "allowances" as guided by whatever cost/benefit considerations as are essential to the rulemaking process.

In determining the contour of the required efficiency level as a function of μ_{nom}, a continuous form, as shown in Figure 28, would appear to be highly desirable. Discontinuities in requirement specification across the friction range would offer the manufacturer little or no relief from the more severe of the specified levels. As shown in Figure 29, a discontinuity in $E_{required}$ at $\mu_{nom} = \mu_1$ will not provide relief to the vehicle development challenge in the regime of μ_{nom} just below μ_1. This is the case because of the fact that the mechanics of tire and brake systems offer no discontinuous characteristics which could be fitted to such a specification.

Given that discontinuities would be avoided, then, the actual contour of the efficiency requirement must derive from the judgment of cost/benefit factors. Clearly, one would be led to considering a non-constant efficiency requirement only through the observation that a constant level specification imposes a large gradient in "cost" over the friction range ("cost" here refers to the economic implications of requiring a vehicle performance level which exceeds currently achieved performance levels). If a steep cost gradient is not perceived, then clearly a fixed level braking efficiency requirement is the answer.

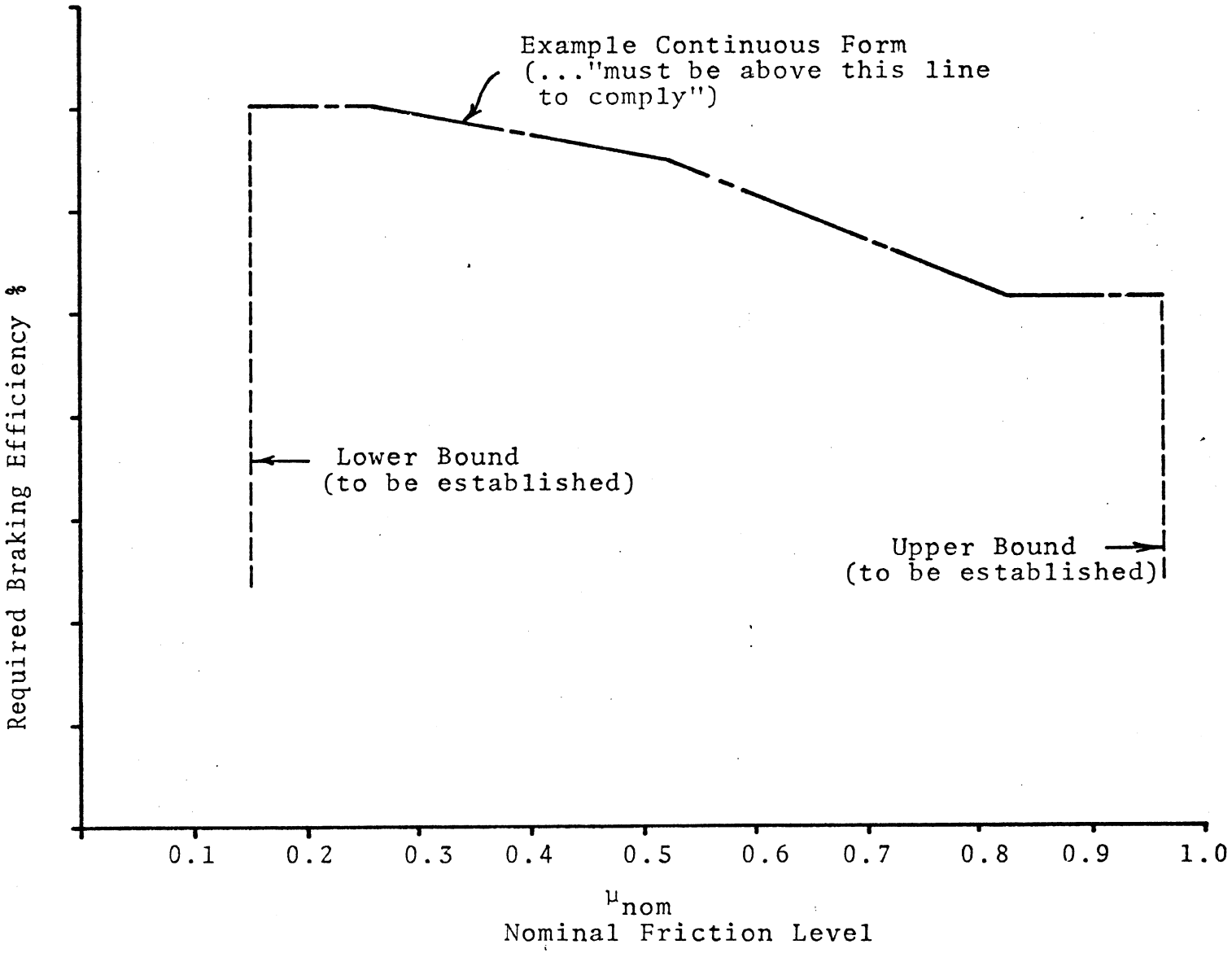

Figure 28. Example braking efficiency requirement showing desired continuous form as a function of μ_{nom}.

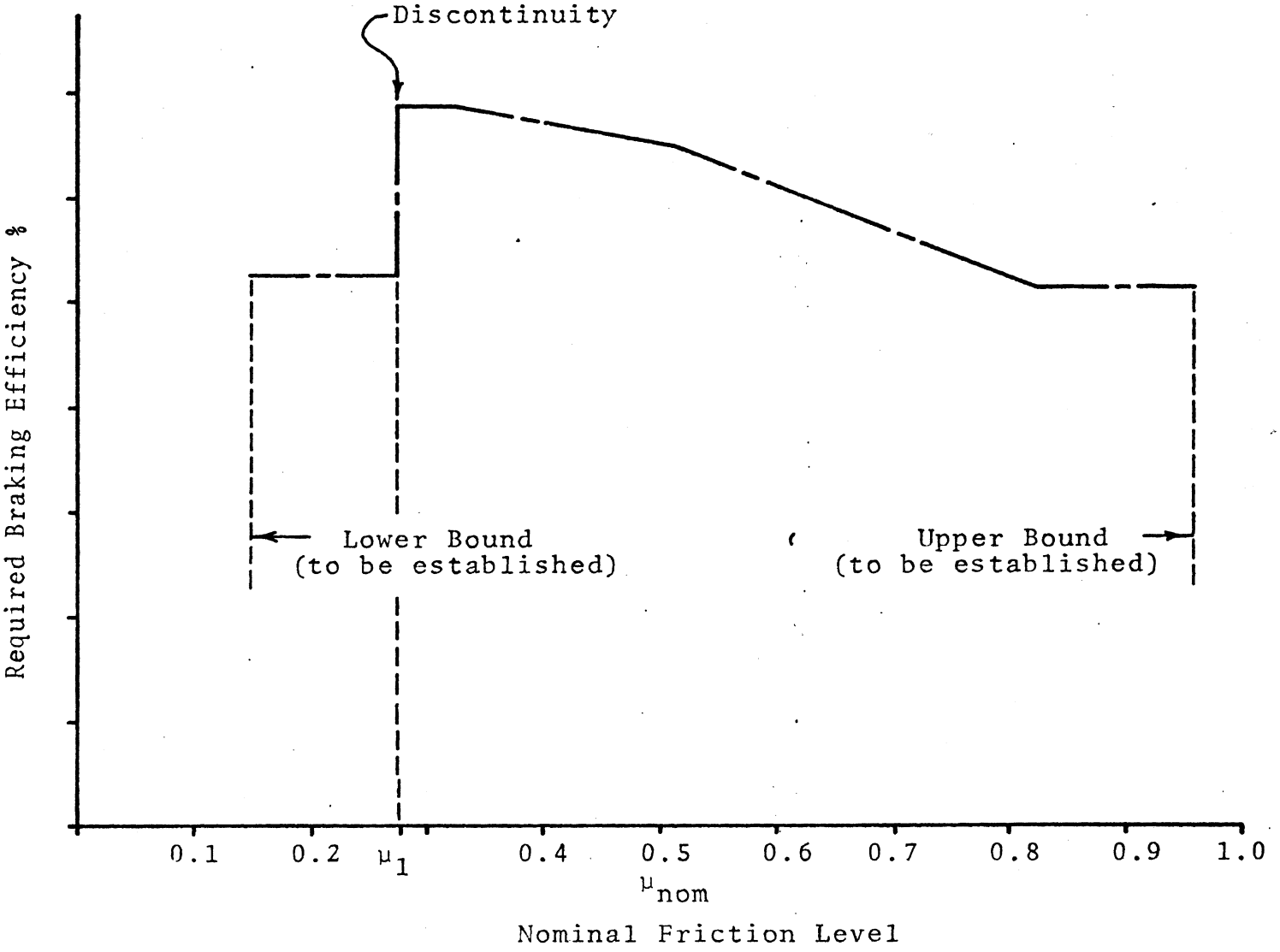

Figure 29. Example braking efficiency requirement showing discontinuity of $\mu_{nom} = \mu_1$.

A primary consideration in the specification of a braking efficiency requirement involves the extent to which the reference tire exhibits a range of traction capability which does not represent the average passenger car tire's performance. With regard to the ASTM G78-15 tire, for example, the limited data available to this study show a significantly reduced peak traction level on wet coated surfaces, as compared to "average" car tire performance. Clearly, if this tire were to be used as a government-defined reference for braking efficiency, the mismatch between its properties and the desired average-like performance would need to be factored into the braking efficiency rule. This could be done by adjusting required efficiency levels upwards in those regimes of μ_{nom} in which the reference tire's traction is sub-average and, conversely, by adjusting requirements downwards for that portion of the μ_{nom} range in which the reference tire is above average in traction capability.

6.0 CONCLUSIONS AND RECOMMENDATIONS

A braking performance characterization has been developed by which the influence of pavement friction becomes normalized to render a measure which is argued to be inherently relevant to traffic safety. Conclusions are presented here which address the quality of this measure as it may be applicable in a standard practice context.

6.1 CONCLUSIONS

1. The braking efficiency technique presented here is capable in concept (and, as has been partially demonstrated, in practice) of accounting for the prevailing frictional constraints which limit a vehicle's braking performance on any paved surface.

2. The developed concept is such that it is comprehensively applicable to vehicles operated in the United States, but it is not international in form due to the fact that the nationally-"representative" passenger vehicle is of markedly different size and weight distribution from one country to the next, with the mean U.S. vehicle probably departing most notably from international mean values of the pertinent parameters.

3. The braking efficiency method itself is totally objective since:

   a) stopping distance performance is evaluated through an open-loop test procedure which is constrained through objective descriptions of initial velocity, wheel lockup, pedal application, and distance measurement, and

b) the normalizing numeric is derived through a mechanistic process of data gathering and processing.

4. The braking efficiency measurements made during demonstration testing showed the method to be quite repeatable on the short term. Long term repeatability of braking efficiency measures, it might be argued, depends not upon the testing method itself but upon the temporal consistency of pavement frictional characteristics and vehicle braking-related properties. It would appear that whatever vehicle and pavement characteristics as might change from day to day or month to month would be adequately accounted for by the complementary measures of vehicle and pavement as make up the braking efficiency method.

5. The test burden associated with the braking efficiency technique is somewhat greater than that currently practiced involving braking effectiveness measurement in conjunction with ASTM skid trailer operation. To the extent that skid trailer measurements are made only infrequently by certain test agencies, the continual operation of the Surface Friction Dynamometer in a braking efficiency method might constitute a considerable increase in burden. In perspective, however, the continual accompaniment of stopping distance measurements with SFD measurements would only be required if pavement friction characteristics were seen to fluctuate significantly and often. Indeed, if that were the case, then it would seem that any surface friction characterization, whether skid numbers as required in FMVSS 105-75 and 121 or SFD measurements as in the braking efficiency method, would be required on a frequent basis.

6. The hardware associated with the measurement of the peak traction of the reference tire has been found to constitute a practical and reliable test tool whose data productivity is comparable to skid trailer operation.

7. The cost of the SFD machine would be comparable, in production, to the cost of commercially-available ASTM skid trailer systems (including trailer, tow vehicle, and data acquisition system).

8. The processing of SFD data, and the subsequent computation of the reference vehicle's stopping distance, involves a rather insignificant cost burden. While the computerized determination of the braking efficiency normalizer costs a trivial amount ($.50 to $1.00 for one surface condition), the manual task employed in reducing tire traction data involves a 3- to 4-hour effort per surface condition. It is clear that on-line peak reading circuitry is feasible here, and would practically eliminate the manual task.

6.2 RECOMMENDATIONS

On the basis of the developments which have been made during this study, we recommend the following:

1. A program of braking efficiency measurements should be conducted to enlighten whatever rulemaking considerations as might ensue from this study. There is a need to:

a) Establish the performance capabilities of contemporary passenger vehicles to provide a scale for interpreting the braking efficiency numeric. This scale will show both the nominal percentage utilization of modern passenger cars as well as the manner in which that utilization is distributed over the friction range.

b) Establish the performance capabilities of commercial vehicles which are configured with the upgraded braking systems required by FMVSS 121. These data should permit an assessment of the extent to which the braking efficiency performance spread between cars and trucks varies over the friction range. Thus, considerations of the need for special car- and truck-applicable requirements can be entertained with an informed view toward the consequences of such specificity, in terms of the spread in braking performance which would prevail in the vehicle population.

2. A survey of peak traction measurements should be conducted over a substantial sample of highways to permit definition of a reasonable upper bound, for the range of the variable μ_{nom}, over which a braking efficiency technique would apply. The measurements, clearly, should be conducted on dry pavements and should include those pavements representing the more aggressive textures which are in common highway usage.

3. Measurements of the shear force potential of a variety of paved surfaces should be made using the ASTM tire to determine the short- and long-term

stability of those characteristics which determine peak traction performance. With these data, an estimate can be made of the frequency of SFD measurements as might be necessary to assure valid characterization of a given surface which is in continual usage as a braking efficiency test facility. Should these measurements indicate substantial short-term variability in peak traction potential, a high level of SFD test burden would be implied. Of course, if such variability is established, one might argue that only by a normalizing braking performance measure can a meaningful characterization be made.

4. In further refinement of the braking efficiency method, work should be done to examine the influence of tire slip rate and load fluctuation on the generation of peak normalized longitudinal force to determine:

   a) the extent to which the delayed spin-down transient of an SFD machine permits measurement of a representative peak traction performance, and

   b) the conditions under which ASTM skid trailer devices, currently in existence, could be acceptable for use in the gathering of traction data for braking efficiency normalization.

5. Further progress should be made in the development of a passive pedal force control element. While automatic brake actuation machines provide an admittedly high quality open-loop braking input, it is clear that a passive device is feasible and surely could be provided at substantially less cost.

6. The qualifications of the reference tire should be evaluated through a program of tire data acquisition. Upon determining the traction properties of a mean passenger car tire over a wide range of friction, the acceptability of the ASTM tire for use in the braking efficiency technique can be evaluated.

APPENDIX A

LITERATURE SURVEY

This literature survey was conducted in fulfillment of Task I of the Braking Efficiency Test Technique study. In conducting this survey, one paper (2)* was found to be a primary source in terms of its direct and immediate background to the present project. Consequently, much of this report is devoted to illuminating and expanding certain points raised by this paper, and hence, the presentation of the literature survey begins with a detailed synopsis of it. The remaining portion of the literature survey is organized as follows:

(1) Velocity and load sensitivity of the peak longitudinal friction coefficient.

(2) Human pedal force and pedal displacement rate potential.

(3) Standard tire representing the mean U.S. tire population in peak longitudinal friction coefficient over a variety of surfaces, both wet and dry.

(4) Theoretical and experimental braking performance measures.

(5) Brake proportioning.

---

*Numbers in parentheses refer to references listed at the end of this Appendix.

R. W. Murphy, "A Procedure for Evaluating Vehicle Braking Performance"

The purpose of Murphy's work was "to develop viable and realistic procedures for determining the braking efficiency of vehicles equipped with four-wheel antilock systems, and to determine by means of these procedures braking efficiencies currently attainable by vehicles equipped with production and/or developmental four-wheel antilock systems."

Braking efficiency has previously been defined as:

$$E = \frac{100\ \bar{A}_x}{\mu\ g} \qquad \text{(A-1)}$$

where

$\bar{A}_x$ is the average maximum sustained deceleration, in ft/sec^2, which a vehicle can achieve without wheel lockup on a given surface

g is the gravity constant, 32 ft/sec^2

μ is the coefficient of friction of the given tire-road interface.

However, this formula assumes that μ is constant throughout the deceleration period. For high friction surfaces, this assumption is approximately correct, but for wet or slippery surfaces, interface friction is a function of vehicle velocity and tire loading. Hence, for his purposes, Murphy defined braking efficiency as:

$$E = \frac{100\ D_i}{D_a} \qquad \text{(A-2)}$$

where

D_i is the ideal stopping distance of the vehicle which would accrue if the braking effort were to be modulated to obtain the maximum tire-road friction force throughout the stop. [Lister determined that maximum braking force occurs at approximately 15% longitudinal slip (3).]

D_a is the actual stopping distance based on experiment.

An experimental program was conducted to determine stopping distances for two cars (a 1971 Chrysler Imperial equipped with "Sure-Brake," a four-wheel antilock system developed jointly by Chrysler and Bendix (4); and a 1971 Buick Riviera equipped with an experimental four-wheel anti-lock system developed by General Motors) at a range of initial velocities and loadings. The tests were run on both dry asphalt and wet jennite.

In the stopping distance tests the brake pedal was applied automatically (insuring open-loop inputs and thereby eliminating the effects of driver skill) at a pedal application rate of 30 in/sec. Driver control was limited to steering inputs with the goal of maintaining the vehicle within a 12-foot lane.

Stopping distance was measured by an electronic counter fed by pulses (1 pulse per foot) from a fifth wheel. The measurement was initiated at the instant of pedal actuation. The HSRI Mobile Tire Tester was used to determine the μ-slip characteristics of the tires used in the stopping tests. Use of this device allowed determination of peak longitudinal friction coefficients at various loads and velocities for use in the ideal stopping distance calculation.

Results

Normalized peak longitudinal force properties of the test tires showed little, if any, sensitivity to load or velocity on dry asphalt, but showed considerable sensitivity to load and velocity on wet jennite. The calculation of ideal stopping distance was tailored to the friction characteristics of the particular tire/test surface combination in question. When peak friction was judged to be insensitive to load and velocity, the equation

$$D_i = \frac{V_i^2}{2g\,\mu_{av}} \qquad \text{(A-3)}$$

where

V_i = initial velocity

μ_{av} = average peak longitudinal friction coefficient

was used. If the peak longitudinal friction coefficient, μ_{x_p}, was judged to be sensitive to velocity, a second-degree polynomial in V (velocity) was fitted to the tire data obtained (assuming the loading was constant) by the method of least squares. In this case, the equation

$$D_i = \frac{1}{g}\int_0^{V_i} \frac{V}{AV^2 + BV + C}\,dV \qquad \text{(A-4)}$$

was employed. It was assumed that the effect of load transfer from rear to front tires was negligible, since a gain in traction on the front tires would be offset by a loss in traction at the rear.

Murphy argued that to fully characterize a vehicle's braking performance, not only is braking efficiency necessary (as a measure of the extent to which the vehicle utilizes the

friction available at the tires), but a measure of the tires' longitudinal tractive qualities is also needed. To fulfill this requirement, the friction performance of the vehicle test tires was rated against the performance of a standard tire. (The standard tire used for these tests was an 8.45-15 Traction Test Standard manufactured by the General Tire Company.) The standard tire was tested for μ_{x_p} at various speeds (fixed load) and inserted in the equation for D_i. A performance measure, the tire factor, was then defined as:

$$\text{Tire Factor:} \quad F = \frac{D_i(\text{std})}{D_i} \tag{A-5}$$

where $D_i(\text{std})$ is the ideal stopping distance using the standard tire and D_i is the ideal stopping distance using the test tire. A second performance measure, the brake system rating, was defined as:

$$\text{Brake System Rating:} \quad R = EF \tag{A-6}$$

where E is the braking efficiency of the vehicle and F is the tire factor. This rating compares the actual brake system performance to that which could be achieved using the standard tire.

A final performance measure was defined:

Wet to Dry Performance Rating:

$$\frac{\dfrac{D_i(\text{wet})}{D_i(\text{dry})}}{\dfrac{D_a(\text{wet}}{D_a(\text{dry})}}$$

This measure gives an indication of the actual vehicle's dry braking performance compared to its wet braking performance

normalized by the dry to wet performance of the vehicle with the standard tires.

Murphy reached the following conclusions:

1. Antilock systems improve the minimum stopping distance capability of cars.
2. The test procedure developed in this study is a viable means of quantifying a vehicle's braking performance.

LOAD AND SENSITIVITY OF PEAK LONGITUDINAL FRICTION COEFFICIENT

A number of investigators have studied the effect of a tire's velocity on the peak braking coefficient obtainable. As a rule, the peak longitudinal friction coefficient decreases with increasing speed for all road surfaces—wet or dry (2, 5-11).

A search of the literature for data relating the effect of loading on the peak longitudinal friction coefficient revealed that data is lacking in this area. Murphy included limited data on loading in his paper (2), but the range was restricted to 1450-1600 lb.

PEDAL FORCE

In the stopping distance experiments proposed in this project, it was desired to input the braking control in an open-loop manner to insure that the results be independent of driver skill. Nonetheless, appropriate parameters for this open-loop pedal application procedure must be established. Hence, the literature was searched to determine a foot pedal force and/or pedal displacement rate that would be representative of a human in an emergency stop.

In an experiment using 105 women employees at the National Bureau of Standards, 50% could not achieve a sustained brake pedal force of 200 lb—the value considered acceptable under a 1970 Federal Motor Vehicle Safety Standard (12).

The maximum pedal force a driver can exert is a non-linear function of the driver's hip joint angle and knee angle (13). Aoki found that 80% of the male drivers he tested could reach a pedal force of 150 lb, however, only with "enormous effort." He recommended that the maximum brake pedal force on a passenger car should be 44 lb. In a later study, using a driver simulator, Aoki determined that from a control standpoint 44 lb was the optimum brake pedal force for actually stopping a vehicle (14).

The foot force capability of people in braking was studied as a function of age, sex, and weight under both standard and induced motivation (15). (It was determined from minimum stopping distance tests that maximum pedal displacement had only a slight effect on the stopping distances attained.) The pedal force that could be attained by at least 5% of the population was:

	Standard Motivation	Induced Motivation
Females	70 lb	100 lb
Males	140 lb	185 lb

It was concluded that an intermediate pedal force level between those measured under "standard" and "induced" motivation would be a reasonable maximum force that drivers should be expected to exert in attaining limit vehicle decelerations. Hence, it was suggested that 85 lb be given as the maximum brake pedal effort necessary to reach a vehicle deceleration of .75g.

A similar study (16) showed the maximum foot pedal force for the fifth percentile female ranging up to 120 lb, depending on test conditions. For the fifth percentile male the range was 120 to 190 lb.

PEDAL DISPLACEMENT RATE

A brake pedal displacement rate of 30 in/sec was used in stopping distance tests at HSRI to study braking efficiency (2), although informal tests conducted at HSRI have shown that two male subjects could apply the brake pedal at rates of 150 to 180 in/sec.

The maximum pedal displacement designed into the brake pedal was shown to have only a slight effect on the average vehicle deceleration achievable (15).

STANDARD TIRE

Data available in the literature was surveyed in an effort to identify a tire for use in this study as a traction reference.

As indicated by a draft of "Standard Specification for Traction Test Control Tires" (unpublished), an SAE standard tire was at one time considered by the SAE Test Procedures Subcommittee (since disbanded). Construction specifications were given, but no performance tests were shown. However, in a study on the tractive qualities of tires in skidding (17) an SAE control tire was used. The data presented in the study showed that the wet friction coefficient for the control tire was significantly below the mean coefficient for the tires tested.

A second standard tire was developed and manufactured by General Tire (18). This tire was intended as a standard skid

test tire to be used to correlate road surface friction measurements. Detailed specifications for the tire's construction were given. Also, the tire's radial deflection was plotted as a function of radial load for three inflation pressures. However, no data was given to determine the tire's suitability as a traction-representative tire.

The third tire considered was the ASTM standard tire. In a large scale systematic tire testing program, 86 tires (2 each of 43 different types representing 90% of the O.E. population) were measured for longitudinal and lateral traction capability on three different wetted surfaces using the HSRI Mobile Tire Tester (19). Four of the tires tested were ASTM standard tires. The μ_{x_p} values of these tires were very close to the mean of all the tires on the wet asphalt and wet concrete surfaces, but they were considerably below the mean on wet jennite.

In another study (20) in which 11 tires (representing all five major tire manufacturers) were studied in dry traction, it was found that the average tire in the sample varied significantly in μ_{x_p} depending on the surface (asphalt or concrete) used. On the other hand, the ASTM tire in the sample showed no significant variation in μ_{x_p} on these two surfaces. Further, the asymmetry of the average sample tire in terms of peak longitudinal and lateral friction coefficients varied significantly over the two surfaces, whereas, again, the ASTM tire showed no signifcant variation in its asymmetry characteristics.

A fourth tire considered was the Goodyear Polyglas Power Cushion. In a study using the HSRI Mobile Tire Tester, 11 different tires were measured on asphalt and concrete surfaces (both wet and dry) to build a traction data base for use in tire model validation work (21). Tires were selected for similarity of tread pattern and tire cord, so that the effect

TABLE A.1

PEAK LONGITUDINAL FRICTION COEFFICIENT AND COMPARISON OF GOODYEAR POLYGLAS POWER CUSHION TIRE WITH TEN OTHER TIRES

Surface	Wet Asphalt			Wet Concrete			Dry Asphalt		Dry Concrete	
Velocity (mph)	20	40	55	20	40	55	20	40	20	40
Goodyear Polyglas Power Cushion	.832	.654	.691	.486	.473	.364	1.126	1.028	.994	.894
Avg. of All Tires	.847	.670	.663	.574	.446	.372	1.106	1.059	1.007	.951
Max. of All Tires	1.118	.800	.818	.877	.582	.545	1.425	1.360	1.237	1.157
Min. of All Tires	.704	.554	.596	.445	.352	.292	.991	.965	.836	.829
No. of Tires With Coef. Higher Than Goodyear Tire	4	2	3	8	2	3	3	4	5	7
No. of Tires With Coef. Lower Than Goodyear Tire	6	8	7	2	8	7	7	6	5	3

of the two tire variables (carcass construction and meridian profile) could be isolated. As shown in Table A-1, the Polyglas tire exhibited the most representative μ_{x_p} of the tire tested.

In a study previously cited, (19), the Polyglas tire also appeared. Its μ_{x_p} characteristics along with the means of the sample tires for the three surfaces are given in Table A-2.

TABLE A-2

Jennite		Concrete		Asphalt	
Polyglas	Mean	Polyglas	Mean	Polyglas	Mean
.37	.32	.69	.62	.57	.57

Referring to the actual distribution of the number of tires versus traction coefficient increment, the Polyglas tire was seen to be moderately representative of the mean (see Figure A.1.

BRAKING PERFORMANCE MEASURES

Experimental

The effectiveness of a vehicle's brakes may be determined by measuring the maximum deceleration capability of the vehicle on a particular surface. This can be done using either of two approaches:

(1) Directly by measuring the actual deceleration during braking.

(2) Indirectly by measuring the initial velocity and the stopping distance. [Using this approach, braking systems of 1972 passenger cars and motorcycles were evaluated by the DOT based on data furnished by vehicle manufacturers (22).]

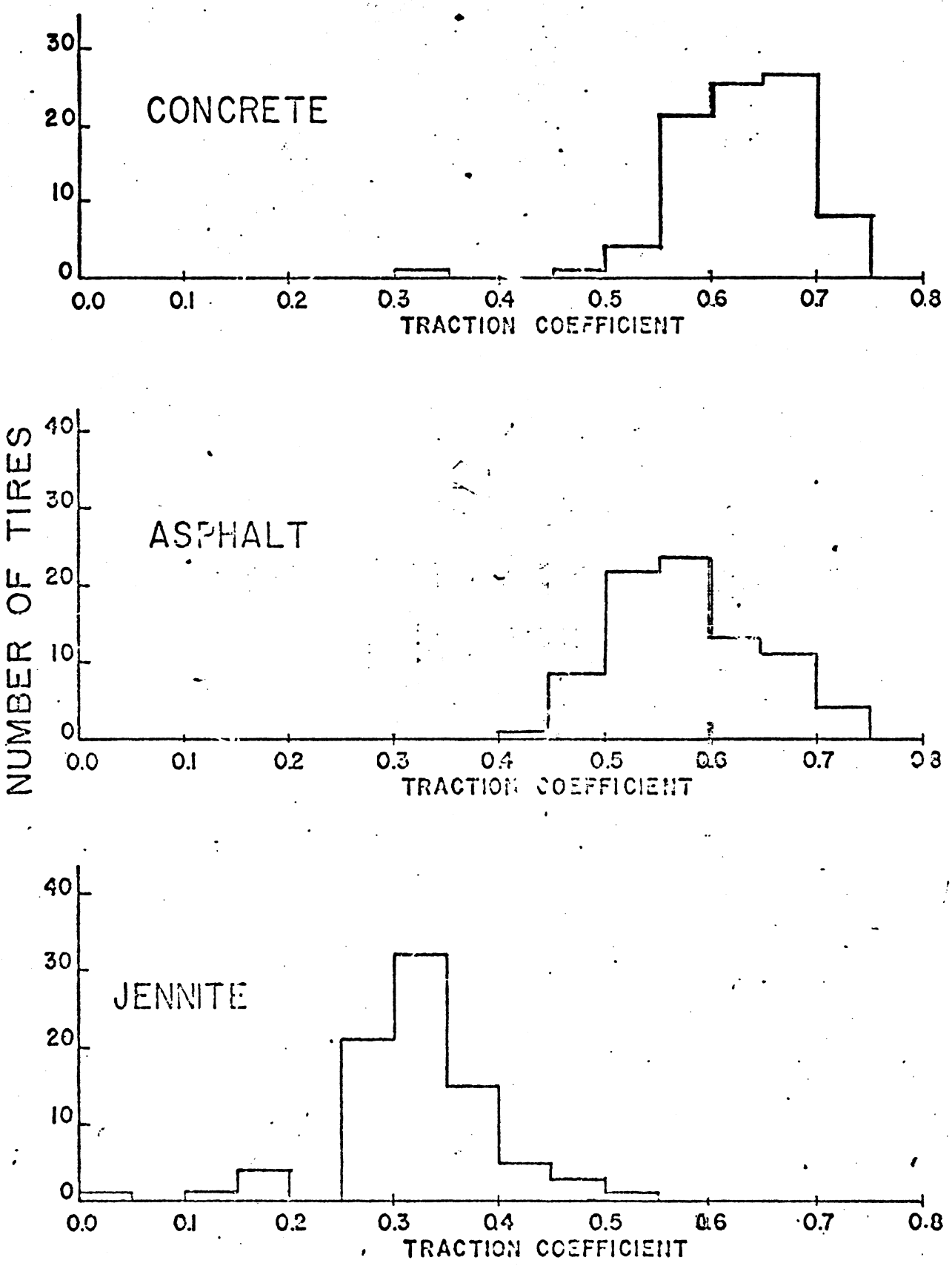

Figure A.1 Distribution of peak longitudinal braking efficiency, μ_{x_p}.

Three methods have been used to measure stopping distance experimentally:

(1) Integration of a fifth wheel velocity signal (23).

(2) A revolution counter attached to the fifth wheel (2, 24).

(3) Direct distance measurement employing an explosively fired chalk pellet to mark the point of brake actuation (25). In this method, account must be taken of the time lag for the chalk pellet to hit the ground.

To measure the instantaneous value of the vehicle's deceleration, two methods have been employed:

(1) Differentiating the velocity of the fifth wheel

(2) Using a decelerometer (24, 26).

The mean deceleration of the vehicle was measured directly by Lister and Sweetland (27) using an instrument of their own design which was carried by the vehicle.

An alternative to actual road testing employs a stationary dynamometer. There are two main types.

(1) The vehicle is anchored, and the braked wheels are driven by rollers.

(2) The vehicle is driven onto a platform and braked sharply, and the reaction force is measured at each wheel on the platform.

The SAE has devised test procedures (28) and performance requirements for braking system based on deceleration levels and stopping distances (28).

Recent government standards have been devised that set more demanding performance levels than the SAE regulations (29, 30).

Experimental and Theoretical Treatments of Braking Effectiveness and Braking Efficiency

The following study is cited in some detail since the experimentation and computer modeling reported are directly applicable to the present project. The research was reported in two documents (31, 32).

The study was conducted in order to determine the braking performance capabilities of buses, trucks and tractor-trailers equipped with standard braking systems. Hence, three integral trucks, three buses, and four tractor-trailer combinations were subjected to a number of brake performance tests. To determine the improvement in braking performance, if any, attributed to advanced braking systems, three additional vehicles were tested:

(1) An integral truck equipped with disc brakes and a full power hydraulic brake actuation system.

(2) A tractor-trailer equipped with proportioning valves, an adaptive braking system, and a trailer brake synchronization device.

(3) A tractor-trailer equipped with a wheel antilock system.

Included in the testing program were maximum deceleration tests and brake balance tests (correct axle-weight proportioning).

The analytical phase of the study was directed towards establishing mathematical procedures for predicting brake effectiveness, braking efficiency, pedal force gain, and thermal response. Equations were developed and presented to include a wide range of options for the vehicle modeled, i.e., number of axles, type of brakes, etc.

Based on the study, recommendations were made to upgrade the braking performance of buses, trucks, and tractor-trailers to a level approaching that of passenger cars.

An interesting analysis of braking efficiency was done by G. R. Olsson, et al. (33).

In that work, the braking efficiency of a vehicle, defined as the ratio of ideal stopping distance to actual stopping distance, was derived in terms of the longitudinal tire slip ratio S_F/S_R (front slip to rear slip), tire properties, and vehicle geometry. The tire traction model used was found in References 34 and 35.

The derivation was developed by applying a limiting process to the equations of motion of a highway vehicle during braking maneuvers at the upper limit of speed number, where:

$$\text{Speed Number} = S = U_o(\mu_o g L)^{1/2}$$

U_o - initial vehicle velocity

μ_o - value of friction coefficient at 0 velocity

g - gravity constant

L - wheelbase of vehicle

The ideal stopping distance was defined as the value obtained when the tire-road friction coefficient, μ, is equal to its value at zero speed—μ_o (a constant). Since this derivation was based on the tire model in Refs. 34 and 35, which was developed assuming dry surfaces, the validity of the derivation is questionable for low friction surfaces.

The equation derived for braking efficiency was:

$$\eta = 1 + A + B + C \qquad \text{(A-8)}$$

where A gives the contribution to efficiency due to the effect of variation of stress over the tire contact patch:

$$A = -\frac{1}{8}\left(\frac{\mu_o\ m\ g}{C_s}\right)\left[\frac{1-S_F}{S_F}\left(\frac{b}{L}\right)^2 + \frac{1-S_R}{S_R}\left(\frac{a}{L}\right)^2\right] \qquad \text{(A-9)}$$

B accounts for the effect of variation of friction with sliding speed:

$$B = -\frac{2}{3}\,VA_s\left(\frac{b}{L}\,S_F + \frac{a}{L}\,S_R\right) \qquad \text{(A-10)}$$

and C accounts for the aerodynamic drag:

$$C = \frac{1}{2}\left(\frac{\rho V^2 C_D A_F}{\mu_o\ m\ g}\right) . \qquad \text{(A-11)}$$

In the above expressions:

a = distance from front axle to c.g. of vehicle

b = distance from rear axle to c.g. of vehicle

μ_o = value of friction coefficient at 0 velocity

m = mass of vehicle

g = gravity constant

S_F = front tire longitudinal slip

S_R = rear tire longitudinal slip

L = wheelbase of vehicle

C_s = tire circumferential stiffness

VA_s = fractional reduction in friction due to sliding speed

ρ = density of air at S.T.P.

C_D = drag coefficient of vehicle

A_F = projected frontal area of vehicle

$\frac{V^2}{2\mu_o g}$ = ideal stopping distance

Dimensionless groups:

$$\frac{\mu_o m\, g}{C_s} = \text{ratio of tire traction force to tire circumferential stiffness}$$

$$\frac{\rho V^2 C_D A_F}{\mu_o\, m\, g} = \text{ratio of aerodynamic drag to tire traction force}$$

For η to be maximum,

$$S_F/S_R = \frac{a}{b} \tag{A-12}$$

with

$$S_R = \frac{3}{16}\ \frac{\mu_o\, m\, g}{C_s}\ \frac{1}{VA_s}\ \frac{a}{L} \tag{A-13}$$

and the restriction that neither S_F nor $S_R > 1$.

BRAKE PROPORTIONING

A vehicle's braking performance can be improved significantly using brake proportioning. This topic was covered as part of two other literature surveys and hence they are reproduced here (15, 31).

The first survey deals with brake proportioning in automobiles. The second concerns trucks and tractor-trailers.

From Ref. 15, pp. 12-13:

When a four-wheeled vehicle decelerates there is a transfer of load (36, 37) onto the front wheels because the body's center of gravity is above the ground plane. To achieve optimum braking, the proportioning of the braking effort between the front and rear axles should match the instantaneous load

distribution (37, 38). Manufacturers build in a front-to-rear proportioning (39), but a brake system having a fixed front-to-rear braking ratio can only achieve optimum performance for a given rate of deceleration (40-42). Typically, brake proportioning is fixed with 60 percent to 70 percent of the braking occurring at the front wheels (39).

A series of tests on vehicles having different weight distributions and different brake proportioning (38) has shown that a front/rear brake ratio equaling the wheel load distribution of the vehicle at a deceleration of 1.0g is desirable if the car is to remain directionally stable when heavily braked on all surfaces. On low coefficient surfaces, however, this would result (36) in premature front wheel lockup and a deceleration less than maximum for that surface. The overall effect of proportioning on the driver-vehicle performance during braking is that, under certain conditions, the driver may be able to apply higher pedal efforts and achieve higher maximum decelerations without incurring wheel lockup.

One solution to the problem of proper proportioning is to vary the brake proportioning with the deceleration of the car. This can be done by controlling the pressure at each axle in correspondence to the axle loading (43-45), but the usual procedure is to limit or proportion the rear brake hydraulic pressure above some fixed upper limit (43). At best, however, these latter methods are only compromises as a result of variations in vehicle loading and brake performance.

From Ref. 31, pp. 12-33:

The coefficient of friction between the tires and the road necessary to prevent the lockup of wheels on the front axle is given by:

$$\mu_x = \frac{F_{X,F}}{F_{Z,F|dyn}} = \frac{(1 - \phi)\cdot(a_x/g)W}{[1 - \psi + \chi(a_x/g)]W} \qquad \text{(A-14)}$$

where

$F_{X,F}$ = brake force on front axle

$F_{Z,F|dyn}$ = vertical force on front axle

ψ = static rear axle load divided by total vehicle weight

ϕ = brake force between tire and roadway generated at the rear axle, divided by total brake force

χ = height of center of gravity divided by wheelbase

The braking efficiency, as determined from the forces acting on the front wheels, can be computed from

$$E_F = \left(\frac{a_x/g}{\mu_x}\right)_F = \frac{1 - \psi}{1 - \phi - \mu_x\chi} \qquad \text{(A-15)}$$

Similarly, the braking efficiency, as determined from the forces acting on the rear wheels, can be computed from

$$E_R = \left(\frac{a_x/g}{\mu_x}\right)_R = \frac{\psi}{\phi + \mu_x\chi} \qquad \text{(A-16)}$$

Friction utilization or braking efficiency, E, is defined as the ratio of the maximum, wheels-unlocked deceleration a_x/g to the coefficient of friction μ_x existing between tire and roadway. Thus, braking efficiency can be expressed as

$$E = \frac{a_x/g}{\mu_x} \qquad \text{(A-17)}$$

In general, E will be different for the individual axles over a wide range of loading and driving conditions due to dynamic weight transfer (1, 40, 46-50) and, in the case of articulated vehicles, due to forces transmitted through the king-pin of the trailer (51, 52).

Integral Trucks with Fixed Brake Force Distribution

Braking efficiency is directly influenced by the distribution of brake force braking effort among the axles. Accordingly, commercial vehicles with a large weight difference, loaded and empty, tend to have reduced braking efficiencies at driving conditions departing from the design point. A fixed brake force distribution is usually selected for integral trucks such that the braking process gives reasonably satisfactory results for the load condition and deceleration level that occur most frequently.

Braking efficiency, E, of the integral motor truck is determined by the center of gravity location, the brake force distribution, and the tire-roadway friction coefficient (2, 46, 47). The brake force distribution, ϕ, is typically not constant during the braking process. At low decelerations, ϕ will depend upon the difference in pushout pressures on front and rear axle, whereas at higher decelerations, ϕ may be affected by fade (51). For a truck with typical values for ϕ, χ, and ϕ, Equations (A-15) and (A-16) produce the result shown in Figure A.2. Note that for the loaded condition, the limiting value of braking efficiency is determined by the front axle, while for the empty condition, the front axle limits up to a μ of 0.68, at which point the rear axle becomes the limiting factor.

The stopping distance that can be achieved prior to wheel lockup is directly related to braking efficiency (46, 47, 50). For a braking efficiency of one, that is, a deceleration in g units equal to the existing friction coefficient, the stopping

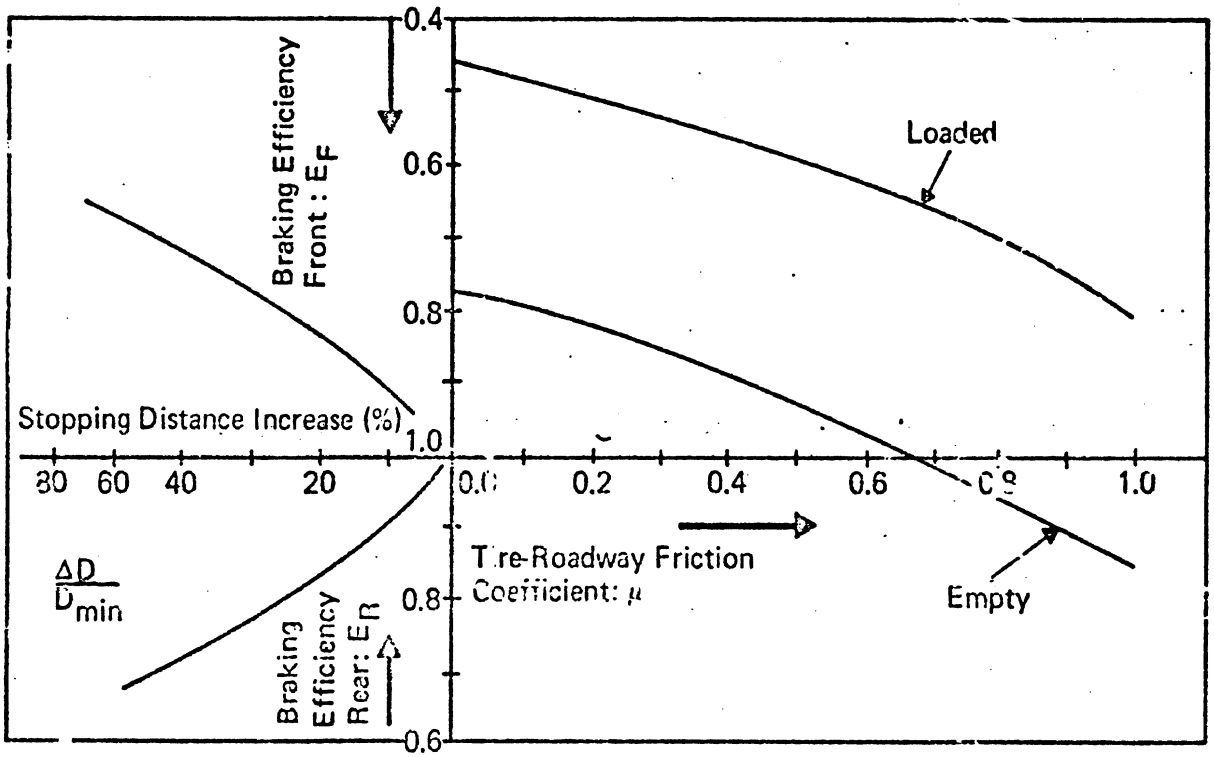

Figure A.2. Braking Efficiency for Two-Axle Vehicle Equipped with Fixed Brake Force

distance of the vehicle is the minimum achievable. If it is assumed that the deceleration, a_x/g, and the friction coefficient, μ_x, remain constant during the braking process, the incremental stopping distance, ΔD, (wheels unlocked), resulting from a braking efficient less than unity, is given by the expression

$$\Delta D = \frac{V^2}{2g}\left(\frac{\mu_x}{a_x/g} - 1\right) \qquad \text{(A-18)}$$

where V = initial speed of the vehicle. On using Equation (A-17), the expression given in Equation (A-18) becomes

$$\frac{\Delta D}{D_{min}} = \frac{1 - E}{E} 100 \ [\%] \qquad \text{(A-19)}$$

where

$$D_{min} = \frac{V^2}{2g\mu_x} = \text{minimum stopping distance} \qquad \text{(A-20)}$$

The increase in stopping distance as calculated from Equation (A-19) for a typical truck is also shown in Figure A.2.

If it were required that the efficiency, E, never be less than a specified value, E_{min}, irrespective of roadway and loading conditions, a very tight bound is placed on the distributions of brake force, ϕ, that will satisfy this requirement. If the requirement for E_{min} is set too high, it will not be possible to achieve it with a fixed brake force distribution. The existence of a fixed value of ϕ that provides $E > E_{min}$ can be checked through the following inequality (47)

$$1 - \mu\chi - \frac{1 - \psi}{E_{min}} \leq \phi \leq \frac{\psi}{E_{min}} - \mu\chi \qquad \text{(A-21)}$$

Application of this inequality to the wet and dry roadway ($0.2 \leq \mu \leq 0.8$) and over the full range of ψ and χ defines an envelope for values of ϕ that yield $E \geq E_{min}$ (47).

Experimental work has been reported by Alexander (38) comparing different fixed brake force distributions and load conditions for passenger cars. In tests of cars with three different brake force distributions, he showed that only one distribution resulted in minimum stopping distance.

The relationships discussed above (Equations (A-15), (A-16), and (A-21)) are also applicable to integral trucks equipped with tandem-axle suspensions. Tandem-axle suspensions are designed to distribute the static load among both axles independent of irregularities in the road surface. They can be classified into three basic groups (according to their attachment to the truck frame) as is indicated in Figure A.3. (a) walking beam suspension, (b) two-elliptic leaf spring suspension, and (c) multiple leaf-multiple rod suspension. [The history of tandem suspensions has been reviewed by Hendrickson (53).] In general, the reaction moments during braking cause a change in load distribution among both axles of the tandem suspension. During braking, the forward axle of a walking beam or multiple leaf-multiple rod suspension will be subjected to an increase in load, while the forward axle of a two-elliptic leaf spring suspension will experience a decrease in axle load from their respective static load values (46, 54-56). Since load transfer among axles of a tandem suspension can lead to premature wheel lockup, tandem-axle geometry and the brake force distribution among individual axles of a tandem suspension have a pronounced effect upon peak, wheels-unlocked deceleration performance.

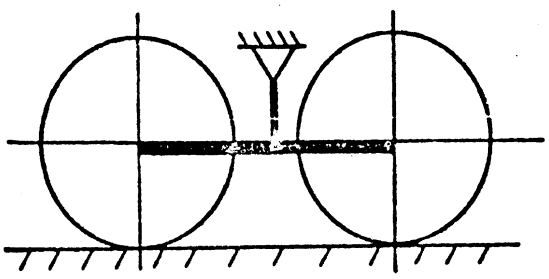

(A) Walking-beam suspension.

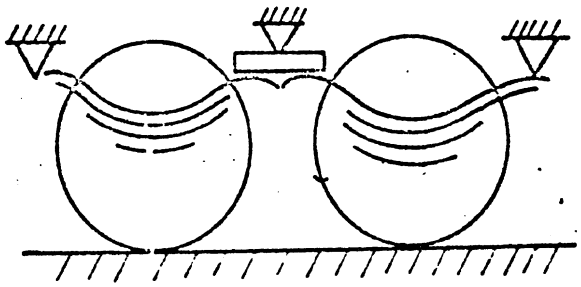

(B) Two-leaf spring suspension.

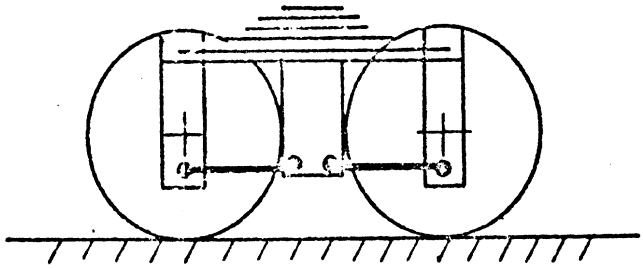

(C) Multiple spring-multiple rod suspension

Figure A.3. Tandem Axle Suspensions

Articulated Vehicles with Fixed Brake Force Distribution

The sum of the dynamic axle loads of each unit of a truck-trailer combination is equal to the weight of the particular unit, assuming no forces are transmitted by the hitch. In the case of a tractor-semitrailer, the axle loads of the tractor are influenced by the loading and brake forces of the trailer. The equations expressing weight transfer, brake forces and decelerations achievable without wheel lockup for a tractor-semitrailer are consequently more complicated than those for the integral truck and the truck-trailer combination (51, 56-62). Experimental work in Europe has indicated that the locking of individual axles influences the stability of the combination in accordance with theoretical predictions (63-65). It has been observed that the tractor-trailer combination is stable with a locked front axle, unstable with the trailer axle locked (producing "trailer swing"), and violently unstable with the tractor axle locked (producing "jackknifing"). The potential for jackknifing is greatest at the beginning of a severe braking process due to the large longitudinal forces that are created at the kingpin if the application and buildup time of the brake force on the trailer is greater than for the tractor (52, 58, 62, 63).

Prevention of wheel lockup appears to be the greatest deterrent to articulated vehicle instability. Assuming that wheel lockup does occur, undesired articulation and directional response can be minimized by having the front wheels lock up first, then the trailer wheels, and then the tractor rear wheels. The often observed practice in the U.S. of disconnecting or removing the front brakes of a tandem-axle tractor is, however, in conflict with the above observation (66). Eliminating the front brakes without changing the baseline distribution of the combination has, generally, an unfavorable influence on the braking performance of the vehicle combination (51).

Several means for determining the optimum fixed brake force distributions on a tractor-semitrailer have been suggested. They consist of either computing the deceleration achievable for a given tire-roadway friction coefficient for several assumed brake force distributions or computing the brake force distribution as a function of vehicle data and the desired range of braking efficiencies (51, 59, 60). Given the brake force produced by a trailer, brake force distribution on the tractor that will yield a minimum stopping distance can be computed from data defining the geometry and loading of the combination (51). A static analysis yields that

$$\phi_{1R} = \frac{A}{E_{1R}} - \mu_{1R} \cdot B \qquad \text{(A-22)}$$

where

$$A = \lambda\psi_1 + (1 - \lambda)(1 - \psi_2)y + \rho(z_2 y + z_1)$$

$$B = \lambda\chi_1 + (1 - \lambda)z_1 - (1 - \lambda)(\chi_2 - z_2)y$$

E_{1R} = braking efficiency produced by tractor rear axle

μ_{1R} = coefficient of friction between tractor rear axle and roadway.

$$\lambda = \frac{W_1}{W}, \quad \rho = \frac{F_{zR}}{W}, \quad W = W_1 + W_2$$

(See Figure A.4 for other symbols.)

Since in most cases the constants A and B in Equation (A-22) are different for the empty and loaded vehicle, Equation (A-22) will usually yield two different values for ϕ_{1R}. For most cases, the tractor rear axle brake force distribution, ϕ_{1R}, should not exceed 50% (64). A relatively small value of ϕ_{1R}, and hence a moderate utilization by the tractor rear axle of road friction in the longitudinal direction, means that

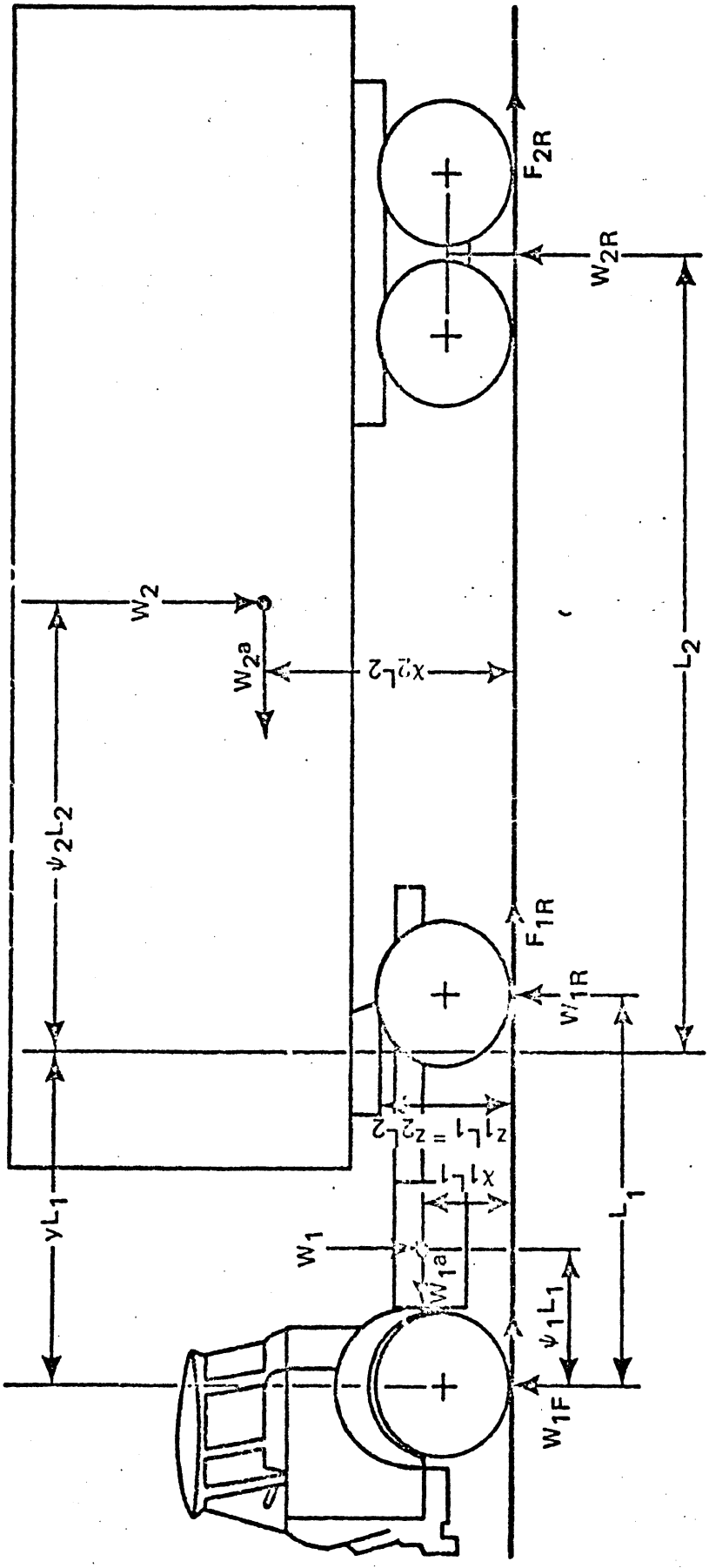

Figure A.4. Geometric and Load Configuration of Tractor-Semitrailer

increased lateral forces are available from the tires for maintenance of directional stability. This result is important since the danger of jackknifing is directly related to the lateral forces that can be produced at the tractor rear axle (62, 63).

Brake forces should be distributed on a truck-trailer combination such that the longitudinal forces at the hitch point are approximately equal to zero during braking. This practice is especially important on combinations in which large differences exist between the loaded and unloaded driving condition (67-69). Time differences in the application of brakes on the individual axles is also an important factor (57, 70). On a semitrailer, for example, if brake torque builds up on the tractor rear axle much faster than on the trailer axle, the combination may jackknife, especially on slippery roadways. This phenomenon can occur very quickly, with the result that the driver loses steering control because he cannot correct for the jackknife in the short time available (71).

It should be noted that dynamic load transfer between the forward and rearward axle of a tandem axle suspension has been neglected in deriving Equation (A-22). This assumption is valid only for tandem axle designs with equalization levers resulting in an approximately constant load distribution. For axles without equalization, however, the reaction moments during braking cause a change in load distribution among the individual axles (51, 54, 55, 72). In this instance, the braking efficiencies of each axle have to be computed individually.

Variable Brake Force Distribution

If the deceleration levels achieved prior to wheel lock, as limited by a fixed distribution of brake force, are considered to be insufficient, a variable distribution of brake

force can be employed. In the latter instance, the brake forces are proportioned so that they more closely approximate the ideal brake force distribution over a wide range of driving conditions. The ideal brake forces are related to the vertical loads on the axles produced by the dynamic weight transfer during the braking process (2, 38, 46, 47, 51, 73-78). A braking efficiency curve typically produced by a braking system with a variable distribution of brake force is shown in Figure A.5. It is clear that the system as designed produces better braking efficiencies on road surfaces with higher coefficients of friction. The braking efficiency curve in Figure A.5 also demonstrates that the designer wanted to avoid lockup of the rear wheels at the higher coefficients of road friction.

For design purposes, it proves to be more convenient to compare the "ideal" pressures (either hydraulic or pneumatic) desired at the wheel cylinders or brake chambers to the pressures actually delivered to the wheel cylinders by the braking system. "Ideal" pressures are those that correspond to the ideal braking forces, i.e., they are dependent upon the dynamic weight transfer (46, 47, 75, 79). Ideal and actual pressures, corresponding to the example used for computing Figure A.5 are shown in Figure A.6.

Proportioning valves have been designed that modulate line pressure as a function of the static or dynamic axle loads (43, 44, 75, 77-84). In the case of static modulation, the valve setting is not affected by suspension movement during the braking process. For dynamic modulation, the proportioning system must, however, be made sensitive to deceleration. For example, suspension deflection during braking has been used to modulate individual brake line pressures. With this type of proportioning, suspension and road noise must be filtered out while still retaining an adequate signal.

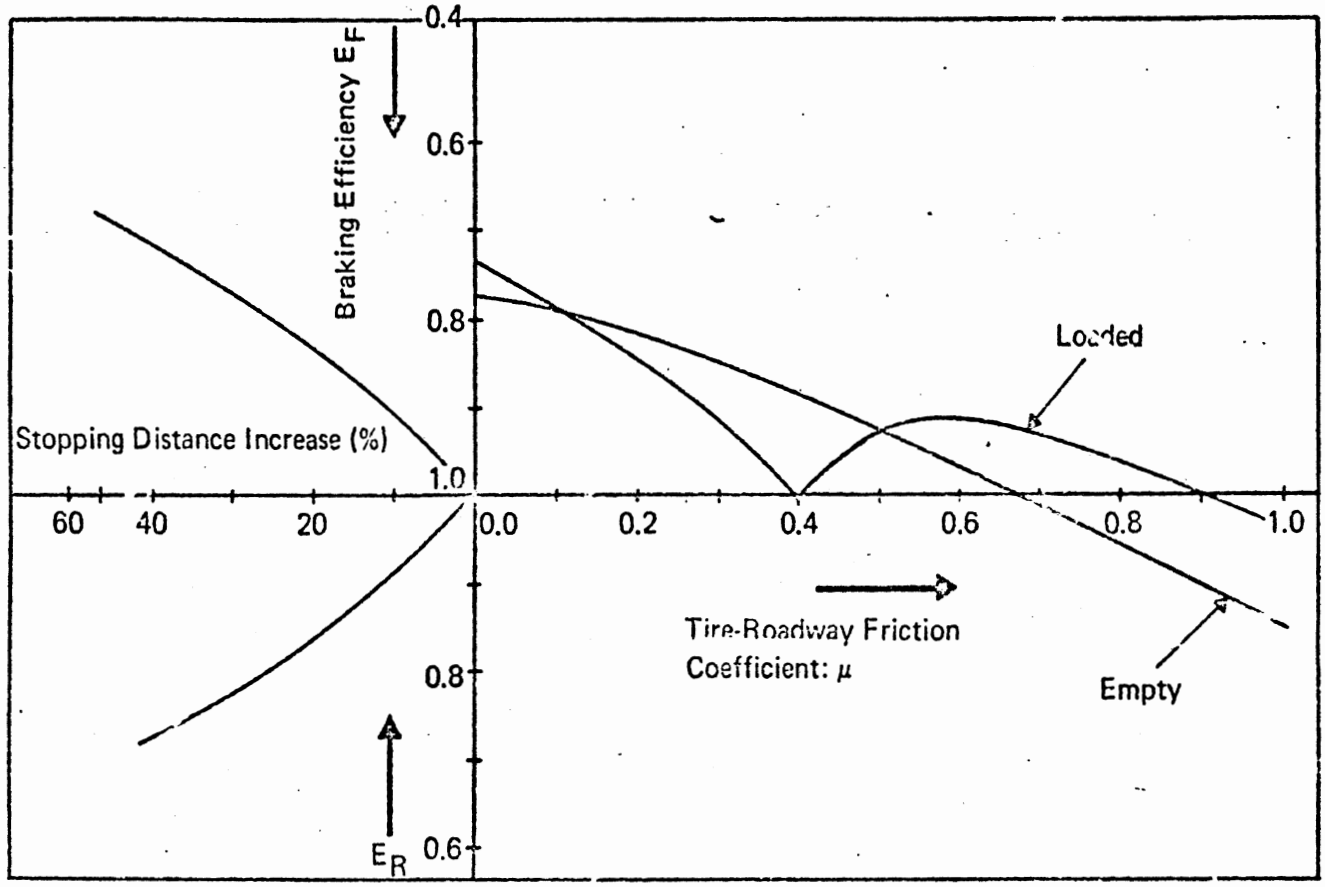

Figure A.5. Braking Efficiency for Proportional Braking

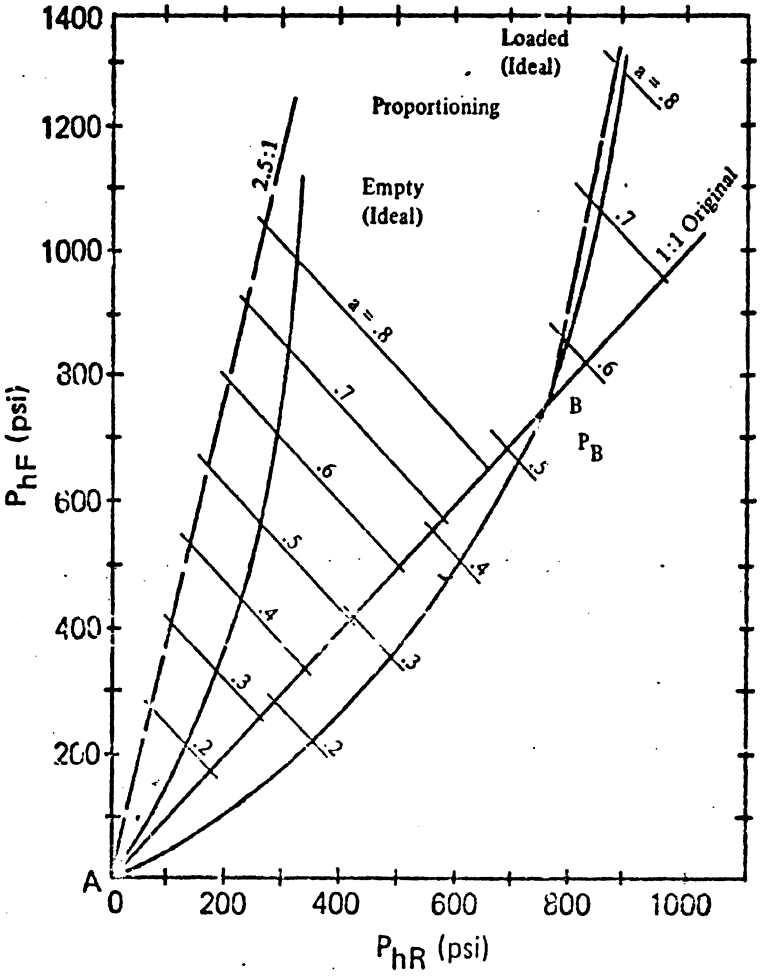

Figure A.6. Ideal and Actual Hydraulic Pressures

The ideal brake forces for a tractor-semitrailer in the loaded and empty driving condition are shown in Figure A.7. These curves show that the ideal brake force on the front axle varies little with change in vehicle loading, whereas the ideal brake force on the rear axle of the tractor and on the trailer axle is heavily influenced by the loading condition (51, 54, 57). Studies have shown that the following procedure is convenient for implementing variable brake torque distribution in an articulated vehicle (44):

(1) The front axle brake force of the tractor is designed to be proportional to brake line pressure.

(2) The brake force at the rear axle of the tractor is determined by a load sensitive proportioning valve. Depending on the design of the valve, the brake torque on the tractor rear axle may vary, for example, from 50 to 120% of the front axle brake torque of the tractor.

(3) It is convenient and sufficient to control the brake force of the trailer axle by a manually positioned limiting valve which has settings for the empty, half-loaded, and loaded conditions resulting in different limiting brake torques on the trailer axle (57, 67, 81-84).

When brake proportioning schemes are employed, it becomes necessary to examine the variability in performance that may result from using different trailers with the same tractor. Calculations of braking efficiency should be made by computing the coefficient of friction required by each axle to achieve a given deceleration without wheel locking. In order to calculate friction utilization, the effective axle loads have to be determined. For tractor-semitrailer and truck-trailer combinations, the equations relating deceleration achievable and tire-roadway friction have the same appearance as those

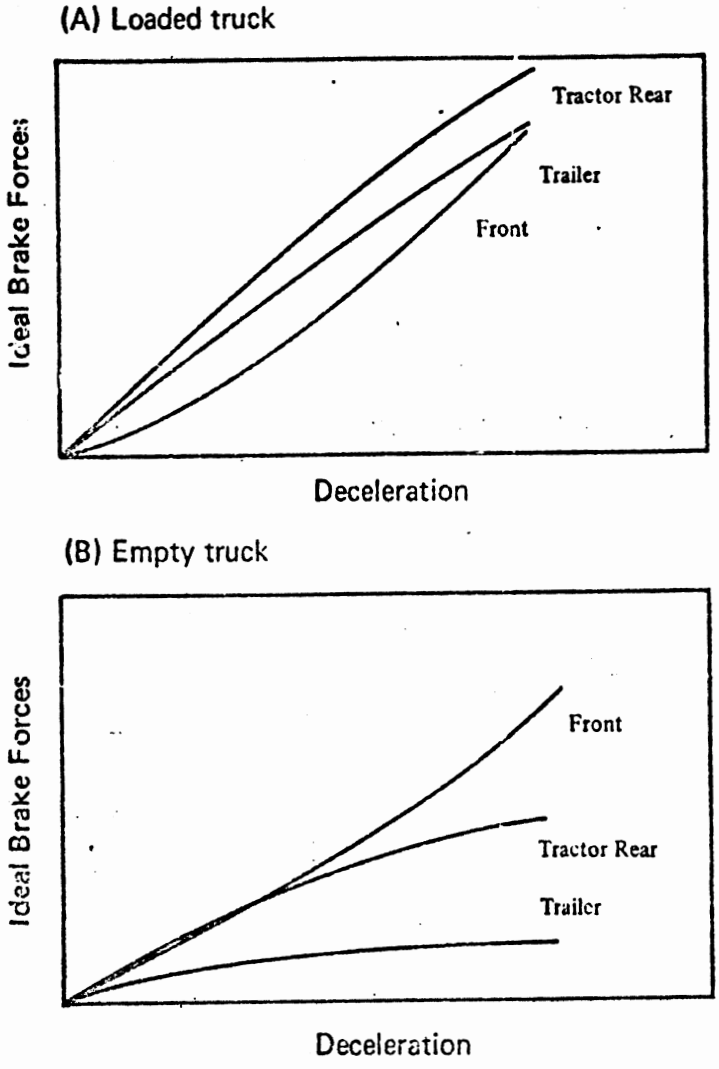

Figure A.7. Ideal Brake Forces on Tractor-Semitrailer

derived for braking systems with fixed distribution of brake torque. For vehicles with proportioning systems, the brake force distribution is determined by the static loads on the tractor rear axle and trailer axle (51, 67, 83, 84) or by the dynamic axle loads (81, 82) during braking.

Since braking systems with proportioning are often implemented by making the line pressure a nonlinear function of the pedal force rather than a function of the actual deceleration of the vehicle or a function of the friction coefficient, it is still possible to lock the wheels, especially on low friction surfaces. Although proportioning can provide a brake force distribution to match a wide range of loading and dynamic driving conditions, a practical system is still subject to some of the basic limitations of systems with fixed torque distribution (78).

WHEEL ANTILOCK SYSTEMS

Recently, antilock systems have been employed to provide brake proportioning. Wheel antilock systems prevent the wheels from locking up during braking by adjusting the braking effort to the traction force available at the tire-roadway interface. These systems were employed on aircraft as early as 1952 (85, 86). Shortly thereafter several antilock devices were introduced for use on automobiles (87-93). However, by 1961 no satisfactory wheel antilock device was in production for road vehicle in Europe (49) or the United States. During the last ten years, extensive research and development has been performed on wheel antilock braking systems for both passenger cars and commercial vehicles (81, 95-121).

REFERENCES

1. Rouse, J.A., "The Distribution of Braking on Road Vehicles," Proceedings of the Symposium on Control of Vehicles During Braking and Cornering, Institute of Mechanical Engineers, London, June 1963.

2. Murphy, Ray W., A Procedure for Evaluating Vehicle Braking Performance, Final Report, Prepared for Department of Transportation, Contract No. DOT-HR-031-1-051, October 1971.

3. Lister, R.D., "Some Problems of Emergency Braking in Road Vehicles," Paper presented at Symposium on Control of Vehicles During Braking and Cornering, London, June 1963.

4. Douglas, J.W. and Schafer, T.C., "The Chrysler 'Sure-Brake'—The First Production Four-Wheel Anti-Skid System," SAE Paper No. 710248, January 1971.

5. Gauss, F., "Braking and Guiding Forces Between Tyre and Road," A.T.Z., Vol. 63, No. 2, February 1961.

6. Harned, J.L., Johnston, L.E., and Scharpf, G., "Measurement of Tire Brake Force Characteristics as Related to Wheel Slip (Anti-Lock) Control System Design," SAE Paper No. 690214, 1968.

7. Holmes, K.E., Braking Force/Braking Slip—Measurements Over a Range of Conditions Between 0 and 100 Percent Slip, Road Research Laboratory Report LR 292, 1970.

8. Holmes, K.E. and Stone, R.D., Tyre Forces as Functions of Cornering and Braking Slip on Wet Road Surfaces, Road Research Laboratory Report LR 254, Ministry of Transport, 1969.

9. Kelley, J.D., Jr., "Factors Affecting Passenger Tire Traction on the Wet Road," SAE Paper No. 680138, January 8-12, 1968.

10. Meades, J.K., The Effect of Tyre Construction on Braking Force Coefficients, Road Research Laboratory Report LR 224, 1969.

11. Staughton, G.C., The Effect of Tread Pattern Depth on Skidding Resistance, Road Research Laboratory Report LR 323, 1970.

12. Radlinski, R.W. and Price, The Brake Pedal Force Capability of Adult Females, NBS Technical Note 552, October 1970.

13. Aoki, K., "Human Factors in Braking and Fade Phenomena for Heavy Applications, Problems to Improve Brake Performance," JSME, 3:587-594, No. 12, 1960.

14. Aoki, K., "Operational Characteristics of Human Beings at Brake Control," J. of Soc. of Auto. Eng. of Japan, March 1964.

15. Mortimer, R.G., Segel, L., Dugoff, H., Campbell, J.D., Jorgeson, C.M., and Murphy, R.W., Brake Force Requirement Study: Driver-Vehicle Braking System Design Variables, Final Report and Summary Final Report, Highway Safety Research Institute, prepared for Dept. of Transportation, Contract FH-11-6952, April 1970.

16. Eaton, D.A. and Dittmeier, H.J., II, "Braking and Steering Effort Capabilities of Drivers," 1970 International Automobile Safety Conference Compendium, SAE, 1970, pp. 153-158, SAE Paper No. 700363.

17. Spelman, R.H., Tarpinian, H.D., Johnson, D.E., and Campbell, K.L., "SAE Study - Wet Pavement Braking Traction," SAE Paper No. 700462, May 1970.

18. Hoefelt, C., Jr. and Bezbatchenko, W., "Pavement Test Standard Tire," The General Tire and Rubber Co., Akron, Ohio, for presentation to ASTM #-17 Committee, Atlantic City, New Jersey, June 26, 1961.

19. Wild, R.E., Wet Traction Test Program, Final Report, Highway Safety Research Institute, prepared for Safety Systems Laboratory, NHTSA, Contract No. DOT-HS-031-2-283, February 1973.

20. Segel, L.,"Tire Traction on Dry, Uncontaminated Surfaces," The Physics of Tire Traction--Theory and Experiment, A Symposium presented by the Research Laboratories of General Motors, October 8-9, 1973.

21. Tielking, J.T., Tire Traction Data Measured by the HSRI Mobile Tire Tester, sponsored by the Motor Vehicle Manufacturers Association, Project 329180, Document 5, March 1973.

22. Department of Transportation, NHTSA, Brakes, A Comparison of Braking Performance for 1972 Passenger Cars and Motorcycles, Vol. 2, Part 1, November 1971.

23. Segel, L., et al., Motor Vehicle Performance--Measurement and Prediction, An Intensive Short Course, Highway Safety Research Institute, Univ. of Michigan, July 9-13, 1973.

24. Starks, H.J.H. and Lister, R.D., "Experimental Investigations on the Braking Performance of Motor Vehicles," Proceedings, Inst. of Mech. Engineers, Automobile Div., No. 1, 1954-5, pp. 31-44.

25. Lister, R.D., "Brake Performance Measurement," Automobile Engineer, Vol. 49, No. 7, July 1959, p. 282.

26. Carpenter, N. and Goddard, E.J., "The Measurement of Braking Performance for Compulsory Motor Vehicle Inspection," J. of Inst. of the Motor Industry, Vol. 4, No. 5, March 1955.

27. Lister, R.D. and Sweetland, R.D., "Measurement of Braking Performance," Automobile Engineer, Vol. 55, No. 1, 1965, pp. 22-27.

28. SAE J843, J937, J992, Service Brake System Performance for Automotive Vehicles, SAE Special Publication SP-299, 1967.

29. Federal Register, Vol. 35, Sept. 25, 1970; Vol. 36, Feb. 27, 1971; Vol. 37, Sept. 2, 1972.

30. Department of Transportation, National Highway Traffic Safety Administration, Docket No. 73-13, Notice 1, June 1973.

31. Murphy, R.W., Limpert, R., and Segel, L., Bus, Truck, Tractor-Trailer Braking System Performance, Vols. 1, 2, and Summary Final Report, Highway Safety Research Institute, prepared for Dept. of Transportation under Contract No. FH-11-7290, March 1971.

32. Murphy, R.W., Limpert, R., and Segel, L., "Development of Braking Performance Requirements for Buses, Trucks, and Tractor-Trailers," presented at Automotive Engineering Congress, Detroit, SAE Paper No. 710046, January 1971.

33. Olsson, G. R. and Fielding, P.G., Applicability of Braking Control Systems to Highway Vehicles, Final Report, Booz-Allen Applied Research, Inc., prepared for Dept. of Transportation, Contract No. FH-11-6859, December 1970.

34. Dugoff, H., Fancher, P.S., and Segel, L., "An Analysis of Tire Traction Properties and Their Influence on Vehicle Dynamic Performance," SAE Paper No. 700377, May 1970.

35. Dugoff, H., Fancher, P.S., and Segel, L., Tire Performance Characteristics Affecting Vehicle Response to Steering and Braking Control Inputs, Final Report, Highway Safety Research Institute, prepared for U.S. Dept. of Commerce, Nat. Bureau of Standards, August 1969.

36. Parker, R.C., "Automobile Braking," The Engineer, 209, March 1960, pp. 498-501.

37. Taborek, J.J., "Mechanics of Vehicles," Bound Series from Machine Design, May-December 1957.

38. Alexander, A.L., Braking Performance of Cars with Different Brake and Weight Distributions, Road Research Laboratory Report LR 130, Ministry of Transport, Crowthorne, 1967.

39. "Engineering Specifications and Statistical Issue," Automotive Industries, 138, 6, March 15, 1968.

40. Chase, T.P., "Passenger-Car Brake Performance—Limitations and Future Requirements," SAE Transactions, Vol. 3, No. 1, January 1949, pp. 26-39.

41. Hofelt, C., "Effect of Speed, Load Distributions, and Inflation Pressure," presented at First International Skid Prevention Conference, Virginia Council of Highway Investigation and Research, University of Virginia, 1959.

42. Parker, R.C. and Newcomb, T.P., "The Performance and Characteristics of Disc Brakes," SAE Paper No. 836 A, April 1964.

43. Furia, A., Schachter, S., and Geneel, P., "Trends in Braking Techniques of European Vehicles," SAE Paper No. 670505, 1967.

44. Eaton, W.C. and Schreur, I.J., "Brake Proportioning Valve," SAE Paper No. 660400, June 1966.

45. "Anti-Skid Device Controlled by Suspension Movement," Engineering, February 7, 1964, p. 216.

46. Limpert, R., An Experimental Investigation of Proportional Braking, M.S. Thesis, Dept. of Mechanical Engineering, Brigham Young University, August 1968.

47. Limpert, R. and Warner, C.Y., "Proportional Braking of Solid-Frame Vehicles," presented at the Automotive Engineering Conference, Detroit, Mich., SAE Paper No. 710047, January 1971.

48. Troost, A., "On the Dynamics of Vehicle Braking," Automobiltechnische Zeitschrift, Vol. 65, No. 1, 1954, pp. 1-4.

49. Strien, H., "Trends in the Development of Vehicle Brakes and Anti-Skid Braking Devices in Europe," presented at the SAE International Congress and Exposition of Automotive Engineering, January 1961.

50. Strien, H., "Factors Influencing Stopping Distance of Motor Vehicles," Automobiltechnische Zeitschrift, Vol. 64, No. 7, 1962, pp. 208-10.

51. Limpert, R., "An Investigation of the Brake Force Distribution on Tractor-Semitrailer Combinations," presented at Automotive Engineering Congress, Detroit, Mich., SAE Paper No. 710044, January 1971.

52. Leucht, P., "The Directional Dynamics of the Commercial Tractor-Semitrailer Vehicle During Braking," SAE Paper No. 700371, May 1970.

53. Hendrickson, E.D., "History of Truck Suspensions--Tandem Suspensions," SAE Paper No. 690096, January 1969.

54. Leuzzi, V., "Braking of Road Vehicles with Tandem Axles Equipped with Equalization," Automobiltechnische Zeitschrift, Vol. 59, No. 3, 1957, pp. 58-61.

55. Goerge, W., "The Effect of Tandem Axles on the Dynamic Axle Loads Especially During Braking," Automobiltechnische Zeitschrift , Vol. 65, No. 11, 1963, pp. 348-353.

56. "Brakes, Brake Balance, and GCW," presented at the 25th Annual Convention of TTMA, Hollywood, Florida, March 1966.

57. Fritzsche, G., "Brake Force Distribution on Tractor-Semitrailers," Automobiltechnische Zeitschrift, Vol. 63, No. 1, 1961, pp. 13-18.

58. Bode, O. and Goerge, W., "Analytical Investigation of the Brake Behavior of Tractor-Semitrailer Combinations," Deutsche Kraftfahrtforschung und Strassenverkehrstechnik, No. 149, 1961.

59. Morse, R.J., "Brake Balance--It Can Be Improved," SAE Paper No. 660398, June 1966.

60. Stump, E., "Brake Force Distribution on Tractor-Semitrailers," Automobiltechnische Zeitschrift, Vol. 64, No. 7, 1962, pp. 203-207.

61. Schmidt, I., The Directional Stability of Two and Three Unit Vehicle Trains, Dissertation, Technische Hochschule Stuttgart, Germany, 1964.

62. Mikulick, E.C., The Dynamics of Tractor-Semitrailer Vehicles--The Jackknifing Problem, Ph.D. Thesis, Cornell University, June 1968.

63. Hales, F.D., et al., The Handling and Stability of Motor Vehicles, Report No. 1966/3, The Motor Industry Research Association, Warwickshire, England, January 1966.

64. Bode, O. and Goerge, W., "Brake Tests with Tractor-Semitrailer Combinations," Deutsche Kraftfahrtforschung und Strassenverkehrstechnik, No. 150, 1961.

65. Wilkens, H.A., Assessment of the Hope Anti-Jackknife Device, Road Research Laboratory Report LR 163, Crowthorne, England, 1968.

66. Stability and Control of Coupled Vehicles, Trucks, Truck Tractors, Semitrailers, and Trailers, Docket No. 69-1, Notice 1, prepared for the Federal Highway Administration by the American Trucking Association, May 1969.

67. Runge, D., "Matching of the Trailer Brake Forces to the Loading of the Combination," Automobiltechnische Zeitschrift, Vol. 69, No. 7, 1967, pp. 211-217.

68. Nelson, P.E. and Fitch, J.W., "Optimum Braking, Stability and Structural Integrity for Long Truck Combinations," SAE Paper No. 680547, August 1968.

69. Bode, O., "Truck-Trailer Braking and Load Matching," Automobiltechnische Zeitschrift, Vol. 60, No. 3, 1958, pp. 79-85.

70. Sido, F., "Analysis of the Time Lag Characteristics of Air Braking Systems Through Scaled Tests," Automobiltechnische Zeitschrift, Vol. 71, No. 3, 1969, pp. 95-100.

71. Oetzel, J.G., "Synchronization of Brakes on Multi-Axle Truck-Trailer Trains," SAE Quarterly Transactions, Vol.6, No. 2, April 1952, pp. 365-372.

72. Strien, H., "Disc Brakes--Drum Brakes," Automobiltechnische Zeitschrift, Vol. 61, No. 9, 1959, pp. 276-279.

73. Toennies, C., "The Varia--Principle for the Braking of Motor Vehicles," Automobiltechnische Zeitschrift, Vol. 60, No. 4, 1958, pp. 99-105.

74. Garcia, J.P., "Braking Improvements," Automobile Engineer, March 1966, pp. 102-106.

75. Oberthür, H. and Baum, F., "Braking-Force Distribution for Hydraulically-Operated Vehicle Brakes," Automobiltechnische Zeitschrift, Vol. 66, No. 8, August 1964, pp. 222-225.

76. "Dunlop Braking Stabilizer," Automobile Engineer, Vol. 53, No. 8, July 1963, pp. 318-320.

77. "Braking Proportional to Load," Automobile Engineer, Vol. 55, No. 12, November 1965, pp. 491-493.

78. Strien, H., "Braking Force Distribution in Cars," Automobiltechnische Zeitschrift, Vol. 67, No. 8, August 1964, pp. 240-245.

79. Eddy, R.T. and Wilson, R.A., "An Approach to Load Sensing Brake Proportioning for Passenger Cars and Light Trucks," SAE Paper No. 660411, June 1966.

80. Cornwell, E.L., "Automatic Load-Sensitive Air Brake Control," Modern Transportation, Vol. 94, No. 2416, 1965, pp. 8-9.

81. Lueck, F.E., Gartland, W.A. and Denholm, M.J., "Proportioning Valve to Skid Control--A Logical Progression," SAE Paper No. 690456, 1969.

82. Mueller, G., "Improved Safety in Braking of Tractor-Semi-trailers and Truck-Trailer Combinations," Automobiltechnische Zeitschrift, Vol. 62, No. 7, 1960, pp. 194-195.

83. Fritzsche, G., "Static Modulation of the Brake Forces on Motor Vehicles and Trailers According to Load and Deceleration," Automobiltechnische Zeitschrift, Vol. 61, No. 8, 1959, pp. 219-224.

84. Mitschke, M., Runge, D., and Bosch, R., "Load-Controlled Brake Force Regulation in Semi-Trucks," Automobiltechnische Zeitschrift, Vol. 68, No. 2, pp. 50-55, and Vol. 68, No. 7, 1966, pp. 253-256.

85. Newcomb, T.P. and Spurr, R.T., Braking of Road Vehicles, Chapman and Hall, 1967, pp. 55-59.

86. Collier, G.H., "Two Methods of Aircraft Skid Control, SAE Paper No. 8B, 1958.

87. "Lockheed Anti-Lock," Autocar, September 14, 1962, p. 423.

88. "The Lockheed Anti-Locking Device," Automobile Engineer, Vol. 52, No. 10, October 1962, pp. 386-389.

89. Lister, R.D. and Kemp, R.N., "Skid Prevention," Automobile Engineer, Vol. 48, No. 10, October 1958, pp. 382-391.

90. Beuchle, F., "The Anti-Lock Device," Automobiltechnische Zeitschrift, Vol. 65, No. 8, 1963, pp. 238-239.

91. Gunsaulus, A.C., "Rolling Wheels Gather No Skids," SAE Transactions, Vol. 61, 1953, pp. 189-195.

92. "Flywheel Overrun Senses Deceleration to Open Brakes," Design News, November 1, 1957, pp. 32-33.

93. "Flywheel Inertia Controls Brake Pressure in Anti-Skid System," Design News, November 9, 1959, p. 15.

94. Neu, H.J. and Helling, J., "Brake Force Control for a Light Truck," Automobiltechnische Zeitschrift, Vol. 71, No. 3, 1969, pp. 71-76.

95. Neu, H.J., "Electronic Brake Force Modulation of Motor Vehicles Equipped with Air Brakes," Automobiltechnische Zeitschrift, Vol. 72, No. 3, 1970, pp. 85-91.

96. Kelstop: The Kelsey-Hayes Anti-Wheel Lock Braking System, Kelsey-Hayes Company, Romulus, Michigan.

97. "New Regulator Equalizes Braking Action," Automotive World, Vol. 33, May 1968, p. 43.

98. Limpert, W.D. and Leiber, H., "A New Method for Prevention of Wheel Locking on Motor Vehicles by Automatic Control of Tire Slip," Automobilismo e Automobilismo Industriale, Vol. 16, No. 2, March-April 1968, pp. 67-81.

99. Limpert, W.D. and Leiber, H., "The Electronic Brake Modulator," Automobiltechnische Zeitschrift , Vol. 71, No. 6, 1969, pp. 181-189.

100. Madison, R.H. and Riordan, H.E., "Evolution of Sure-Track Brake System," SAE Paper No. 690213, January 1969.

101. Harned, J.L. and Johnston, L.E., "Anti-Lock Brakes," Automotive Safety Seminar, Paper No. 21, General Motors Corporation, 1968.

102. Horne, W.B., "Skidding Accidents on Runways and Highways Can Be Reduced," Astronautics and Aeronautics, Vol. 5, No. 8, August 1967, pp. 48-55.

103. Haviland, G.S., "Automatic Brake Control for Trucks—What Good Is It?" SAE Paper No. 680591, September 1968.

104. Falkevich, B.S. and Yudakow, B.F., "Investigation of the Handling of a Vehicle with Anti-Locking Device During Braking in a Turn," Avtomobil'naya Promyshlennost', No. 5, May 1968, pp. 22-24.

105. "Anti-Skid Device Controlled by Suspension Movement," Engineering, February 7, 1964, p. 216.

106. "Vacuum Servo Reverses Action to Correct Wheel Skid," Design News, Vol. 21, March 20, 1968, pp. 28-29.

107. "Anti-Skid Device," Automobile Engineer, July 1958, pp. 248-254.

108. "Anti-Skid Systems," Aircraft Engineering, January 1968, p. 14.

109. "Commercial Vehicle Braking: State of the Art," Automobile Design Engineering, November 1968, pp. 44-52.

110. Puleo, G., "Automatic Brake Proportioning Devices," SAE Paper No. 700375, May 1970.

111. Latvala, B.F. and Morse, R.J., "Adaptive Anti-Lock Braking—A Reality for Air-Braked Vehicles," SAE Paper No. 700112, January 1970.

112. Denholm, M.J., et al., "Make Trucks Stop Too," SAE Paper No. 700114, January 1970.

113. Fisher, D., "Brake System Component Dynamic Performance Measurement and Analysis," SAE Paper No. 700373, May 1970.

114. Phase II Report on the Study of Applicability of Anti-Skid and Load Proportioning Systems for Highway Vehicles, Contract No. FH-11-6859, prepared for the Federal Highway Administration by Booz-Allen Applied Research, Inc., July 1, 1969.

115. Hickner, G.B. and Howard, D.W., "Analog Simulation as a Design Tool for Advanced Braking Concepts," SAE Paper No. 700157, January 1970.

116. Schaefer, T.C., et al., "Design and Performance Considerations for a Passenger Car Anti-Skid System," SAE Paper No. 680458, 1968.

117. Gredeskul, A.B., "An Experimental Investigation of the Locking of a Braked Wheel," Avtomobil'naya Promyshlennost', No. 3, 1965.

118. Orzhevski, I.S., "On the Analysis of the Operation of an Anti-Locking Device," Avtomobil'naya Promyshlennost', No. 10, 1966.

119. Balkin, V.D. and Petrov, M.A., "An Analytical Investigation of Wheel Braking with an Anti-Locking Device in the Braking System," Avtomobil'naya Promyshlennost', No. 11, 1965.

120. "Anti-Skid Device for Commercial Vehicles (Anti-Lock)," Engineer, Vol. 224, July 14, 1967, p. 53.

121. Lomaka, S.I., "An Experimental Investigation of Anti-Locking Devices for the Vehicle Braking Process," Avtomobil'naya Promyshlennost', No. 12, 1963.

122. Fancher, P.S., Ervin, R.D., Grote, P., MacAdam, C.C., and Segel, L., Limit Handling Performance as Influenced by Degradation of Steering and Suspension Systems, Final Report, (Vol. 1 & 2), Prepared for National Highway Traffic Safety Administration, U.S. Dept. of Transportation, Contract DOT-HS-031-1-126, November 1972.

123. Tcheng, Y. and Majcherczyk, R., "Measurement of the Tire Adherence to the Pavement and Skid Resistance Qualities," Second International Conference on Vehicle Mechanics, Paris, France, 1971.

APPENDIX B

DESIGN OF THE SURFACE FRICTION DYNAMOMETER AND PROCEDURES FOR ITS USE

The following discussion of Surface Friction Dynamometer (SFD) operation is organized into three sections. A general description of the SFD and its major components is given in Section B.1. Section B.2 is concerned with general operating details, some of which may even be classified more accurately as maintenance but are nonetheless covered here. Section B.3 regards operation of the SFD in the immediate tire testing environment.

B.1 GENERAL DESCRIPTION

For purposes of detailed consideration, the SFD is conveniently broken down into several subsystems.

1) Mechanical system
2) Pneumatic system
3) Brake system
4) Hydraulic system
5) Instrumentation system

Each of these systems is discussed in the following sections.

B.1.1 MECHANICAL SYSTEM. The mechanical system is designed to (1) locate the test wheel, (2) react test wheel forces and transmit them to the vehicle frame, and (3) facilitate mounting of various components of the remaining systems.

A sketch of the static member of the mechanical system appears in Figure B.1. The basic frame of this member is a horizontal, U-shaped section constructed of steel channel. This structure is bolted to the base vehicle frame via the shimming blocks and mounting flanges. At the rear of this

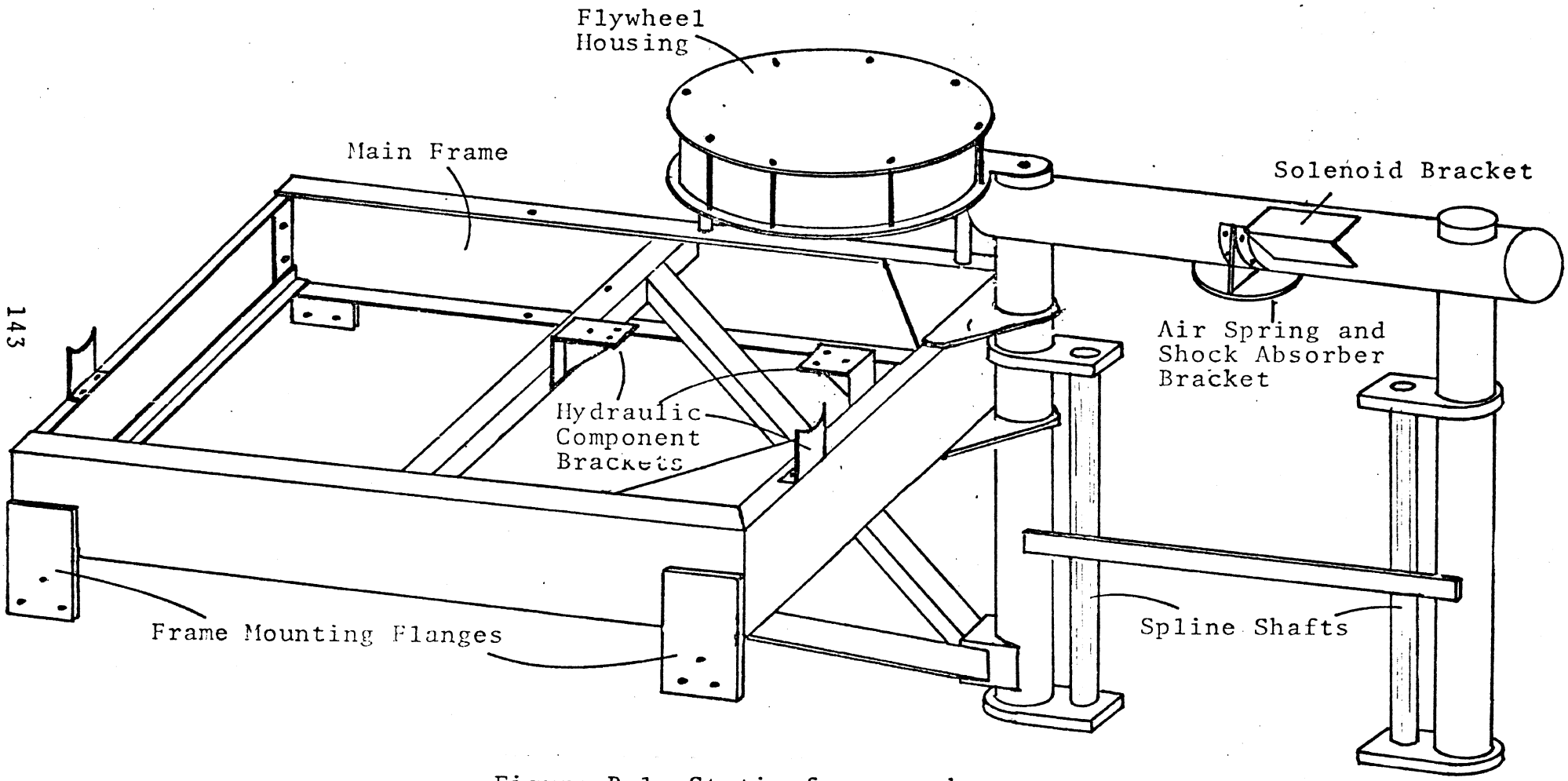

Figure B.1 Static frame member.

frame is mounted an inverted U-shaped structure incorporating three sections of steel pipe and braced by several sections of square steel tubing. A vertical ball spline shaft is mounted to each of the vertical pipe members via mounting flanges. The flywheel housing is mounted above the basic frame. Virtually all remaining SFD components located in the truck bed area (with the exception of the pneumatic system reservoir) mount directly to this frame structure. This results in a modularized system which may readily be transferred to a new base vehicle when desired.

The test wheel carriage (WC), the second major component of the mechanical system, appears in Figure B.2. The WC is situated within the U of the pipe structure and is located by the ball spline shafts. The WC is basically a welded aluminum box structure to which are bolted four aluminum pillow blocks. These pillow blocks each retain a ball spline outer race assembly through which the ball spline shafts pass. The upper surface of the WC provides a mounting surface for the air spring. While the upper half of the WC is fully enclosed, the lower half is open on one side (reference Figure B.3). Thus a cavity is provided in which the biaxial load cell is mounted. The load cell is bolted to a machined surface on the rear face of the WC. Coaxial with the load cell, on the opposite side of the rear face, is mounted the test wheel hydraulic pump via the pump bracket. Additional brackets for shock absorber and lifting cylinder are located on the WC as are protective housings for the ball spline assemblies.

The test wheel spindle assembly is mounted to the face of the biaxial load cell. This structure is a modified left-front 1974 Oldsmobile Toronado spindle assembly. It includes a single cylinder, floating caliper disc brake.

Located within the hollow center of the load cell is a double universal joint assembly which couples the test wheel hydraulic pump to the wheel spindle drive shaft.

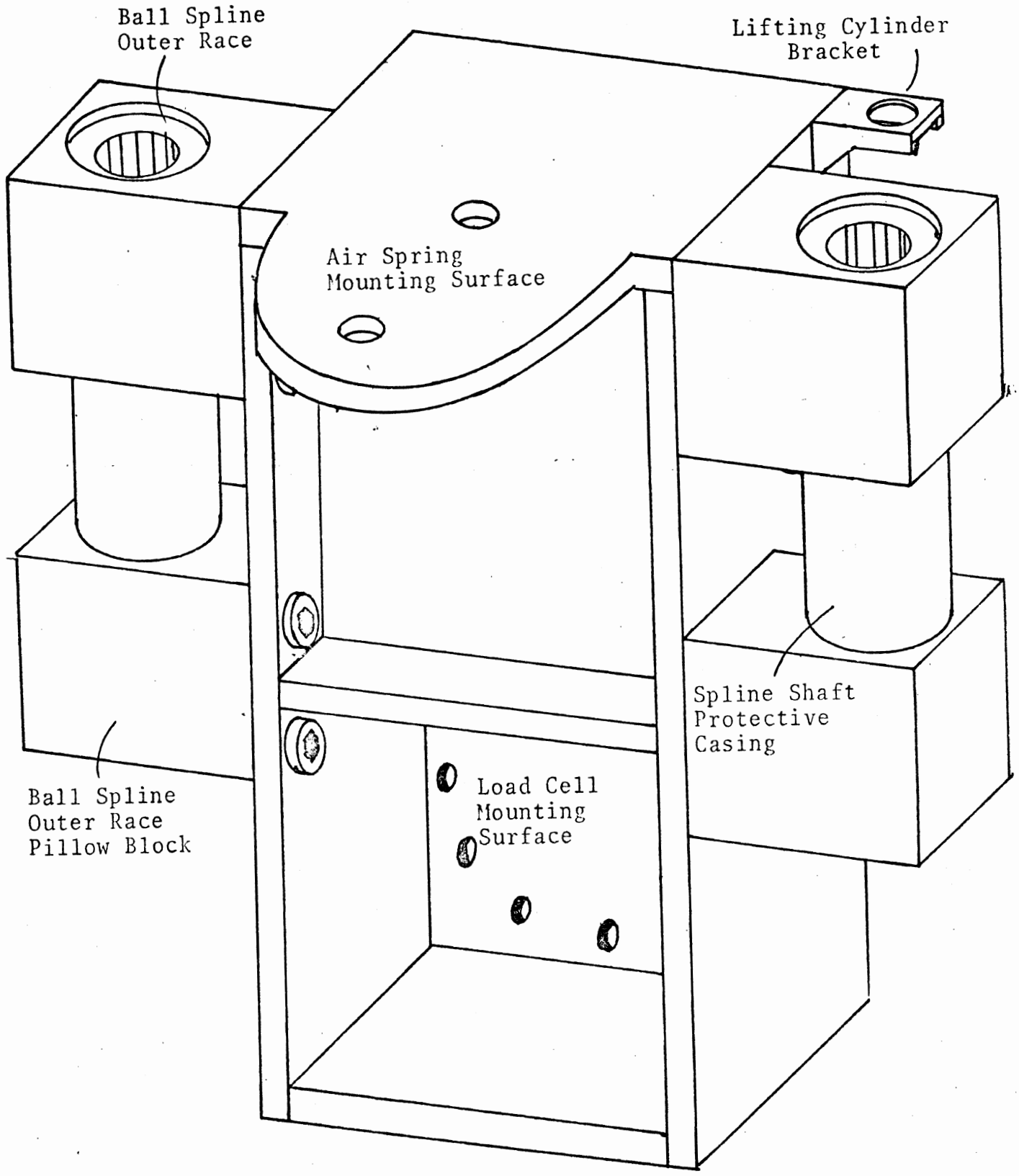

Figure B.2 Test wheel carriage.

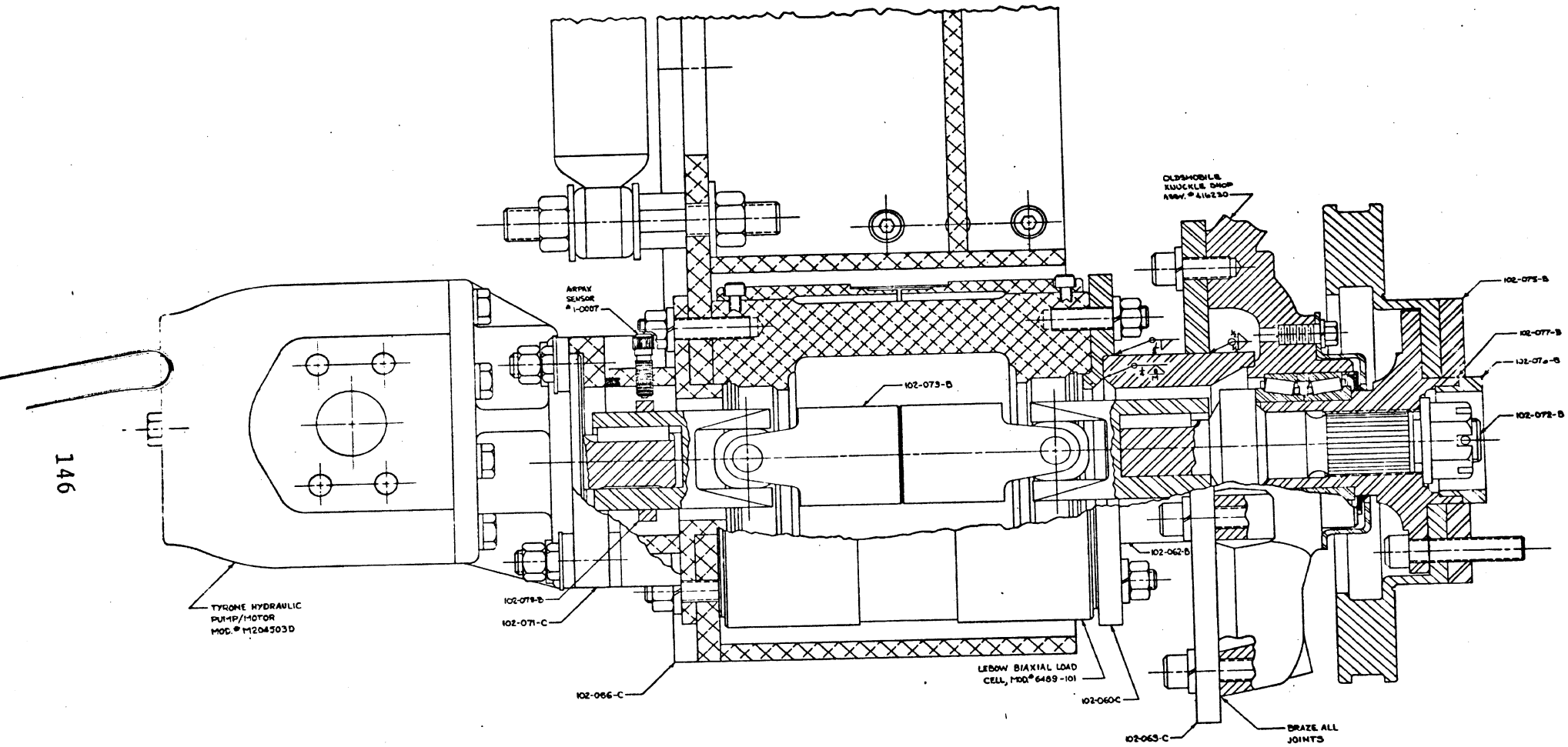

Figure B.3. Test wheel area assembly drawing.

B.1.2 PNEUMATIC SYSTEM. A schematic diagram of the pneumatic system appears in Figure B.4. The pneumatic system performs a number of functions, namely:

1) Provides vertical test wheel loading and control.
2) Provides for lifting of the test wheel.
3) Powers and controls the test wheel brake system.
4) Powers the hydraulic system charging pump.
5) Provides compressed air for test wheel inflation pressure maintenance.

The pneumatic system is powered by an engine-mounted air compressor which charges two, 13-gallon storage tanks. System controls are located in the cab, as was shown in Figure 14.

Test wheel vertical loading is accomplished by a low rate air spring which bears on the WC. Vertical load is controlled by regulating air pressure to the spring. A precision regulator located in the truck cab provides this function. Input and exhaust control of the spring is provided by a three-way solenoid valve which may be remotely controlled from the cab or manually controlled at the test wheel area. Use of an air spring loading system provides a relatively low rate vertical coupling between the vehicle and the test wheel. Such a coupling is desirable for attenuating the tire load fluctuations which derive from the vertical displacement oscillations of both the test wheel and the base pickup truck vehicle.

The test wheel may be lifted from the roadway via the action of an air cylinder acting on the WC. This cylinder is also controlled remotely from the cab or manually at the test wheel area by a solenoid valve. A limit switch which senses the fully extended position of the lifting cylinder disables the air spring solenoid whenever the cylinder is not extended, thus preventing conflict in remote cylinder and air spring commands.

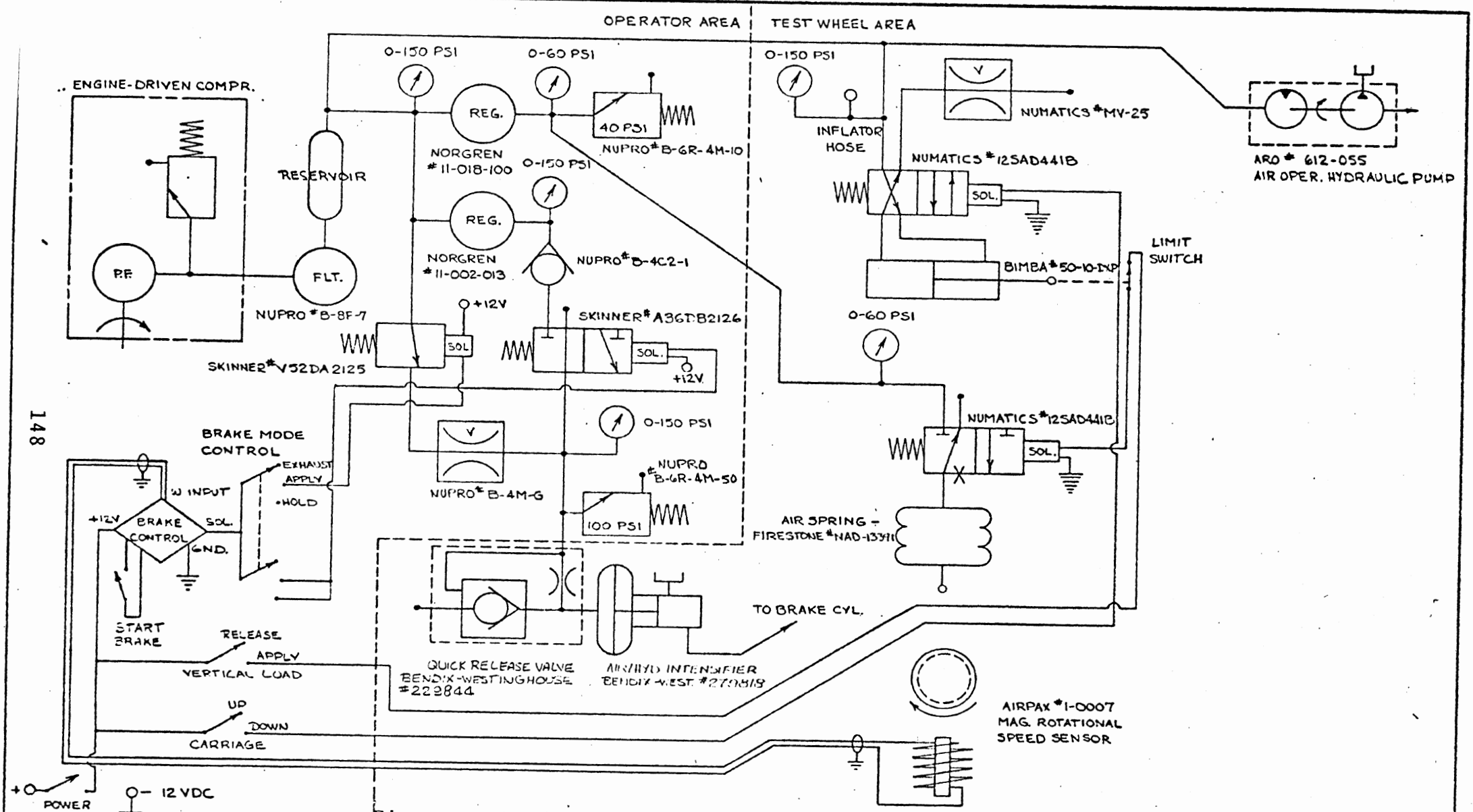

Figure B.4 Schematic diagram: The pneumatic system

The test wheel brake system is powered and controlled by the pneumatic system. The hydraulic test wheel brake system is pressurized by an air/hydraulic pressure intensifier with an area ratio of 20:1. Input air to this intensifier is supplied by the pneumatic system. The design of the pneumatic system provides for the development of brake system fluid pressure by way of a step-fronted-ramp time history. (See Figure B.5.) This function is employed because it allows a relatively small time rate of change of system pressure during the period of test wheel lockup without requiring an excessively long brake application period. Thereby, a minimum over-torque of the test wheel brake is insured, enhancing the "delayed spin-down" feature of the flywheel-coupled test wheel. The height of the initial step is determined by a brake pressure regulator setting; the slope of the ramp by a throttle valve setting. (Both control devices are mounted on the control panel in the truck cab.)

There are three modes of operation of the brake-associate portion of the pneumatic system; exhaust, apply, and hold. In the exhaust mode, the intensifier is vented to the atmosphere through a quick-release valve. In the apply mode, intensifier air chamber pressure is controlled according to the step-fronted ramp function. The hold mode maintains intensifier pressure constant at its value at the time when the hold mode was selected. Mode selection is controlled by a switch in the cab. An additional feature of the brake system mode control is the test wheel "antilock" system. A magnetic pick-up is installed in the test wheel pump bracket and observes the rotational motion of the universal joint by sensing the passage of teeth of a gear mounted on the joint. (See Figure B.3.) The output of the pick-up is fed to an electronic circuit which behaves as a latching switch. When a test wheel velocity of less than 2 mph is sensed, the switch is thrown

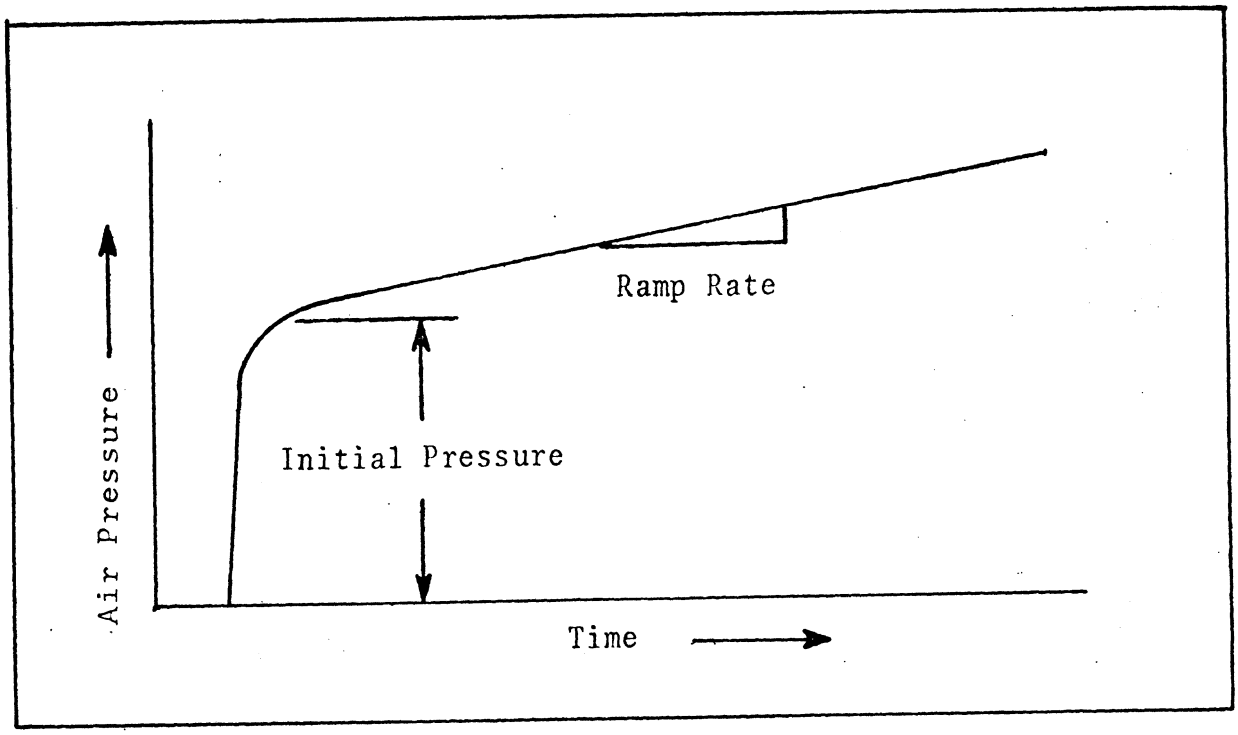

Figure B.5. Step fronted ramp function.

and locked, causing the brake system to be in exhaust mode regardless of operator selected mode. A push-button (labeled "Start") is provided on the control panel in the cab which unlatches and/or overrides this circuit. The presence of this "antilock" feature prevents excessive wear and flat spotting of the test tire.

The hydraulic system which is associated with flywheel/test wheel coupling requires a charging pump whose function is to replenish the hydraulic fluid lost through pump leakage. A pneumatic-powered hydraulic pump is provided for this function.

A high pressure air output line is provided in the test wheel area for the maintenance of test tire inflation pressure, and as a junction for coupling the pneumatic system to an external compressed air source.

B.1.3 THE BRAKE SYSTEM. The brake system, shown schematically in Figure B.6, is a hydraulic system whose input device is the aforementioned air/hydraulic intensifier and whose output device is the test wheel disc brake caliper. The air/hydraulic intensifier is primarily designed for use in air-over-hydraulic truck braking systems. As such, in normal use it is expected to displace a considerably larger volume of fluid than that required for operation of the single passenger car brake caliper of the SFD. Certain design details of the intensifier would result in excessive wear of the master cylinder piston seal if the fluid displacement were limited to the small amount deriving from test wheel brake application. Consequently, a dummy caliper, plumbed in parallel to the brake caliper, has been provided. This caliper has been modified with a stroke limiter and return spring. It functions as a capacitor in the brake system, and increases the displacement of the intensifier appropriately.

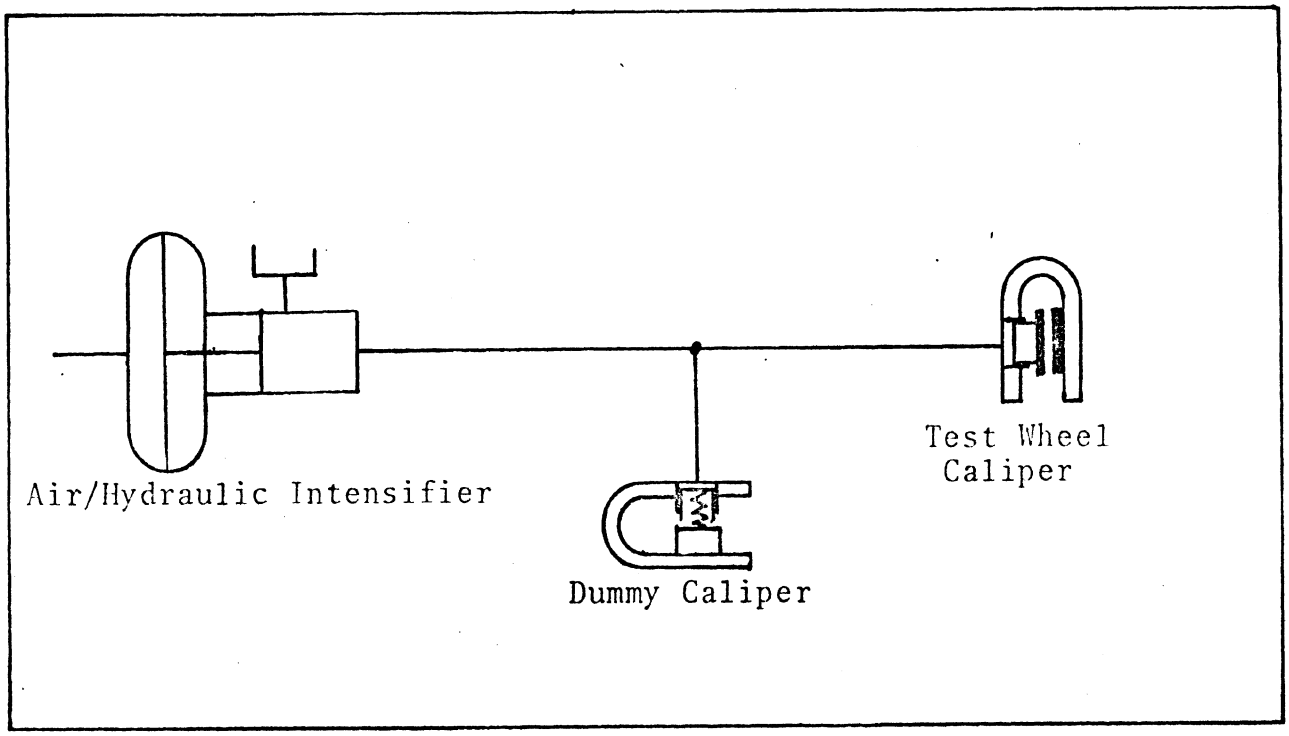

Figure B.6. Schematic diagram: The brake system.

B.1.4 THE HYDRAULIC SYSTEM. A schematic diagram of the hydraulic system appears in Figure B.7. The basic function of the system is to serve as a hydrostatic transmission coupling the rotational degree of freedom of the test wheel and flywheel. The main hydraulic circuit, composed of test wheel- and flywheel-driven pumps plumbed in a "loop," serves this purpose. The remaining hydraulic system components are auxiliary to this purpose.

The maximum design pressure of the hydraulic circuit is 3000 psi. To insure that this pressure is not exceeded, two relief valves set at 2900 psi are provided, one each in the lines connecting the pumps.

The additional inertia provided by the flywheel greatly increases the response time of the test wheel lock-up cycle. Nonetheless, due to the relief valve function, test wheel lock-up may occur while substantial kinetic energy remains in the flywheel. If lock-up is sustained (by overriding the brake system antilock circuit), as is sometimes the case, this kinetic energy is absorbed by heating of the hydraulic fluid. Consequently, the output of the relief valves is input to a "heat tank." This tank serves as both a thermal capacitor, by providing a relatively large volume of hydraulic fluid, and as a convective heat transfer device to expel heat to the atmosphere.

The output of the heat tank returns fluid to the main hydraulic system via a pair of check valves. This output line also serves as a portion of the replenishing circuit which replaces fluid lost from the main circuit due to pump leakage. To complete the replenishing circuit, the heat tank is also serviced by the pneumatic-powered replenishing pump which provides fluid from the system reservoir at a pressure equal to existing pneumatic system reservoir pressure.

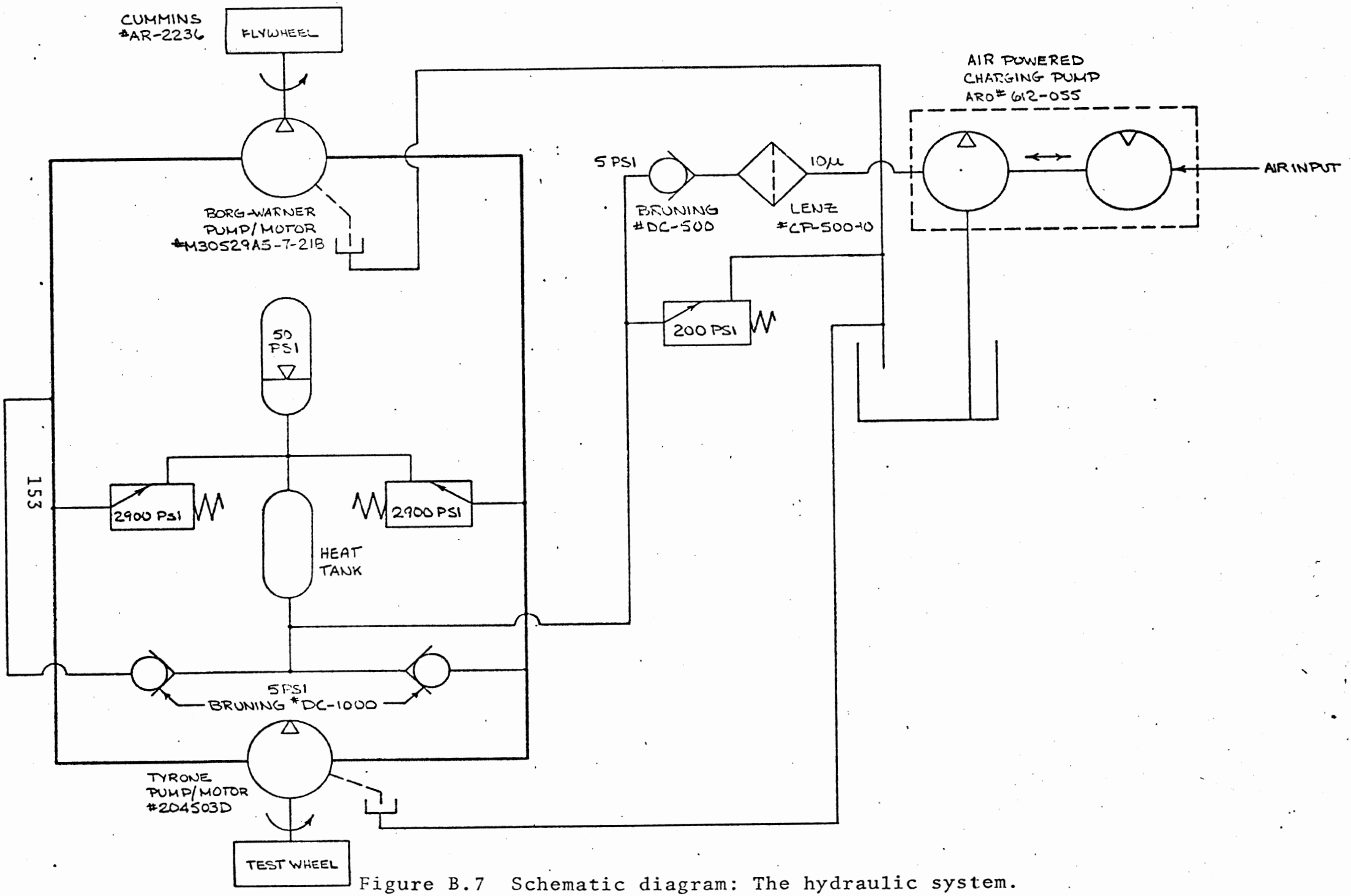

Figure B.7 Schematic diagram: The hydraulic system.

The heat tank is also fitted with a one-quart accumulator to absorb surges in the system, and with a large volume safety relief valve. This valve is set to 200 psi and returns fluid to the system reservoir.

B.1.5 INSTRUMENTATION SYSTEM. In addition to the electronics associated with the test wheel antilock system, electronic instrumentation provides analog signals of F_x, F_z, F_x/F_z and V. Although normal operation calls for continuous recording of F_x/F_z, F_z and V by ink pen recorder, F_x/F_z may readily be replaced by F_x. Vehicle velocity is also displayed digitally to the driver. A galvomometer displayed to the operator provides for the monitoring of test wheel brake temperature. Scematic diagrams of the instrumentation system appear in Figures B.8 and B.9.

Transducers for the system are (1) the biaxial load cell, (2) a fifth wheel-mounted, d.c. tachometer generator, and (3) a iron-canstantan thermocouple.

Two strain gauge bridge conditioning devices provide power, signal amplification and calibration shunt resistor switching services for their respective load cell channels. An encapsulated analog multiplier/divider circuit provides the F_x/F_z computation. Various passive networks are employed to filter analog signals being recorded.

Several binding post pairs are provided on the control panel for signal monitoring and external recorder input. Four switches are provided for internal signal routing and various system calibration requirements.

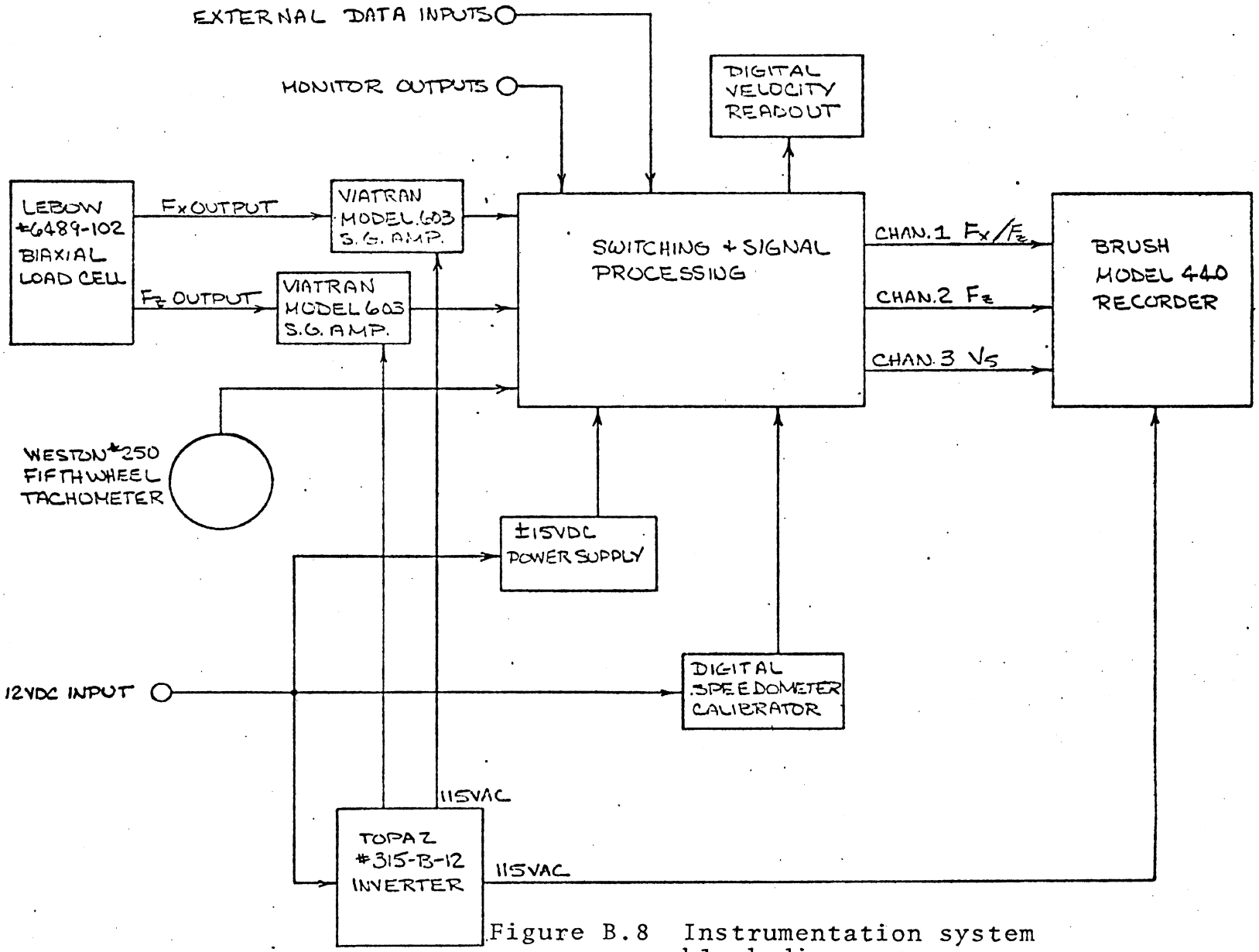

Figure B.8 Instrumentation system block diagram

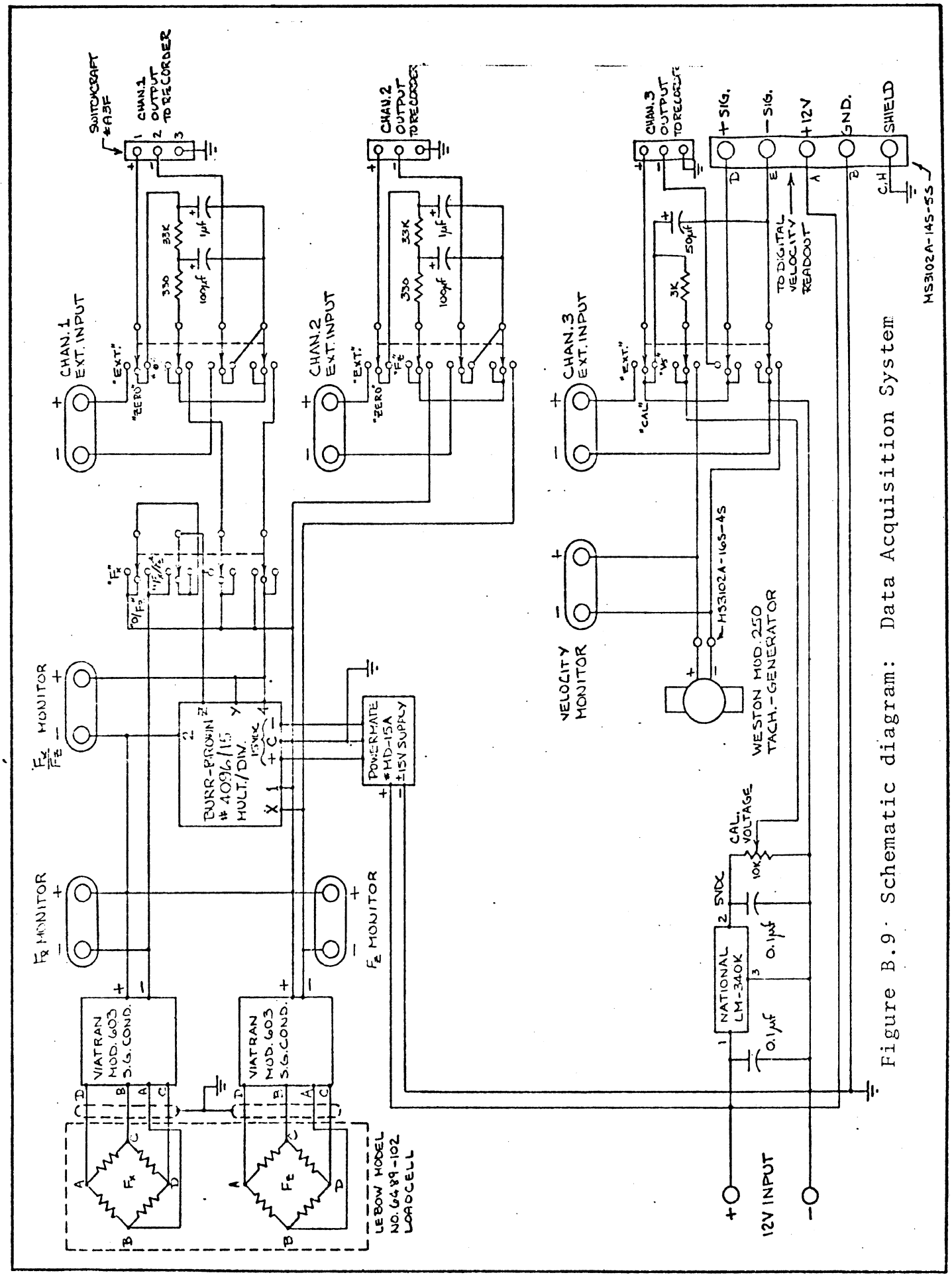

Figure B.9 Schematic diagram: Data Acquisition System

B.2 SFD: GENERAL OPERATING INFORMATION

Each of the five major systems of the SFD (mechanical, pneumatic, brake, hydraulic, and electrical) demands some attention with regard to maintenance or general operation. Each is addressed separately.

B.2.2 MECHANICAL SYSTEM. The mechanical system is composed mostly of structural members and thus requires little attention. Of most concern is the maintenance of the ball bearing spline assemblies. Periodically they should be checked with regard to:

1) Integrity of their isolation or sealing mechanisms; i.e., the condition of the four bellows and the various areas of rubber sealant material.

2) Lubrication of both the inner and outer ball spline races.

Note that if disassembly of the ball spline is ever warranted, the individual ball bearings are not retained by the outer race upon removal of the inner race (i.e., the spline shaft). As the inner race is removed, a dummy race, such as a cardboard cylinder, should be simultaneously installed.

The only other point of maintenance in the mechanical system is the flywheel support bearing which should receive periodic lubrication. To obtain access to this bearing:

1) remove flywheel housing cover

2) remove two bolts attaching flywheel to flywheel hub and replace with eyebolts of similar thread

3) using eyebolts, lift flywheel from housing

4) flywheel bearing is now exposed.

B.2.2 PNEUMATIC SYSTEM. The power source for the pneumatic system is an engine-mounted air compressor (nominally, a truck air brake system compressor). In normal operation, the compressor is controlled by a governor located on the right fender inside the engine compartment. The governor is set to maintain reservoir air pressure between 110 and 140 psi. Mounted on the head of the compressor is a mechanical governor override consisting simply of a bracket, bolt and locking wing nut. By tightening the bolt, the compressor valve control lever may be depressed, thus causing the compressor to idle regardless of reservoir pressure. This is most convenient when transporting the SFD as a normal highway vehicle. Whenever compressed air supply is required, the override bolt would be backed off sufficiently to allow clearance between it and the valve control arm.

To insure adequate air supply at all times during operation, a rather large reservoir volume (26 gallons) is provided. A substantial time period (10 to 15 minutes) may be required for the system compressor to charge this reservoir. To avoid this delay and to allow system operation without operating the truck motor, the system may be linked to an independent air supply of less than 140 psi via the flexible air line located at the test wheel area.

Normal operation of the pneumatic system may result in the accumulation of considerable condensation in the air reservoir. The tanks are arranged serially relative to the compressor such that most condensation occurs in the passenger side tank. The water valve located on the bottom of this tank should be used daily to drain this condensation. Tanks should be under pressure during this procedure to facilitate flushing. Occasionally, the plug in the driver side tank should be removed to check for water. This plug should not be removed while the tank is pressurized.

In addition to the pneumatic system control functions available in the cab of the vehicle, the air spring and lift cylinder solenoid valves may be operated manually from the test wheel area. The button protruding from the solenoid coils activates the valves. Actuation of the cylinder valve lowers the test wheel, actuation of the air spring valve pressurizes the air spring.

The pneumatic system is equipped with three overload relief valves. One, located on the reservoir, relieves the entire system at 150 psi in case of governor failure. The other two are located in the instrumentation cabinet. One is set at 40 psi and prevents overload of the test wheel load cell by limiting air spring pressure. The other prevents over-pressurizing the hydraulic brake system by limiting air/hydraulic intensifier input pressure to 100 psi.

B.2.3 THE BRAKE SYSTEM. Periodic maintenance of the brake system should include:

1) Maintenance of adequate fluid in the system reservoir, located on the air/hydraulic pressure intensifier.

2) Periodic bleeding and/or flushing of the brake system fluid lines.

3) Periodic replacement of disc brake pads.

Bleeding of the brake lines is accomplished in the same manner as for any automotive brake system, except that the master cylinder is stroked by using the pneumatic system. Both the test wheel brake caliper and the dummy caliper should be bled.

Disc brake pads should be replaced by those for a 1974 Oldsmobile Toronado front brake.

B.2.4 THE HYDRAULIC SYSTEM. Hydraulic system operation is virtually automatic. The system requires attention only in terms of maintenance.

Fluid level in the system reservoir should be maintained to the level of the sight glass provided.

The system should be bled periodically. Two open-ended valves, one on the forward end of the heat tank, and one on the passenger side forward end of the piping network, are provided for this purpose. When bleeding, the pneumatic system should be pressurized and the front end of the entire vehicle lifted such that the bleed points are at high points of the fluid system.

In the event that a large fluid volume is lost from the hydraulic system such that major air contamination of the main system loop occurs, the system should be charged with an independent hydraulic fluid source with a delivery capacity of roughly 5 gpm. The source should be connected to the quick-disconnect fitting located at the rear of the test wheel pump. A return line to the source should be provided via the bleed valve on the piping network. With the flywheel motor restrained from rotating and the test wheel motor free to rotate, fluid should be pumped into the system for several minutes, thus purging the test wheel motor. This procedure should be repeated with the test wheel motor constrained and the flywheel motor free to rotate. During this activity, hydraulic fluid will be delivered to the system reservoir via the pump drain lines. Reservoir fluid level is maintained during this procedure by operation of the charging pump and the heat tank bleed valve.

The hydraulic system fluid is cleansed via the filter at the charging pump exit. The filter should be periodically inspected and replaced when necessary.

The accumulator located on the heat tank should be nitrogen-precharged to 50 psi. Proper precharge pressure should be checked periodically, with the pneumatic system pressure at zero, and with hydraulic system pressure relieved through opening of the heat tank bleed valve.

B.2.5 ELECTRICAL SYSTEM. The power source for the SFD electrical system is the 12-volt vehicle electrical system. The main fuse for the SFD system is located on the right front wheel fender inside the engine compartment. The main power switch is a large red palm button located on the control panel in the aft passenger area of the cab. The 12-volt vehicle power is used directly to operate the various air solenoid valves and control panel indicator lights. The 12-volt supply is converted to 110-volt, 60 cycle AC by an inverter located within the instrumentation cabinet. The AC supply powers the recorder and the strain gauge excitation units, as well as a ± 15-volt DC power supply which, in turn, feeds the F_x/F_z division circuitry. A voltage regulator, within the driver-display speedometer package, provides 5 v. DC for DVM power. An adjustable voltage regulator located in the instrumentation cabinet provides calibration voltage for the velocity data circuit.

All AC power is distributed via an AC plug strip located on the inside forward wall of the instrumentation cabinet. This strip may be conveniently plugged into any AC utility outlet, rather than the inverter, to avoid battery drain during a garage-site operation.

Several points of adjustment, not generally used in daily activity, but of interest here, are provided in the electrical system.

A velocity calibration adjustment is located inside the instrumentation cabinet on the aft side of a small chassis box mounted on the cabinet front panel. Adjustment of this trim pot varies the calibrator voltage available to the velocity measurement system.

A gain adjustment for the driver-display digital speedometer is located on the right side of the speedometer housing. This trim pot behaves as a voltage divider relative to the speedometer DVM input.

The test wheel "antilock" circuitry, located in a chassis box on the aft wall of the instrumentation cabinet, has two adjustment points. These are trim pot adjustments and may be accessed through holes on the chassis box cover. (Adjustment should be made with the cover in place to avoid the effects of extraneous noise.) As indicated on the cover, one adjustment is for signal sensitivity and one is for antilock trigger velocity adjustment.

Physical calibration of the instrumentation system transducers (load cell and fifth wheel) should be accomplished periodically.

An extensive physical calibration of the load cell was undertaken in March of 1974 to ascertain its gain, linearity, hysteresis and cross-talk effects. During calibration, all loads were applied in the test wheel plane to assure that moments deriving from the offset of this plane from the load cell face were accounted for. Data from the calibration are reviewed in Tables B-1 through B-6 and in Figures B.10 and B.11. The resulting load readings associated with the calibration resistors installed in the two strain gauge condition units appear in Table B-7.

Physical calibration of each load cell channel should be accomplished periodically, possibly prior to each major use of the device. Cross-channel calibration should be accomplished occasionally.

TABLE B-1

SFD LOAD CELL CALIBRATION: F_z CALIBRATION

Conditions of Load:

1) F_x = 0.0 lbs.
2) F_z applied through cell centerline

Calibration Shunt Resistor Readings, SFD Cell:

F_z Channel

Lebow Resistor Applied at Cell:	Reading	Shunt Terminals
	1514	B - D
	1508	C - D

HSRI Resistor Installed in F_z Viatran:	Reading	Calibration Switch Position
	1514	left
	1520	right

SFD Load Cell Readings	Calibration Load Cell Readings (lb)		
F_z	Cell #1	Cell #2	Avg.
0	0	0	0
246	237	239	238
359	350	348	349
409	399	400	400
515	497	501	499
623	605	605	605
718	695	696	696
805	776	778	777
918	888	891	890
1007	975	980	978
1100	1074	1075	1074
1220	1188	1188	1188
1310	1274	1275	1274
1411	1373	1374	1374
1510	1473	1474	1474
1600	1562	1562	1562
1720	1677	1677	1677
1840	1797	1797	1797
1900	1854	1857	1856
1995	1945	1949	1947
1895	1854	1856	1855
1800	1760	1760	1760
1700	1666	1666	1666
1600	1565	1567	1566
1490	1459	1461	1460

TABLE B-1 (Continued)

1382	1353	1356	1354
1310	1283	1287	1285
1165	1142	1146	1144
1090	1069	1073	1071
1002	981	990	986
870	853	861	857
800	785	791	788
720	707	714	710
590	581	590	586
472	467	473	470
400	397	406	402
330	330	338	334
09	01	08	04

TABLE B-2

SFD LOAD CELL CALIBRATION: F_z CALIBRATION AND F_x ZERO OFFSET RESULTING FROM F_z

Condition of Loading:

1) F_x = 0.0 lbs.
2) F_z = applied through cell centerline

Calibration Shunt Resistor Readings, SFD Cell:

F_z Channel

HSRI Resistor Installed in F_z Viatran:	Reading	Calibration Switch Position
	1514	left
	1520	right

F_x Channel

Lebow Resistor Applied at Cell:	Reading	Shunt Terminals
	1501	B - D
	1498	C - D

SFD Load Cell Readings		Calibration Load Cell Reading (lb)
F_x	F_z	F_z
0	0	0
2	270	261
5	542	524
7	816	789
11	1058	1024
15	1300	1258
20	1556	1509
25	1809	1755
28	1988	1930
25	1578	1531
20	1064	1030
16	608	590
14	370	359
10	0	0
22	1240	1205
29	1940	1885
16	362	351
10	0	0

TABLE B-3

SFD LOAD CALIBRATION: F_x CALIBRATION, BRAKE TORQUE AND F_z EFFECT ON F_x

Conditions of Load:

1) F_z = 0.0 lbs.
2) F_x = applied at approximately 11 inch moment arm from cell centerline

Calibration Shunt Resistor Readings, SFD Cell:

F_x Channel

Lebow Resistor Applied at Cell:	Reading	Shunt Terminals
	1501	C - D
	1498	B - D

HSRI Resistor Installed in F_x Viatran:	Reading	Calibration Switch Position
	1502	Left
	1499	Right

SFD Load Cell Readings	Calibration Load Cell Readings (lb)		
F_x	Cell #1	Cell #2	Avg.
0	0	0	0
-137	-134	132	133
-328	-323	321	322
-510	-500	499	500
-630	-625	620	622
-735	-724	721	722
-844	-833	830	832
-1035	-1019	1016	1018
-1134	-1122	-1115	1118
-1199	-1185	1180	1182
-1347	-1328	-1325	1326
-1459	-1442	1436	1439
-1590	-1569	1564	1566
-1689	-1671	1665	1668
-1729	-1707	1702	1704
-1785	-1764	1758	1761
-1444	-1421	1415	1418
-1269	-1244	1240	1242
-1094	-1070	1067	1068
-934	-908	907	908
-803	-781	777	779
-659	-636	635	636
-529	-511	507	509
-416	-398	396	397
-303	-290	289	290
-194	-183	181	182
+5	+9	-9	-9

TABLE B-4

SFD LOAD CELL CALIBRATION: F_x CALIBRATION, F_z EFFECT ON F_x

Condition of Load:

1) Nominally F_z = 925 lbs.

2) F_x = applied at approximately 11 inch moment arm from cell centerline

Calibration Shunt Resistor Readings, SFD Cell:

F_x Channel

Lebow Resistor Applied at Cell:	Reading	Shunt Terminals
	1501	C - D
	1498	B - D

SFD Load Cell Readings	Calibration Load Cell Readings (lb)	
F_x	F_x	F_z
0	0	925
-101	98	916
-193	188	918
-305	299	912
-412	406	915
-528	520	909
-657	648	908
-763	749	904
-897	883	919
-1031	1017	928
-1118	1100	926
-1281	1258	921
-1395	1376	918
-1522	1494	915
-1617	1592	917
-1704	1674	920*
-1715	1691	935
-6	0	0

*Brake Slips. Following data contaminated.

TABLE B-5

SFD LOAD CELL CALIBRATION: F_x CALIBRATION,
BRAKE TORQUE EFFECT ON F_x AND F_z ZERO OFFSET RESULTING FROM F_x

Conditions of Load:

1) F_z = 0.0 lbs.
2) F_x = applied at approximate 15 inch moment arm from cell centerline

Calibration Shunt Resistor Readings, SFD Cell:

F_x Channel

Lebow Resistor Applied at Cell:	Reading	Shunt Terminals
	1501	C - D
	1498	B - D

F_z Channel

HSRI Resistor Installed in F_z Viatran:	Reading	Calibration Switch Position
	1516	Left
	1518	Right

SFD Load Cell Readings		Calibration Load Cell Readings (lb)
F_x	F_z	F_x
0	0	0
-248	-5	243
-589	-6	581
-818	-7	806
-1063	-9	1042
-1301	-10	1280
-1550	0	1513*
-655	-2	622
-316	0	296
-9	6	2

*Brake Slips. Following data contaminated.

TABLE B-6

SFD LOAD CELL CALIBRATION: F_x CALIBRATION

BRAKE TORQUE EFFECT ON F_x AND F_z ZERO OFFSET RESULTING FROM F_x

Conditions of Load:

1) F_z = 0.0 lbs.
2) F_x = applied at approximately 11 inch moment arm from cell centerline

Calibration Shunt Resistor Readings, SFD Cell:

F_x Channel

Lebow Resistor Applied at Cell:	Reading	Shunt Terminals
	1501	C - D
	1498	B - D

F_z Channel

HSRI Resistor Installed in F_z Viatran:	Reading	Calibration Switch Position
	1516	Left
	1518	Right

SFD Load Cell Readings		Calibration Load Cell Readings (lb)
F_x	F_z	F_x
0	0	0
-218	-3	214
-464	-5	454
-773	-6	760
-976	-7	958
-1315	-10	1295
-1545	-11	1514
-1721	-9	1690
-856	0	820
-552	1	515
-193	2	169
-20	6	0

TABLE B-7

SHUNT CALIBRATION VALUES FOR THE SFD LOAD CELL*

Data Channel	Viatram Calibration Switch Position	Equivalent Load in Pounds
F_z	Left	-1473
F_z	Right	1479
F_x	Left	1478
F_x	Right	-1474

*Values in this table are for shunt resistors installed in Viatram units as determined in March, 1974.

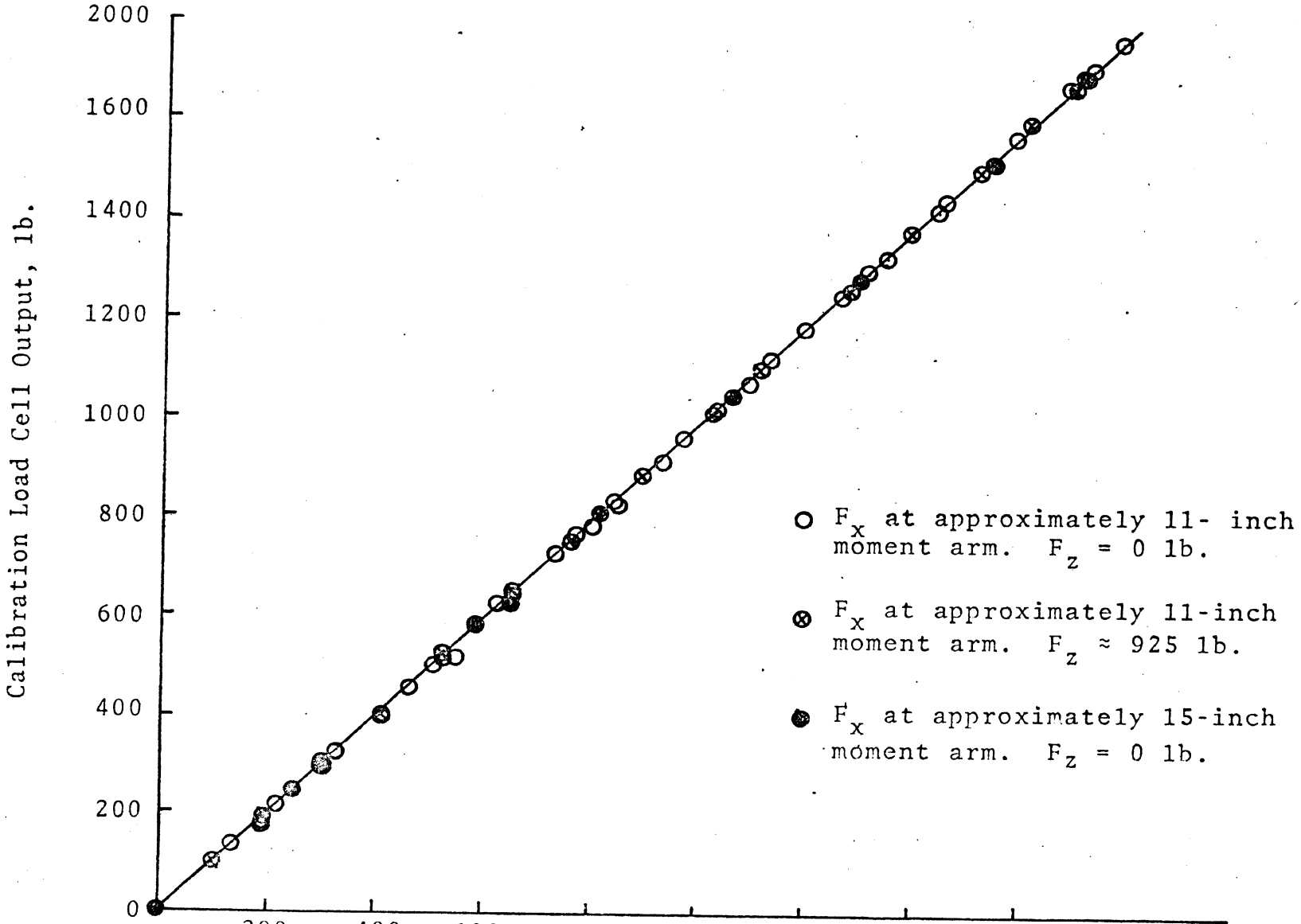

Figure B.10 Load cell calibration, F_x

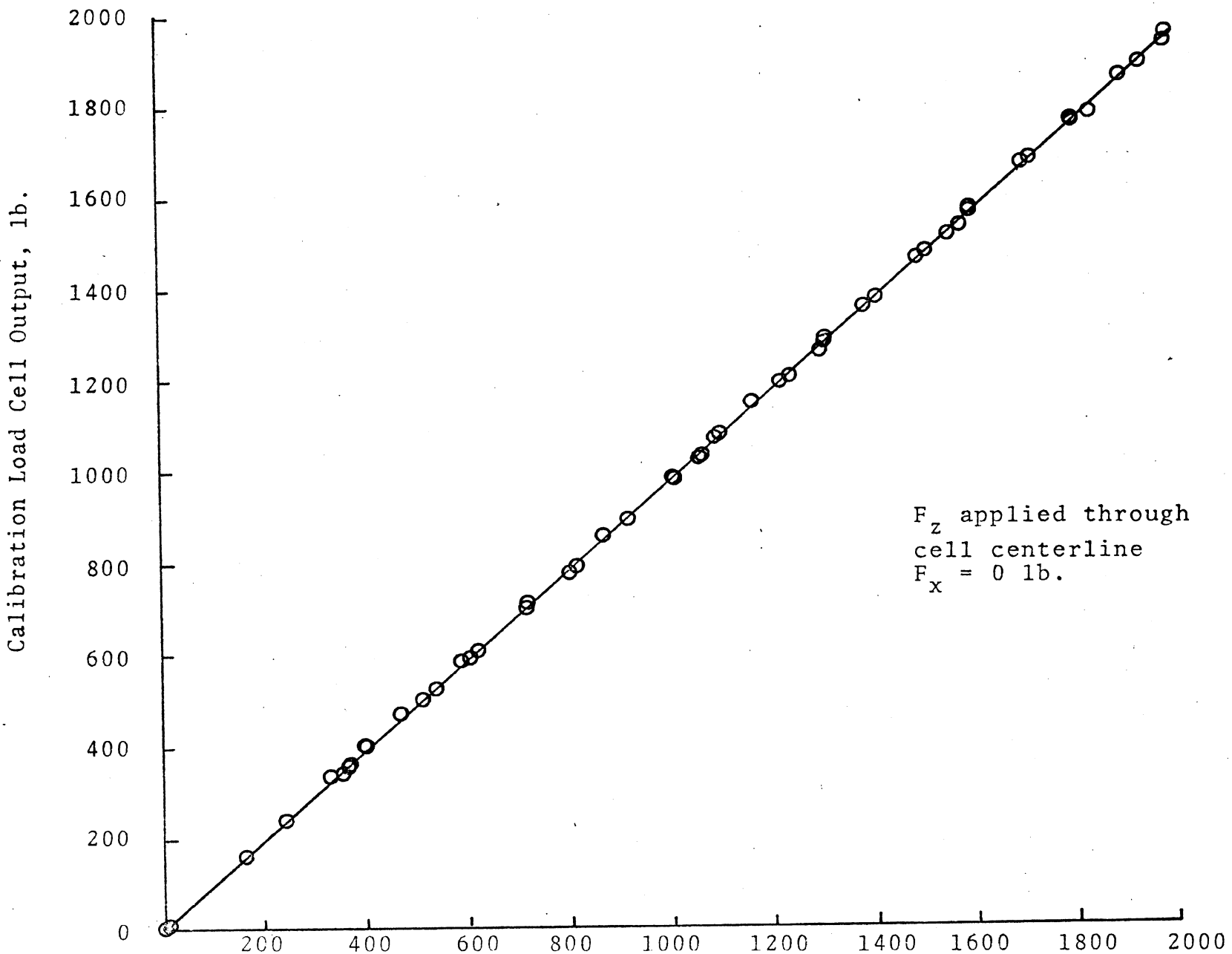

Figure B.11 Load cell calibration, F_z

Similarly, physical calibration of the fifth wheel velocity transducer should be done regularly, either by comparison with a similar device of assured accuracy or by a distance travel/time interval procedure.

The encapsulated divider circuit contained in the instrumentation system should occasionally be checked for linearity and consistency of gain. A calibration check of this device resulted in the data appearing in Figure B.12. The significant results of the calibration are the confirmation of the linearity of the device and of the consistency of its gain (10.05) over the range of denominator voltages commonly encountered in the conduct of the braking efficiency test technique (1.35 to 4.00 v; approximately equivalent to F_z readings of 500 to 1500 lbs.). The zero shift phenomenon, indicated by f(D) data does not damage the utility of the device, for it may be compensated for in the pretest instrumentation calibration procedure as outlined in Section B.3.2.

B.3 SFD TEST PROCEDURE OPERATING INSTRUCTIONS

The following paragraphs outline the procedure which should be followed in preparing for and performing peak longitudinal friction tire tests using the SFD. Particular attention should be paid to system calibration and brake application rate programming.

B.3.1 VEHICLE PREPARATION. Start the engine and turn on power to the instrumentation system. Turn on the power switches of the recorder and strain gauge conditioners. (To insure that the AC inverter is on, check the paper feed function of the recorder. If AC power is not present, turn on inverter from rear of instrumentation cabinet.) Charge the pneumatic system either by allowing sufficient time for

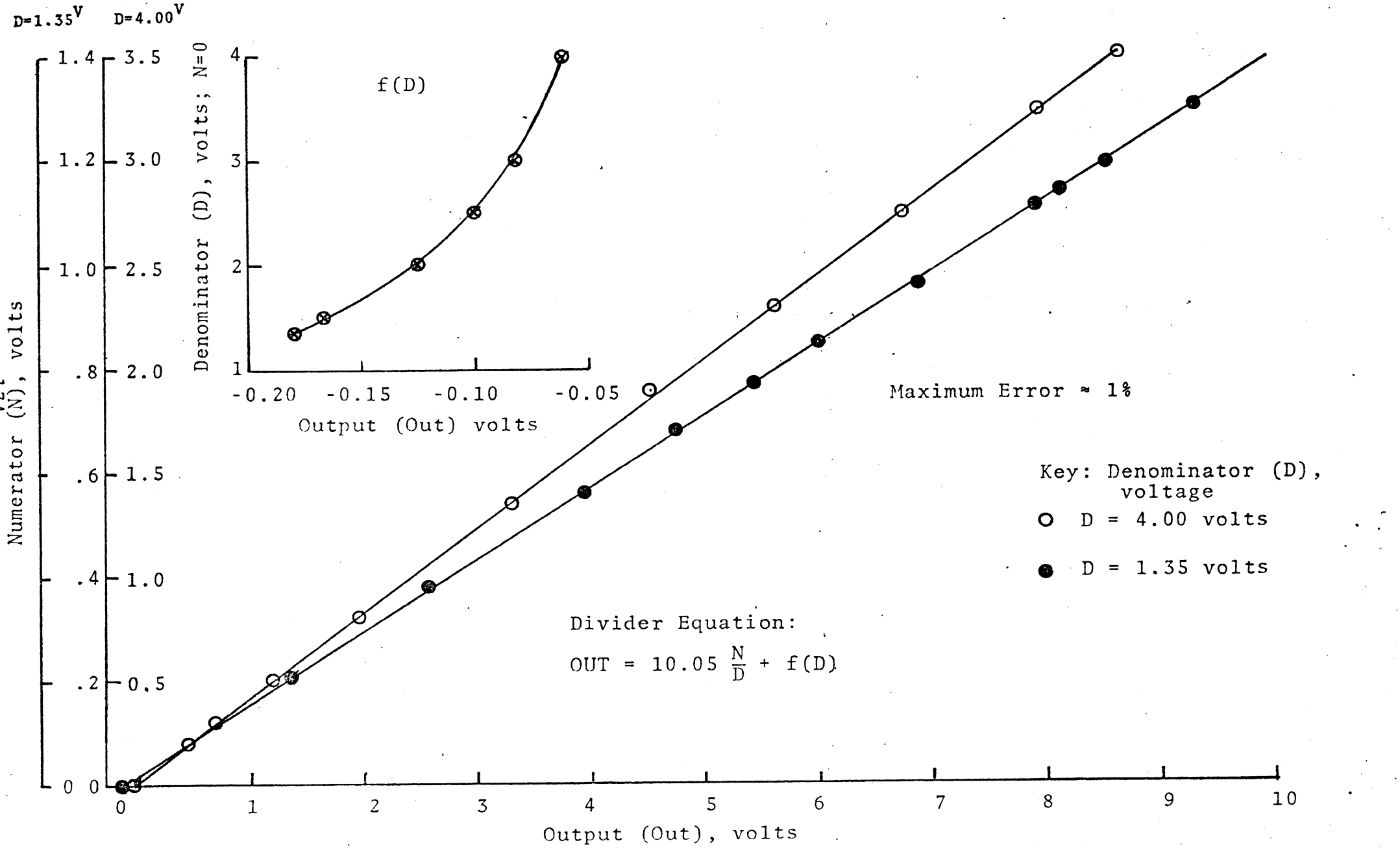

Figure B.12. Divider circuit calibration.

the engine-mounted compressor to fill the reservoir or by connecting a house pneumatic supply to the system via the air hose available at the test wheel area. Allow 15 minutes for instrumentation warm up.

A mechanical latch is provided at the extreme rear of the right-hand truck frame rail for support of the test wheel when the pneumatic system is not pressurized. When sufficient pressure is obtained for the lift cylinder to support the test wheel structure, release this latch so that the wheel may be lowered.

Lower the velocity fifth wheel (but never back vehicle with the fifth wheel down).

B.3.2 CALIBRATION PROCEDURE. Instrumentation calibration should be accomplished with the SFD parked and the instrumentation warmed up.

B.3.2.1 Velocity Calibration. Place the input control switch for channel 3 (located above the recorder) to "V_5." Using the channel 3 position control of the recorder, position the ink pen to zero (right-hand edge of the data grid). Check the fifth wheel driver-display speedometer for a zero reading. To apply the calibration voltage, place the channel 3 input control switch to "Cal." Using the gain and sensitivity adjustments of the recorder, obtain the indicated miles per hour corresponding to the calibration voltage. Lock the sensitivity and position controls in place. Check driver speedometer for a similar indicated velocity. If necessary, adjust speedometer with trim pot on right side of the speedometer case. Return the input control switch to "V_5." Note that fifth wheel voltage output level is such that the system may conveniently be calibrated such that milivolts/division scale on the gain selector may be interpreted as

miles per hour, full scale. For instance, with the selector at 50 milivolts/div., sensitivity may be adjusted such that full-scale deflection corresponds to 50 mph. With sensitivity so adjusted, system gain is easily and accurately switched to other settings such as 100 or 20 mph full scale with the gain selector.

B.3.2.2 Vertical Load (F_z) Calibration. Lift the test wheel out of contact with the ground to insure a true zero value of F_z. (Place the carriage control switch to "UP.") Place the input selector switch for channel 2 in the "Zero" position. Using the channel 2 position adjustment on the recorder, position the pen in the zero position (right edge of the data grid). Switch the input selector to "F_z." Using the zero adjustment on the F_z signal conditioning unit, adjust recorder pen to zero. (To increase accuracy of adjustment, place the channel 2 gain selector to a high sensitivity position.) With the gain selector at an appropriate position, and the sensitivity adjusted fully clockwise (that is, "x1"), place the calibration switch of the F_z conditioning unit to the right position and check for an output of approximately 4 volts on the recorder. If necessary, make adjustment with the conditioning unit "Span" adjuster. If span adjustment is needed, repeat zero adjustment of conditioning unit.

(The preceding adjustments of the F_z conditioning unit are necessary for proper voltage input to the divider circuit which calculates F_x/F_z. If F_x/F_z is not to be recorded, accurate zero adjustment is not critical.)

Set the channel 2 gain selector to 100 milivolts/volt. Assuming a full-scale value of 2000 lbs., place the F_z calibration switch to the right and, using the channel 2 sensitivity control, adjust for the proper F_z load reading (1479 lbs. as indicated by load cell calibration of March, 1974). The gain control selector may now be used to obtain the desired full-scale deflection, e.g., 50 milivolts/div. = 1000 lb. full scale.

B.3.2.3 Normalized Brake Force (F_x/F_z) Calibration. (Must be preceded by F_z calibration.) Lift the test wheel out of contact with the ground. Place the input selector switches for channel 1 to the "Zero" position (i.e., right-hand switch to "Zero," left-hand switch in any position). Position the pen to the zero position (right edge of data grid). Switch the input selectors to F_x (i.e., right-hand side switch to "•", left-hand switch to F_x). Using the zero adjust on the F_x signal conditioning unit, adjust recorder pen to zero. (To improve the accuracy of this adjustment, select a high sensitive gain position.) With the gain selector at an appropriate position and the sensitivity adjustment fully clockwise, place the calibration switch of the F_x conditioning unit to the left. Check for an output of approximately three volts on the recorder. If necessary, adjust the conditioner "Span." If span adjustment is necessary, repeat zero adjustment. Place the left-hand input selector switch to F_x/F_z and the gain selector switch to 100 milivolts/div. With the F_z calibration switch to the right, use the recorder position adjust to obtain a zero reading. With the F_z calibration switch to the right and the F_x calibration switch to the left, use the sensitivity adjustment to obtain the proper reading, assuming a full-scale value of 1. (As per load cell calibration of March , 1974, the proper F_x/F_z calibration reading was 1.00, i.e., F_x = 1478, F_z = 1479.) Lower test wheel onto surface and load wheel to desired vertical load by adjusting air spring pressure and observing F_z readout. Place left-hand input selector switch to "$0/F_z$" and adjust recorder pen to zero using the recorder position adjustment. Place the left-hand selector switch to F_x/F_z.

The gain selector switch is now an indicator of the full-scale F_x/F_z reading. For example:

50 milivolts/div → F_x/F_z = .5 at full scale

100 milivolts/div → F_x/F_z = 1.0 at full scale

200 milivolts/div → F_x/F_z = 2.0 at full scale

In the preceding procedure, zero and span adjustments of the F_x conditioning unit assure proper voltage input to the divider circuit. The following adjustments of position and sensitivity provide for proper system gain. The final adustment of pen zero position nulls the zero offset of the divider circuit, as explained in Section B.1.5.

The final zero position adjustment must be repeated whenever tire vertical load changes are made.

B.3.2.4 Brake Force (F_x) Calibration. Lift the test wheel out of contact with the ground. Place the right-hand input selector switch for channel 1 to "Zero" and adjust the pen position to read zero, i.e., the right edge of the data grid. With the recorder gain selector on an appropriate value, the sensitivity control fully clockwise, and the input selector switches to "F_x" (left-hand switch on "F_x", right-hand switch on "•"), use span and zero adjustments of the F_x conditioning unit to obtain a zero reading output of zero volts, and a calibration output of approximately three volts, as was described in Section 2.3. (When F_x rather than F_x/F_z is to be measured, this procedure is not as critical, but should be undertaken to insure reasonable use of the instrumentation capability.)

Set the channel 1 gain selector to 100 milivolts/volt. Use the pen position adjustment to obtain a zero reading. Assuming a full-scale deflection equal to 2000 lb., place the F_x calibration switch to the left and adjust recorder sensitivity to obtain the proper reading in pounds (1478 lb. as of cell calibration of March, 1974). Recheck zero pen position.

Channel 1 is now calibrated for recording F_x. The appropriate full-scale reading may be selected using the gain selector switch, e.g.,

100 milivolts/volt → F_x = 2000 lb. full scale

50 milivolts/volt → F_z = 1000 lb. full scale

B.3.3 AIR SYSTEM OPERATION. Control inputs for the air system are available on the upper portion of the instrumentation cabinet. These inputs are associated with test wheel carriage control, test wheel load control, and brake system control. The following sections deal with each topic, respectively.

B.3.3.1 Carriage Control. Position of the test wheel carriage can be controlled from the vehicle cab using the toggle switch marked "Carriage." This switch remotely controls a four-way air solenoid at the test wheel area which controls air to the lift cylinder. The "Up" position causes the test wheel to be raised from the surface while the "Down" position causes it to be lowered to the surface. (Note that the "Up" position corresponds to deactivation of the valve. Failure of electrical power to the valve therefore raises the wheel.)

The valve may also be controlled manually from the test wheel area, when the control switch is deactived (Up). To activate the valve and lower the wheel, depress the button protruding from the solenoid coil. Rotate the button to lock the valve in its activated condition.

B.3.3.2 Test Wheel Load Control. Vertical loading of the test tire may be controlled remotely from the cab area. Air spring pressure adjustment and readout plus a Release/Apply control switch are available within the "Load System" section of the control panel. To adjust vertical load, lower the

test wheel onto the surface and set load control switch to "Apply." While observing the F_z readout on the pen chart recorder, adjust air spring pressure to obtain the desired F_z.

Functionally, the air spring pressure adjust operates a precision air regulator whose output is input to a three-way solenoid valve. This valve is located at the test wheel area, but is remotely controlled by the Release/Apply switch. (This valve may also be controlled manually in the same manner as the carriage control solenoid.) The valve causes pressurization of the air spring in the "Apply," or activated, condition and exhausts the air spring in the "Release" position. The air spring pressure readout gauge indicates air pressure output of the pressure regulator.

An added feature of the load control system prevents remote activation of the air spring unless the wheel carriage is fully down. A limit switch mounted at the rear of the support structure interrupts the "Apply" command signal unless the lift cylinder is fully extended. Thus, the test tire load cannot be applied remotely unless the carriage is "Down." Furthermore, when the carriage is commanded "Up" the air spring will be exhausted regardless of whether a "Release" command is given.

B.3.3.3 Test Wheel Brake Control. The test wheel brake system of the SFD is an air-over-hydraulic brake system. Operator control of the system is attained through open-loop control of the air input to the air/hydraulic pressure intensifier. Additional control is obtained through the action of an electronic test wheel "antilock" system.

A general description of the pneumatic portion of the brake control system appeared in Section B.1.2. Operation of the brake system is very simple as a result of this control arrangement. After making proper adjustments of initial

pressure and application rate, the mode selection switch may be left on "Apply." Pressing the "Start" button begins each test cycle while action of the antilock system ends each test cycle.

The adjustments of "Initial Pressure" and "Application Rate" allow for the programming of the step-fronted ramp brake application. As indicated in Figure B.5, this function allows for a low value of $\frac{dP}{dt}$ at the time of the occurrence of peak F_x (a property advantageous to elongating peak F_x in time) without requiring an unreasonably long application time.

Experience indicates that initial pressures corresponding to 60-70% of the pressure required for lock-up and a rate setting resulting in lock-up occurring 2 1/2 to 3 seconds after starting the run results in "good" data traces.

A trial lock-up cycle, conducted in the "Hold" mode may assist in determining the proper initial pressure setting. With initial pressure adjusted low and the mode switch in "Hold," start a test cycle. Slowly increase brake pressure by increasing the initial pressure setting until wheel lock occurs. The initial pressure readout now indicates the required pressure for lock-up. Initial pressures may now be adjusted accordingly. (Brake temperature will affect lock-up pressure due to fade effects. An effort should be made to perform this test at a representative brake temperature.)

One or two additional trial tests should be sufficient to establish the appropriate "Application Rate" setting.

Functionally, the initial pressure setting controls an air regulator whose output is routed to the air/hydraulic pressure intensifier in the "Apply" and "Hold" modes. The application rate setting controls a precision needle valve, which bleeds additional air into the intensifier in the "Apply" mode.

As a final point, the antilock function can be overridden by maintaining activation of the "Start" button. By this method, it is possible to gather locked-wheel data with the SFD.

B.3.3.4 Performing a Tire Test. Tire testing may commence after preparing the SFD as described in earlier sections. A typical test procedure is described below.

Adjust the load control system for the desired vertical load with the vehicle parked. With the vehicle moving over the test surface, additional adjustment of the vertical load may be desired to compensate for (1) the unique character of the surface on which the vehicle was parked during static adjustments and (2) dynamic effects on load due to nonlinear shock absorber effects and air system dynamic effects.

Instruct the driver to attain the desired test speed. Test should be conducted at as constant a velocity as possible. The operating of the air/hydraulic braking system and the "squeal" of the test tire are quite audible from the SFD cab. These cues, plus the readout of the fifth wheel speedometer are available to assist the driver in his control task of maintaining velocity. Perfect maintenance of vehicle velocity at high speeds, high test tire loads, and on high friction surfaces is virtually impossible. (This problem is somewhat attenuated in the SFD compared to skid trailers due to the presence of only one test tire.) In such cases, the test cycle should commence at one or two mph above the desired speed.

It is desirable to lower the test tire onto the test surface while parked or at rather low speeds. This procedure lessens the work load placed on the hydraulic system and elongates test tire life. When a non-rotating test tire is lowered onto the surface at speed, the inertia of the flywheel is accelerated rapidly. This results in substantial

F_x generation at the tire-road interface and in maximum pressure in the hydraulic system over a sustained time period.

With test tire down, load adjusted, and proper test velocity established, a lock-up cycle is initiated by pressing the brake system "Start" button (mode control switch on "Apply".)

More than one lock-up cycle may be desired on a single pass over the test surface. If so, sufficient time for the flywheel to "spin up" should be allowed between cycles. During a lock-up cycle, the flywheel is decelerated somewhat. When the test brake is released, a brake force is required to spin up the test wheel and flywheel will, nonetheless, be evident for a short period of time, as shown in Figure B.13. The next lock-up cycle should not be initiated until F_x has subsided to a constant value (attributed to the sum of rolling resistance, brake drag, and bearing and hydraulic system losses) as shown in the figure.

Between passes over the subject surface, the test tire may be maintained in a variety of conditions as the SFD traverses other areas of the test facility; namely:

1) Up
2) Down and Unloaded
3) Down and Loaded

The choice of conditions is largely governed by experience in terms of maintenance of the desired test tire inflation pressure. (See Section 4.3.1.) However, negotiation of tight turns should be avoided with the tire down and loaded. This practice will avoid subjecting the test tire to unnecessary and undesirable wear and subjecting the tire support structure, including the load cell, to unnecessary loading.

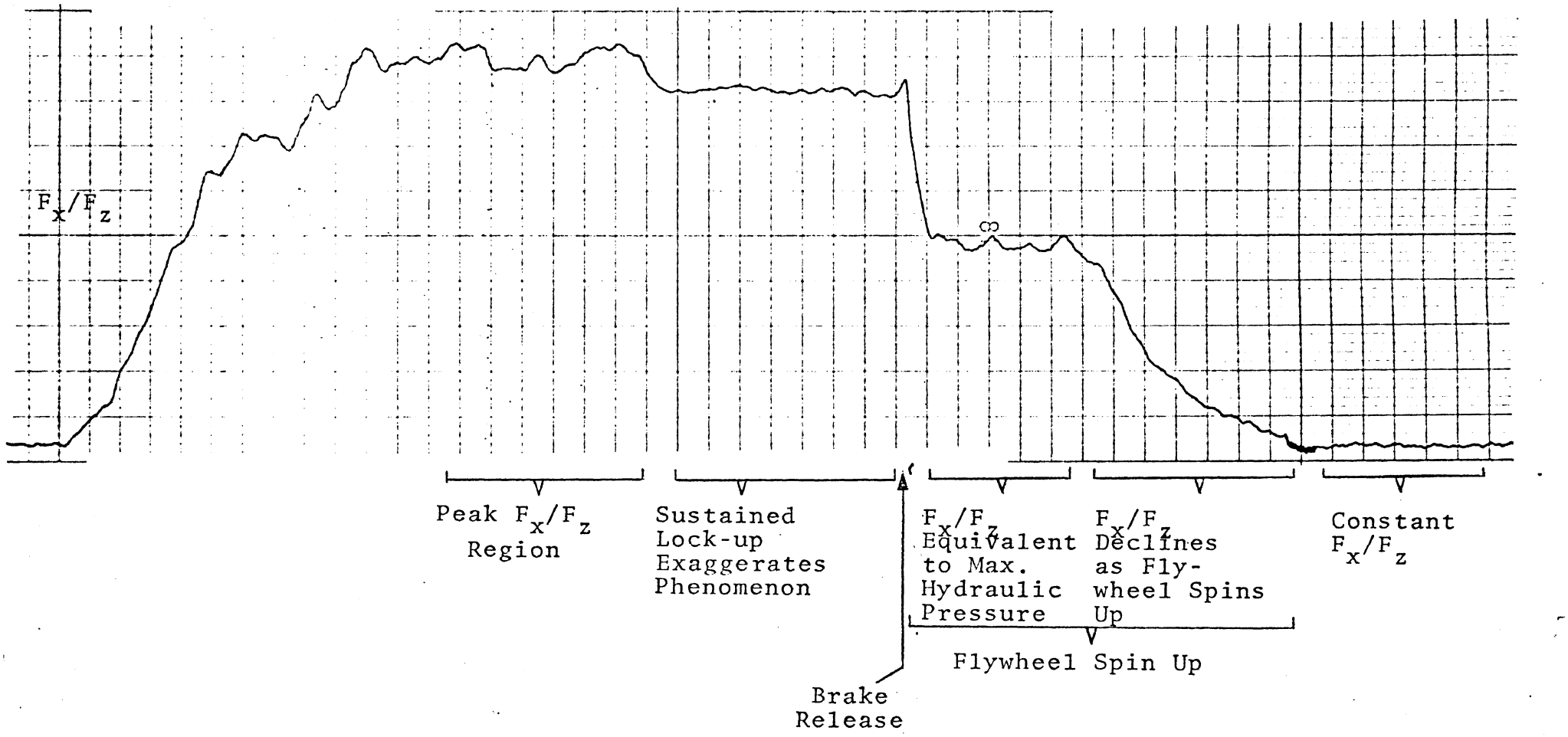

Figure B.13. Flywheel Spin Up Phenomenon

APPENDIX C

PROCEDURE AND PROGRAM FOR REDUCING AND HANDLING THE BRAKING EFFICIENCY TEST DATA

C.1 INTRODUCTION

After conducting a braking efficiency test program, both SFD tire data and vehicle performance data must be reduced in order to procure the final braking efficiency numeric for the test vehicle. This appendix outlines the data handling process developed in this study. Section C.2 outlines data reduction, i.e., the extraction of peak longitudinal friction numerics from the tire data. Section C.3 reviews data processing, i.e., computations performed upon the data which lead to the braking efficiency numeric. Included in this section is a description of

(1) the mathematical computations

(2) the digital computer program which performs these computations.

C.2 DATA REDUCTION

The vehicle stopping distance data requires no reduction activity other than the discarding of invalid data, i.e., stops in which wheel lock occurred. However, point-wise data for processing must be extracted from the SFD tire data. The SFD is equipped for the continuous recording of

F_z	test tire vertical load
F_x/F_z	test tire normalized brake force
V_5	SFD velocity

The reduction of data for each individual tire test is concerned with producing a single value of each of these three measures

for processing. The reduction procedure is as follows:

1. The maximum value of F_x/F_z occurring during a tire test is recorded as μ_p for that test.
2. The maximum and minimum values of F_z recorded within ± .05 sec. of the occurrence of μ_p are averaged. This average value is recorded as the value of F_z for that test.
3. The value of V_5 measured at the occurrence of μ_p is recorded as the velocity of that test.

C.3 DATA PROCESSING*

C.3.1 THE MATHEMATICAL COMPUTATION. The braking efficiency of a vehicle is defined in this document as:

$$E = \frac{DI}{DA} \times 100\% \qquad (C.1)$$

where DA is the actual stopping distance of the vehicle being tested and DI is the ideal stopping distance of the reference vehicle.

Equation (C.1) represents the last in a series of three computations required for data processing. In inverse chronological order, the remaining two are:

(1) The computation of DI, the ideal stopping distance

(2) The computation of the parametric constants for the reference tire equations (see Section 3.2).

The following section addresses these two computations respectively.

---

*Notation in this section may differ somewhat from that used elsewhere in this document. Notation used in this section is equivalent to that used in the digital computer program used for data processing.

C.3.1.1 The Ideal Stopping Distance Computation. The ideal stopping distance is defined as that distance necessary for the reference vehicle to come to a complete stop from the point of brake actuation, assuming quasi-static load transfer and with the vehicle's braking system utilizing the full friction potential of the reference tire/test surface throughout the stop. This potential is realized (conceptually and in the DI computation) by insuring that the longitudinal slip of the vehicle's tires is continuously adjusted to maintain the peak longitudinal friction available at all instantaneous loads and velocities during braking (see Section 3.2).

In equation form:

$$DI = \int_{t_f}^{o} V dt \qquad (C.2)$$

where

V is the instantaneous velocity of the reference vehicle during the stop,

t is time

and t_f is the time taken for the reference vehicle to come to a complete stop after the instant of brake actuation.

Equation (C.2) can be transformed to an integration in V:

$$DI = \int_{o}^{V_o} \frac{V dV}{A_x} \qquad (C.3)$$

where

V_o is the reference vehicle's velocity at the instant of brake actuation

and A_x is the instantaneous deceleration of this vehicle.

In addition to Equation (C.3), the operating equations of the decelerating vehicle system are:

$$A_x = \frac{F_{x_F} + F_{x_R}}{W/G} \tag{C.4}$$

$$F_{x_F} = 2(\mu_F)F_{z_F} \quad , \quad F_{x_R} = 2(\mu_R)F_{z_R} \tag{C.5}$$

$$F_{z_F} = \frac{1}{2}\left[\frac{W(L - a)}{L} + \frac{W \cdot H \cdot A_x}{GL}\right] ,$$

and

$$F_{z_R} = \frac{1}{2}\left[\frac{W(a)}{L} - \frac{W \cdot H \cdot A_x}{GL}\right] . \tag{C.6}$$

where

F_{x_F} is the sum of the instantaneous longitudinal shear forces of the front tires

F_{x_R} is the sum of the instantaneous longitudinal shear forces of the rear tires

μ_F is the instantaneous peak longitudinal friction coefficient of a single front tire

μ_R is the instantaneous peak longitudinal friction coefficient of a single rear tire

F_{z_F} is the instantaneous load on a single front tire

F_{z_R} is the instantaneous load on a single rear tire

G is the acceleration due to gravity

and W, L, H, and a are the reference vehicle's weight, wheelbase, height of c.g. above ground, and distance of c.g. aft of the front axle, respectively.

As outlined in Section 3.2, the traction performance of the reference vehicle's tires, front and rear, respectively, are characterized by:

$$\mu_F = AF \cdot V^2 + BF \cdot V + CF \tag{C.7a}$$

and

$$\mu_R = AR \cdot V^2 + BR \cdot V + CR \tag{C.7b}$$

where AF, BF, CF, AR, BR, and CR are parametric constants. (Procedures for determining these constants appear in the following section.)

Using Equations (C.3)-(C.7) and the definitions:

$$A = AF - AR \qquad D = (L - a)AF + a(AR)$$

$$B = BF - BR \qquad E = (L - a)BF + a(BR)$$

$$C = CF - CR \qquad F = (L - a)CF + a(CR)$$

Equation (C.3) may be transformed to:

$$DI = \int_0^{V_o} \frac{[L - H(AV^2 + BV + C)]}{G(DV^2 + EV + F)} \tag{C.8}$$

The analytical solution to Equation (C.8) is:

$$DI = M(V_o) + P\frac{(V_o)^2}{2} + \frac{Q}{2D}\ln\left|\frac{D(V_o)^2 + E(V_o) + F}{F}\right| + (N - \frac{QE}{2D})I \tag{C.9}$$

where

where

$$M = \frac{H}{G}\left(\frac{AE}{D^2} - \frac{B}{D}\right),$$

$$N = \frac{H}{G}\left(\frac{FB}{D} - \frac{AEF}{D^2}\right),$$

$$P = -\frac{H}{G}\,\frac{A}{D}\,, \tag{C.10}$$

$$Q = -\frac{L}{G} - \frac{H}{G}\left(C - \frac{FA}{D} - \frac{EB}{D} + \frac{AE^2}{D^2}\right),$$

$$R = E^2 - 4DF$$

$$\text{and } I = \begin{cases} \dfrac{1}{\sqrt{R}}\ \ell n\left|\left[\dfrac{2D(V_o)+ E - \sqrt{R}}{2D(V_o)+ E + \sqrt{R}}\right]\left(\dfrac{E + \sqrt{R}}{E - \sqrt{R}}\right)\right| & \text{for } R > 0 \\ \dfrac{2}{\sqrt{-R}}\ \arctan\left[\dfrac{2D(V_o)+E}{\sqrt{-R}}\right] - \arctan\left(\dfrac{E}{\sqrt{-R}}\right) & \text{for } R < 0 \\ \dfrac{4D(V_o)}{2D(V_o)E+E^2} & \text{for } R = 0 \end{cases} \tag{C.11}$$

C.3.1.2 Computing the Tire Descriptor Parametric Constants. The parametric constants, AF, BF, CF, AR, BR, CR, are fitted to the tire data using a least squares linear regression technique. Ignoring the notation F and R (denoting front and rear) the coefficients are:

$$COEFS = (X^T X)^{-1} X^T(\mu) \tag{C.12}$$

where

$$COEFS = \begin{pmatrix} A \\ B \\ C \end{pmatrix} \tag{C.13}$$

$$X = \begin{bmatrix} 1 & V_1 & V_1^2 \\ 1 & V_2 & V_2^2 \\ \vdots & \vdots & \vdots \\ 1 & V_N & V_N^2 \end{bmatrix} \qquad \text{(C.14)}$$

and

$$\mu = \begin{bmatrix} \mu_{p_1} \\ \mu_{p_2} \\ \vdots \\ \mu_{p_N} \end{bmatrix} \qquad \text{(C.15)}$$

and N is the number of data points gathered at the appropriate vertical load. The computation is, of course, performed once for "front tire" data gathered at F_{z_F} and once for "rear tire" data gathered at F_{z_R}.

C.3.2 THE DIGITAL COMPUTER PROGRAM.

C.3.2.1 Program Function. A flow chart of the computer program appears in Figure C.1.

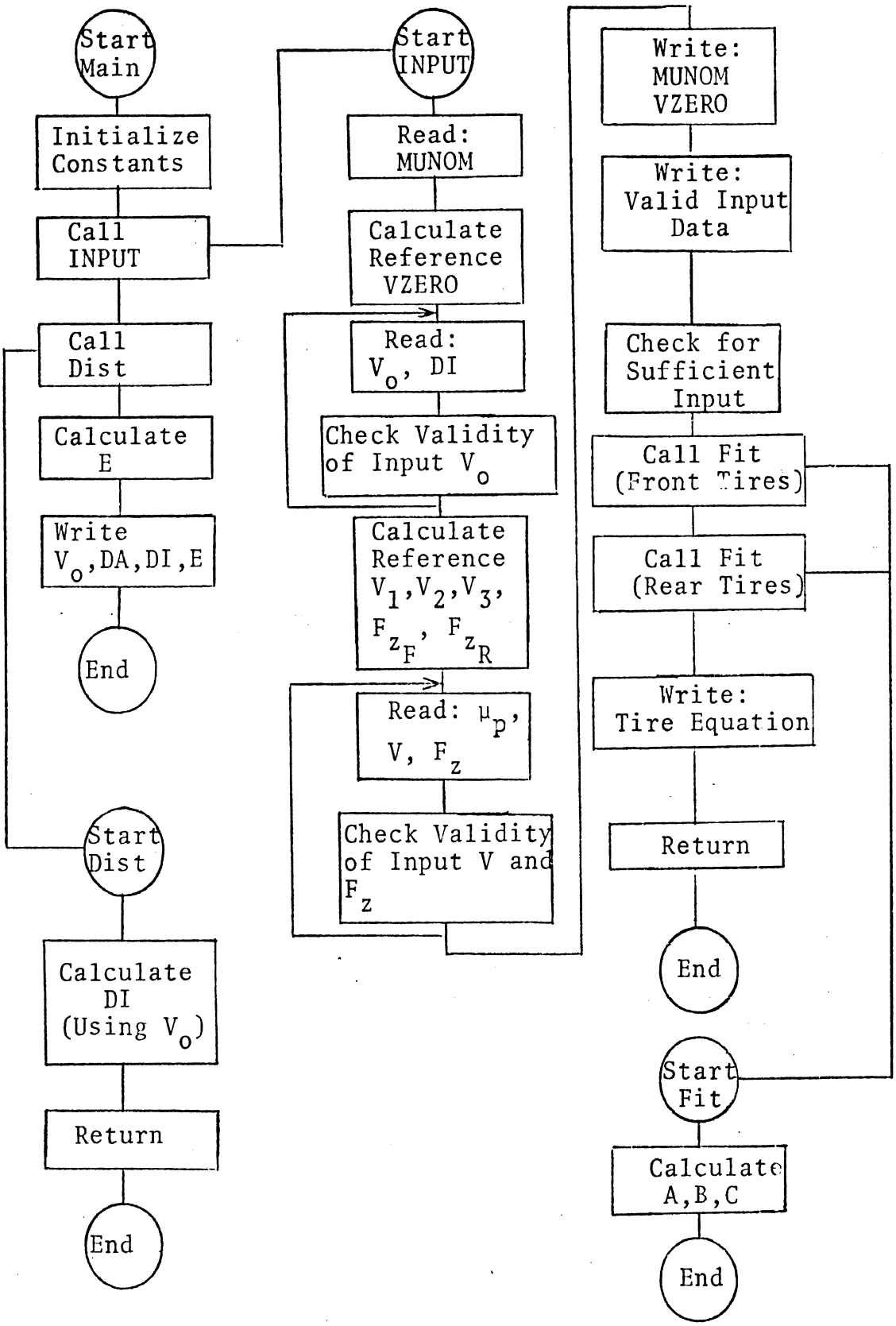

Figure C.1. Braking efficiency computer program flow chart.

The program performs five functions:

(1) Screens input data for validity. The initial velocity of vehicle stopping distance tests is checked to be within ± 2 mph of V_o as prescribed by Figure 9 (Section 3.3). The velocities and vertical loads of tire test input are checked (as per the validity definitions given in Section 3.3).

(2) Determines if sufficient tire data is given (as outlined in Section 3.3).

(3) Determines the parametric constants of the tire equations from the input data.

(4) Calculates the ideal stopping distance of the reference vehicle (stopping from the same initial velocity as the test vehicle).

(5) Calculates the test vehicle's braking efficiency.

A listing of the computer program, written in Fortran IV, follows.

```
CCCCCCCCCCCCCCCCCCCCCCCCC
C
C       MAIN PROGRAM
        REAL L,MUNOM
        DIMENSION V(100),D(100)
        COMMON /CON/ SMALA,G,H,L
        COMMON /VARS/ DA,MUNOM,VZERO
        COMMON /IO/ IR,IW
  672   IR=5
        IW=6
        SMALA=4.35
        G=32.17
        H=1.875
        L=9.383
        CALL INPUT(V,D,NUM,KEYERR)
        IF(KEYERR.NE.0) STOP 1
  200   WRITE(IW,930)
  930   FORMAT('0',50('*')/'0',T15,'BRAKING EFFICIENCY'/T4,'VZERO(MPH)',
     1   4X,'DA(FT)',6X,'DI(FT)',4X,'EFFICIENCY(%)')
        I=I-1
        DO 300 J=1,NUM
        VEL=V(J)*1.4667
        CALL DIST(VEL,DI)
        E=DI/D(J)*100.
  300   WRITE(IW,920) V(J),D(J),DI,E
  920   FORMAT(4X,F10.3,2X,F10.3,2X,F10.3,4X,F6.2)
        GO TO 672
        END
CCCCCCCCCCCCCCCCCCCCCCCCC
C
        SUBROUTINE INPUT(V,D,K,KEYERR)
        REAL MUNOM,MUF,MUR,MUT
        DIMENSION EZF(60),VF(60),MUF(60),KOUNT(6),XF(60,3),VFSO(60)
        DIMENSION EZR(60),VR(60),VRSO(60),XR(60,3),MUR(60),V(100),D(100)
        COMMON /VARS/ DA,MUNOM,VZERO
        COMMON /ABC/ AF,BF,CF,AR,BR,CR
        COMMON /IO/ IR,IW
        EQUIVALENCE (XF(1,2),VF(1)),(XF(1,3),VFSO(1))
        EQUIVALENCE (XR(1,2),VR(1)),(XR(1,3),VRSO(1))
C INITIALIZE FIRST COLUMNS OF BOTH XF AND XR TO 1.0
        DATA XF /60*1.0/, XR /60*1.0/
        KEYERR=0
        READ(IR,900) MUNOM
  900   FORMAT(F20.0)
        VEL=VZERO
        IF(MUNOM.LE.0.25) VMU=20.
        IF(MUNOM.GT.0.25.AND.MUNOM.LE.0.75) VMU=40.*MUNOM+10.
        IF(MUNOM.GT.0.75) VMU=120.*MUNOM-50.
        KVMU=2.*VMU+.5
        VMU=KVMU/2.
  100   CONTINUE
  300   K=1
  320   READ(IR,940) V(K),D(K)
  940   FORMAT(2F20.0)
        IF(V(K).EQ.0.0.OR.K.GE.100) GO TO 340
        IF(ABS(V(K)-VMU).GT.2.0) GO TO 320
        K=K+1
        GO TO 320
  340   K=K-1
        DO 350 I=1,12
```

```
350 KOUNT(I)=0
    VC1=.913*VMU
    KVC1=2.*VC1+.5
    VC1=KVC1/2.
    VC2=.707*VMU
    KVC2=2.*VC2+.5
    VC2=KVC2/2.
    VC3=.408*VMU
    KVC3=2.*VC3+.5
    VC3=KVC3/2.
    FC1=994.+370.*MUNOM
    KFC1=FC1/10.+.5
    FC1=10.*KFC1
    FC2=859.-370.*MUNOM
    KFC2=FC2/10.+.5
    FC2=10.*KFC2
    DELTAV=2.0
    DELTAF=50.0
    NF=1
    NR=1
375 READ(IR,950) FZT,VT,MUT
950 FORMAT(3F20.0)
    IF(FZT.EQ.0.0) GO TO 550
    J=1
    IF(ABS(FZT-FC1).LE.DELTAF) GO TO 380
    J=2
    IF(ABS(FZT-FC2).LE.DELTAF) GO TO 380
    GO TO 375
380 I=1
    IF(ABS(VT-VC1).LE.DELTAV) GO TO 400
    I=2
    IF(ABS(VT-VC2).LE.DELTAV) GO TO 400
    I=3
    IF(ABS(VT-VC3).LE.DELTAV) GO TO 400
    GO TO 375
400 I=3*(J-1)+I
    KOUNT(I)=KOUNT(I)+1
410 IF(J.EQ.2) GO TO 425
    FZF(NF)=FZT
    VF(NF)=VT
    VFSQ(NF)=VT*VT
    MUF(NF)=MUT
    NF=NF+1
    GO TO 375
425 VR(NR)=VT
    FZR(NR)=FZT
    VRSQ(NR)=VT*VT
    MUR(NR)=MUT
    NR=NR+1
500 N=N+1
    GO TO 375
550 NF=NF-1
    NR=NR-1
    WRITE(IW,955) VMU,MUNOM
955 FORMAT('0VMU= ',F7.2,'  MPH'/' MUNOM= ',F8.3)
    WRITE(IW,970) (FZF(I),VF(I),MUF(I),I=1,NF)
970 FORMAT('0',T16,'TIRE DATA'/'0',5X,'FZ(LB)',6X,'V(MPH)',8X,'MU'/
   1  (3X,F10.3,2X,F10.3,2X,F10.3))
    WRITE(IW,980) (FZR(I),VR(I),MUR(I),I=1,NR)
980 FORMAT((3X,F10.3,2X,F10.3,2X,F10.3))
```

```
  600 DO 650 I=1,6
      IF(KOUNT(I).GE.5) GO TO 650
      KEYERR=1
      WRITE(IW,960) I
  960 FORMAT(' ***ERROR:  LESS THAN FIVE DATA POINTS IN MATRIX ',
     1  'POSITION ',I2,'***')
  650 CONTINUE
      IF(KEYERR.NE.0) RETURN
      CALL FIT(AF,BF,CF,XF,MUF,NF)
      CALL FIT(AR,BR,CR,XR,MUR,NR)
      AF1=AF/.464876
      AR1=AR/.464876
      BF1=BF/.681818
      BR1=BR/.681818
      WRITE(IW,800)AF1,BF1,CF,AR1,BR1,CR
  800 FORMAT('0',50('*')/'0',T15,'TIRE EQUATIONS'/2X,'FRONT TIRES:'/
     1        2X,'MUP=',F11.3,'*V**2 +',F11.3,'*V +',F11.3/2X,
     2        'REAR TIRES:'/2X,'MUP=',F11.3,'*V**2 +',F11.3,'*V +',
     3        F11.3)
      RETURN
      END
CCCCCCCCCCCCCCCCCCCCCCCCC
C
      SUBROUTINE DIST(VEL,DI)
      REAL M,N,L,I
      COMMON /CON/ SMALA,G,H,L
      COMMON /VARS/ DA,MUNOM,VZERO
      COMMON /ABC/ AF,BF,CF,AR,BR,CR
      A=AF-AR
      B=BF-BR
      C=CF-CR
      D=(L-SMALA)*AF+SMALA*AR
      E=(L-SMALA)*BF+SMALA*BR
      F=(L-SMALA)*CF+SMALA*CR
      M=H/G*(A*E/(D*D)-B/D)
      N=H/G*(B*E/D-A*E*E/(D*D))
      P=-H*A/(G*D)
      O=L/G-H/G*(C-A*E/D-E*B/D+A*E*E/(D*D))
      R=E*E-4.*D*F
      IF(ABS(R).LE.0.000001) GO TO 200
      IF(R.LT.0.0) GO TO 100
  300 I=ALOG((2.*D*VEL+E-SQRT(R))/(2.*D*VEL+E+SQRT(R))*
     1  (E+SQRT(R))/(E-SQRT(R)))/SQRT(R)
      GO TO 400
  100 I=2./SQRT(-R)*(ATAN((2.*D*VEL+E)/SQRT(-R))-ATAN(E/
     1  SQRT(-R)))
      GO TO 400
  200 I=2./E-2./(2.*D*VEL+E)
  400 DI=M*VEL+P*VEL*VEL/2.+O/(2.*D)*ALOG((D*VEL*VEL+
     1  E*VEL+F)/F)+(N-O*E/(2.*D))*I
      RETURN
      END
CCCCCCCCCCCCCCCCCCCCCCCCC
C
      SUBROUTINE FIT(A,B,C,X,Y,N)
C FROM THE EMPIRICAL DATA CONTAINED IN MATRIX X AND VECTOR Y. FIT
C  COMPUTES A, B AND C.  N IS THE NUMBER OF ENTRIES IN THE
C  MATRIX AND THE VECTOR.
      DIMENSION R(3),X(60,3),Y(60),XTRAN(3,60),PROD(3,3),L(3),M(3)
      DIMENSION EXTRA(3,60)
```

```
C PUT X-TRANSPOSE IN XTRAN
      DO 10 I=1,3
      DO 10 J=1,N
   10 XTRAN(I,J)=X(J,I)
C CALCULATE THE PRODUCT OF XTRAN TIMES X
   15 DO 20 J=1,3
      DO 20 I=1,3
      PROD(I,J)=0.0
      DO 20 K=1,N
   20 PROD(I,J)=PROD(I,J)+XTRAN(I,K)*X(K,J)
C INVERT THE RESULTING MATRIX
      CALL MINV(PROD,3,D,L,M)
      IF(D.EQ.0.0) STOP 10
      DO 30 I=1,3
      DO 30 J=1,N
      EXTRA(I,J)=0.0
      DO 30 K=1,3
   30 EXTRA(I,J)=EXTRA(I,J)+PROD(I,K)*XTRAN(K,J)
C MULTIPLY THE RESULT BY THE VECTOR OF MUS
      DO 40 I=1,3
      R(I)=0.0
      DO 40 K=1,N
   40 R(I)=R(I)+EXTRA(I,K)*Y(K)
      C=R(1)
      B=R(2)*.681818
      A=R(3)*.464876
      RETURN
      END
```

C.3.2.2 Program Input. The computer program requires the following input form:

Data	Format
TEST SURFACE MUNOM	F10.4
VEHICLE STOPPING DISTANCE DATA	
INITIAL VELOCITY (MPH), STOPPING DISTANCE (FT)	2F10.4
.	.
.	.
.	.
.	.
.	.
(UP TO 100 DATA SETS. ONE SET PER LINE)	.
.	.
.	.
.	.
.	.
0.0 (INDICATES END OF VEHICLE DATA)	F10.4
TIRE TEST DATA	
LOAD (LB), VELOCITY (MPH), μ_p	3F10.4
.	.
.	.
.	.
.	.
(UP TO 60 DATA SETS. ONE SET PER LINE)	.
.	.
.	.
.	.
0.0 (INDICATES END OF DATA)	F10.4

C.3.3.3 Program Output. An example of program output is presented below. Note that the tire data echo contains only valid tire data according to the reference tire test matrix scheme presented in Section 3.3.

Similarly, output under the heading "Braking Efficiency" reflects calculations only for those vehicle tests input whose initial velocities were considered valid.

--------651607----------651607----------651607-----

VMU= 57.00 MPH
MUNOM= 0.890

TIRE DATA

FZ(LB)	V(MPH)	MU
1300.000	24.000	0.950
1280.000	24.000	0.920
1290.000	25.000	0.940
1290.000	24.000	0.920
1310.000	23.500	0.930
1300.000	24.000	0.910
1320.000	40.000	0.850
1300.000	41.000	0.870
1300.000	39.500	0.850
1320.000	41.000	0.850
1290.000	42.000	0.850
1300.000	52.000	0.820
1290.000	50.500	0.830
1300.000	52.000	0.830
1280.000	52.000	0.820
1300.000	52.000	0.810
510.000	41.500	0.880
520.000	41.500	0.970
530.000	42.500	0.910
540.000	40.000	0.930
510.000	41.500	0.960
550.000	24.000	0.980
510.000	24.000	0.980
530.000	23.000	0.920
510.000	23.000	0.960
530.000	23.500	1.000
490.000	52.000	0.960
490.000	52.000	0.930
490.000	52.000	0.950
520.000	51.500	0.930
500.000	51.500	0.930

****

TIRE EQUATIONS

FRONT TIRES:
MUP= 0.521E-04*V**2 + -0.778E-02*V + 0.109E 01
REAR TIRES:
MUP= 0.996E-04*V**2 + -0.848E-02*V + 0.111E 01

****

BRAKING EFFICIENCY

VZERO(MPH)	DA(FT)	DI(FT)	EFFICIENCY(%)
56.600	186.100	119.719	64.33
56.700	186.000	120.164	64.60
58.000	185.900	126.014	67.79
56.500	189.600	119.276	62.91
56.500	195.200	119.276	61.10

C.3.3.4 Dictionary of Computer Program Terms.

AF, BF, CF, AR, BR, CR	Coefficients for Equation (C.7). [AF and AR are in units of $(sec/ft)^2$; BF and BR are in units of sec/ft; CF and CR are dimensionless.
D	Matrix containing actual stopping distances (DA) associated with initial velocities (VZERØ) stored in matrix V.
DA	Actual stopping distance (ft) of test vehicle.
DELTAF	Allowable tolerance (lb) in FC1 and FC2 for tire tests (equal to 50 lb).
DELTAV	Allowable tolerance (mph) in VC1, VC2, and VC3 for tire tests (equal to 2 mph).
DI	Ideal stopping distance of reference vehicle equipped with reference tires.
DIST	Subroutine used to compute DI.
E	Braking efficiency (%) of test vehicle.
FC1, FC2	Tire loads (lb) to be used in determining the peak longitudinal friction coefficients for the standard tire FC1 = 994 + MUNOM (370) lb, FC2 = 859 - MUNOM (370) lb.

FIT	Subroutine used to determine coefficients AF, BF, CF, AR, BR, and CR.
FZF	See MUF
FZR	See MUR
FXT	See MUT
G	Gravity constant (equal to 32.17 ft/sec^2).
H	Vertical distance from ground to c.g. of reference vehicle (equal to 1.875 ft).
INPUT	Subroutine to read in data and to check data for consistency.
IR	Read device number.
IW	Write device number.
KEYERR	Flag, initially set to 0. If set to 1 in subroutine INPUT, program will stop when control is returned to main routine.
KØUNT	Counter for the number of data points in each of the six tire matrix positions.
L	Wheelbase of reference vehicle (equal to 9.383 ft.).
MUF	Matrix containing peak longitudinal friction coefficients (μ_{xp}) obtained from the tire tests using a load in the range FC1 ± DELTAF. FZF and VF are matrices containing the corresponding tire load and velocity, respectively, for each μ_{xp} in MUF.

MUNØM	Nominal coefficient of friction for test surface.
MUR	Matrix containing peak longitudinal friction coefficients (μ_{xp}) obtained from the tire tests using a load in the range FC2 ± DELTAF. FZR and VR are matrices containing the corresponding tire load and velocity, respectively, for each μ_{xp} in MUR.
MUT	Entered peak longitudinal friction coefficient corresponding to load FZT and velocity VT.
NF	Counter for number of tire data points put into matrix XF.
NR	Counter for number of tire data points put into matrix XR.
SMALA	Horizontal distance from center of front axle to c.g. of standard vehicle (equal to 4.35 ft.).
V	See D
VC1, VC2, VC3	Velocities (mph) at which tire tests should be run (within tolerance of DELTAV). VC1 = .913 VMU mph, VC2 = .207 VMU mph, and VC3 = .408 VMU mph. (All to the nearest 1/2 mph)
VEL	VZERØ in ft/sec.
VF	See MUF
VFSQ	Matrix containing squared values of each element in VF.
VR	See MUR

VRSQ	Matrix containing squared values of each element in VR.
VMU	Computed value of VZERØ (mph) using MUNØM
VT	See MUT
VZERØ	Velocity (mph) at instant of brake actuation.
XF	Matrix with first column containing 1'S, second column containing VF, and third column containing VFSQ. Used in subroutine FIT to determine AF, BF, and CF.
XR	Matrix with first column containing 1'S, second column containing VR, and third column containing VRSQ. Used in subroutine FIT to determine AR, BR, and CR.

APPENDIX D

PROCEDURE FOR CONDUCT OF THE BRAKING EFFICIENCY TEST TECHNIQUE

D.1 SCOPE AND APPLICATIONS

The Braking Efficiency Test Technique is applicable to the measurement of the limit braking performance of any highway vehicle. It constitutes a method whereby the limit stopping distance which is achievable with a constant effort braking input is normalized using a reference stopping distance value which is computed. The computed reference value accounts for the prevailing friction potential of the test surface, but is not adjusted in any way to account for the particular test vehicle being examined. The computation of the reference normalizer requires the gathering of a special set of tire-pavement traction data using a reference tire and a mobile dynamometer device.

D.2 TEST PROCEDURE - VEHICLE STOPPING DISTANCE

D.2.1 GENERAL. Successive straight-line stops are conducted, from a described initial velocity, gathering data defining the shortest stopping distance achievable without incurring lockup of any wheel. These stops are conducted with constant pedal effort.

D.2.2 DEFINITIONS.

Lockup - A condition in which the angular velocity of a vehicle's wheel has reduced below a level corresponding to ω and which has exceeded that level for more than x seconds, while the vehicle is at a speed above V.

Stopping Distance - The elapsed distance traveled in stopping a vehicle following initiation of movement at the service brake control element.

μ_{nom} - A nominal measure of the peak normalized longitudinal force capability (peak F_x/F_z) of the reference tire, deriving at a vertical load of 925 lbs., and a test velocity V_t within the range $.707V_o - 5 \leq V_t \leq .707V_o + 5$ (mph)

V_o - The nominal initial velocity of the stopping distance test. V_o is determined, knowing μ_{nom}, according to the relationship shown in Figure D.1.

D.2.3 TEST CONDITIONS.

Surface - Any straight, paved surface whose grade does not exceed 1% and whose μ_{nom} measure is between 0.40 and 1.05.*

Initial Velocity - Equal to $V_o \pm 2$ mph.

Brake Control Input - To be a constant effort input ± 5% of the nominal steady value.

D.2.4 CONDUCT OF THE STOPPING DISTANCE TESTS. From the desired initial velocity, the brake control input is applied while steering control is exercised to maintain the

*Upper and lower bounds of the μ_{nom} range are tentatively suggested as reasonable values, but as suggested in the "recommendations" section of this report, further research is required for the establishment of solidly defensible values.

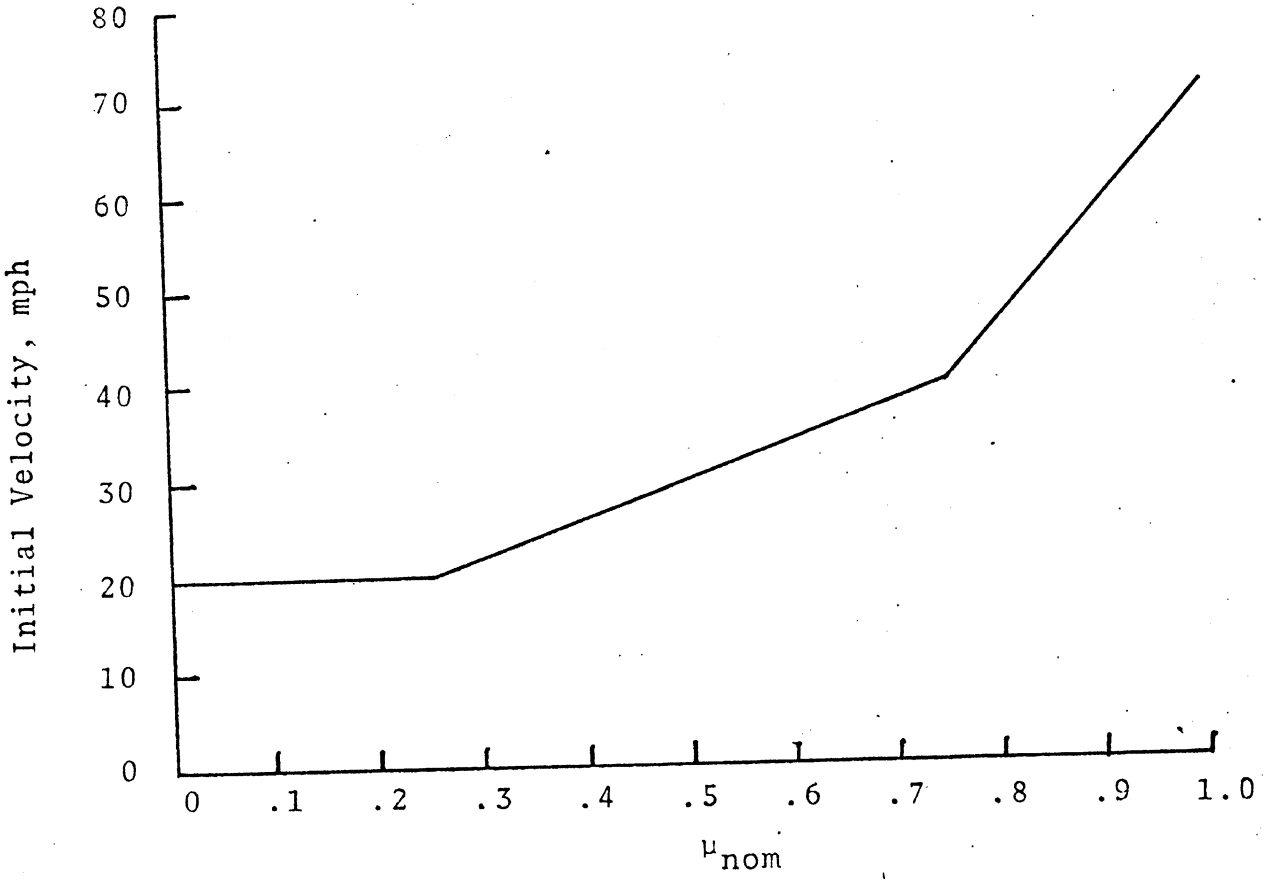

Figure D.1 Initial velocity as a function of μ_{nom}.

vehicle within a 12-foot lane. In manual transmission vehicles, the clutch is depressed prior to brake application; automatic transmission vehicles are maintained in a normal drive gear throughout the braking process.

Iterative tests are made to determine a virtually maximum control input level at which wheel locking is not incurred. A maximum of 15 runs are to be made in selecting the control input level at which minimum stopping distance data are to be taken. With anti-wheel-lock-equipped vehicles an iterative activity may not be necessary if minimum stopping distance accrues at a braking input level which causes anti-locking modulations.

Upon determining the brake control input level at which performance is to be assessed, five successive stops are to be conducted at that input level.

D.2.5 ACQUIRED DATA. For each of the five performance-assessment stops, the stopping distance and initial velocity values are to be tabulated.

D.3 TEST PROCEDURE - TRACTION PERFORMANCE OF THE REFERENCE TIRE

D.3.1 GENERAL. A set of tests are to be conducted using a mobile dynamometer device, in which a reference tire is to be operated over a matrix of two vertical loads and four velocities. The peak normalized longitudinal force measurements obtained will be used in characterizing the prevailing friction condition of the surface upon which measurements were made.

D.3.2 DEFINITIONS.

V_I - Nominal velocity of the mobile dynamometer at which tire traction data is gathered—subscript, I, identifies each of (4) velocity conditions.

F_{zT} - Nominal vertical load applied to the reference tire—subscript, T, identifies each of (2) load conditions.

Reference Tire - The ASTM Traction Standard tire (belted bias-ply - size G78-15) as defined in ASTM E501-73.

Peak F_x/F_z - The peak value which is observed in the filtered F_x/F_z time history. The raw F_x/F_z signal is to be passed through a critically damped second-order filter whose natural frequency is 5 Hz.

D.3.3 TEST CONDITIONS.

Surface - The tire traction measurements are to be made on the subject surface and under such surface conditions as prevailed during gathering of the previously described stopping distance data.

Path of the Test Tire - The test tire is to be operated over the nominal location of the wheel paths which were established during vehicle tests. Data should

be taken only over that length of pavement which was traveled during the stopping process of the vehicle tests.

F_{zT} Tire Vertical Load - The reference tire is to be tested at each of two vertical loads, F_{zF} and F_{zR}, where,

$$F_{zF} = 994 + 370\ (\mu_{nom}) \quad \text{lbs}$$

$$F_{zR} = 859 - 370\ (\mu_{nom}) \quad \text{lbs}$$

as shown in Figure D.2.

V_I, Test Velocity - At each vertical load level, the reference tire is to be tested at each of four values of velocity, V_{1-4}, in which:

$V_1 = .920\ V_o$

$V_2 = .735\ V_o$ (V_o is defined from μ_{nom} as shown in Figure D.1)

$V_3 = .483\ V_o$

$V_4 = .200\ V_o$

Reference Tire Inflation Pressure - During measurement operations the reference tire sample is to be maintained at a "warm" inflation pressure value of 27 psi.

Reference Tire - Tread Depth - A reference tire sample is to be utilized in measurement operations only when groove depth exceeds 0.165 inches in every groove.

D.3.4 CONDUCT OF THE TESTING SEQUENCE. An evaluation of μ_{nom} is required first, as defined earlier. An iterative set of tests may be needed to attain a measured value for

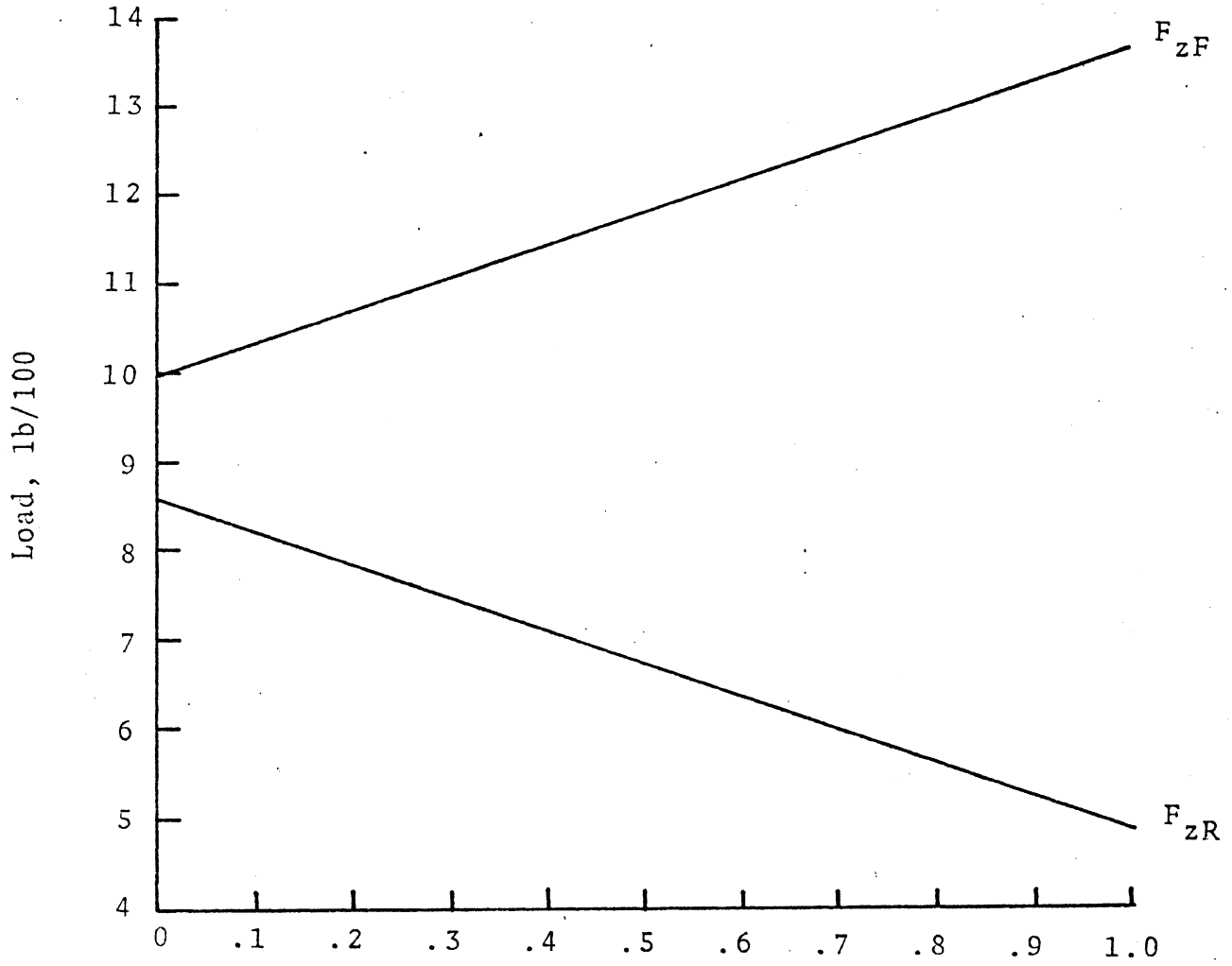

Figure D.2 Tire test loads as a function of μ_{nom}.

μ_{nom} at a velocity which is within 5 mph of the (.707 × V_o) value—where V_o is defined as a function of μ_{nom} in Figure D.1—and at a load of 925 lb. ± 50 lb.

With μ_{nom} established, values of $V_{1\to4}$, F_{zF}, and F_{zR} can be determined. At each of the eight load and velocity combinations, a minimum of five valid tire tests are to be conducted. A tire test is considered valid when it incorporates an F_{zT} condition which is within ± 50 lbs. of the desired load and a V_I condition which is within ± 2 mph of the desired velocity, while the test tire is inflated to within ± 1 psi of the desired 27 psi value.

The test itself involves the imposition of a full cycle of longitudinal slip to the reference tire—from the freely rolling zero slip condition to the locked wheel, 100% slip condition and then back to zero slip again. The slip sweep is to be sufficiently slow, in time, that the tire's longitudinal force response shall remain within ± 10% of its peak value for periods of at least .200 seconds.* The locked wheel condition is to be limited to less than .200 seconds.

D.3.5 DATA REQUIREMENTS. Each of the five repeat runs at each tire test condition must be represented by a set of data describing the values of:

1. test velocity, V_I
2. tire vertical load, F_{zT}, and
3. normalized longitudinal force, F_x/F_z

as were measured at the occasion of peak F_x/F_z during the slip cycle. These forty (8 conditions × five repeats) sets of data then are input to the braking efficiency computation program.

---

*The peak value retention time of .200 seconds is tentatively suggested as a reasonable value.

APPENDIX E
THE VARIABLE BRAKING VEHICLE

The Variable Braking Vehicle (VBV) has been conceived as a research tool for (a) the human factors investigation of man-machine interactions during braking, (b) the engineering evaluation of innovative brake system configurations, and (c) as a means for determining the ability of brake diagnostic devices to detect degradations in vehicle braking performance. In concept, such a vehicle requires a control and instrumentation system by which the braking action at each wheel may be independently programmed, controlled, and monitored. These goals have been achieved for rear wheel braking control by means of the system configuration diagrammed* in Figure E.1.

The Model Reference Computer (MRC) is the central component in the VBV system. This computer is a programmable, special-purpose, analog device which serves as an electronic analog of any proposed brake system whose performance is to be synthesized. The analog inputs required by the MRC are supplied by means of an extensive instrumentation system. The outputs of the MRC command two electrohydraulic control systems which actuate the left and right rear brakes of the vehicle independently. The instrumentation system, the MRC, and the electrohydraulic control systems are collectively designated the Model Reference Control System (MRCS). Together they produce braking actions at the rear wheels of the vehicle which are in accord with the outputs of the mathematical model of the brake system programmed on the MRC. The extension of this design to include front wheel braking control is under

---

*Subscripts 1 and 2 are used to designate the left-rear and right-rear control systems, respectively.

consideration but is not necessary for the work of the proposed program.

A 1969 Chevrolet Townsman station wagon equipped with a 396 cubic inch displacement (CID) engine, automatic transmission, power brakes, manual steering, and air conditioning was used as the foundation vehicle for the development of the VBV. The car was purchased with disc brakes on the front wheels and duo-servo drum brakes on the rear wheels.

The vehicle has been extensively modified during the construction of the VBV. In order to provide more consistent brake performance, the rear-axle drum brakes were replaced by disc brakes having two calipers per disc. One set of left and right calipers is dedicated to the VBV control system, while the second set is part of a completely independent emergency braking system. The emergency brakes are actuated by a pedal and master cylinder located next to the normal brake pedal. Both chambers of the master cylinder have been routed to the brakes on the front wheels. The air conditioning compressor and hoses have been removed from the engine compartment to make room for a hydraulic pump and a heavy duty alternator. The heat exchanger of the air conditioning system has been utilized as part of the hydraulic power system.

The various pieces of equipment associated with the MRCS and its ancillary systems are distributed throughout the car as shown in Figure E.2.

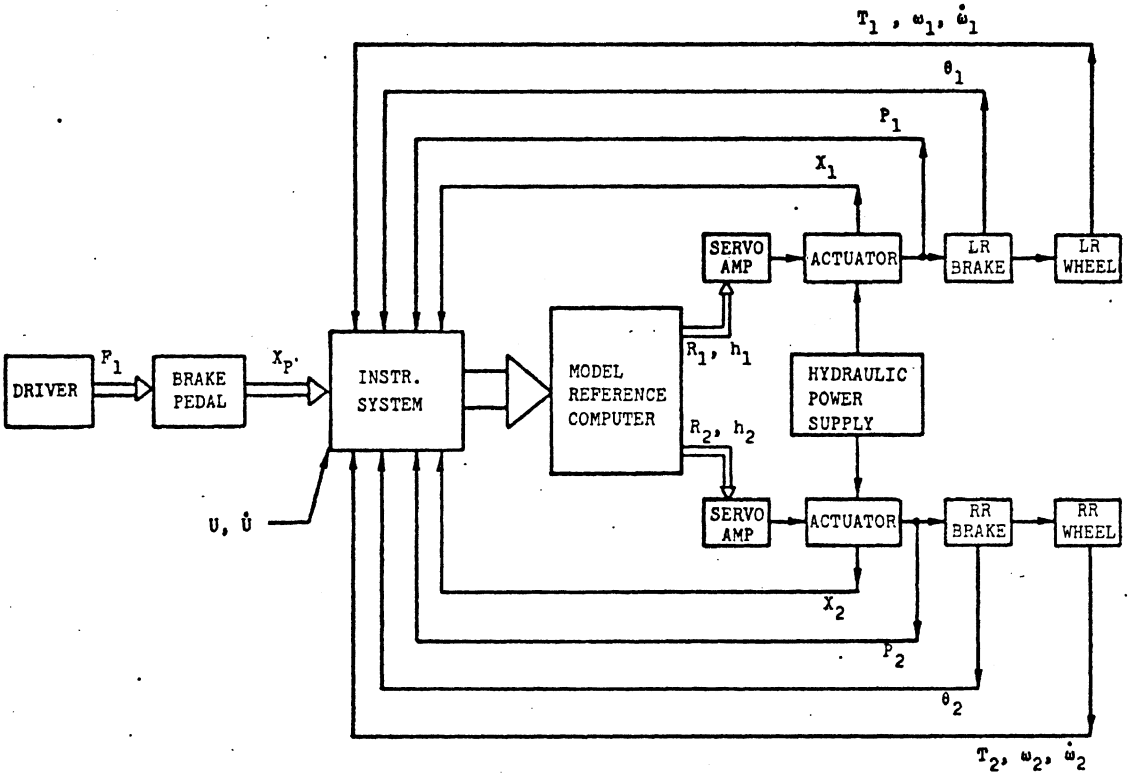

Figure E.1 Model-Reference Control System (MRCS)

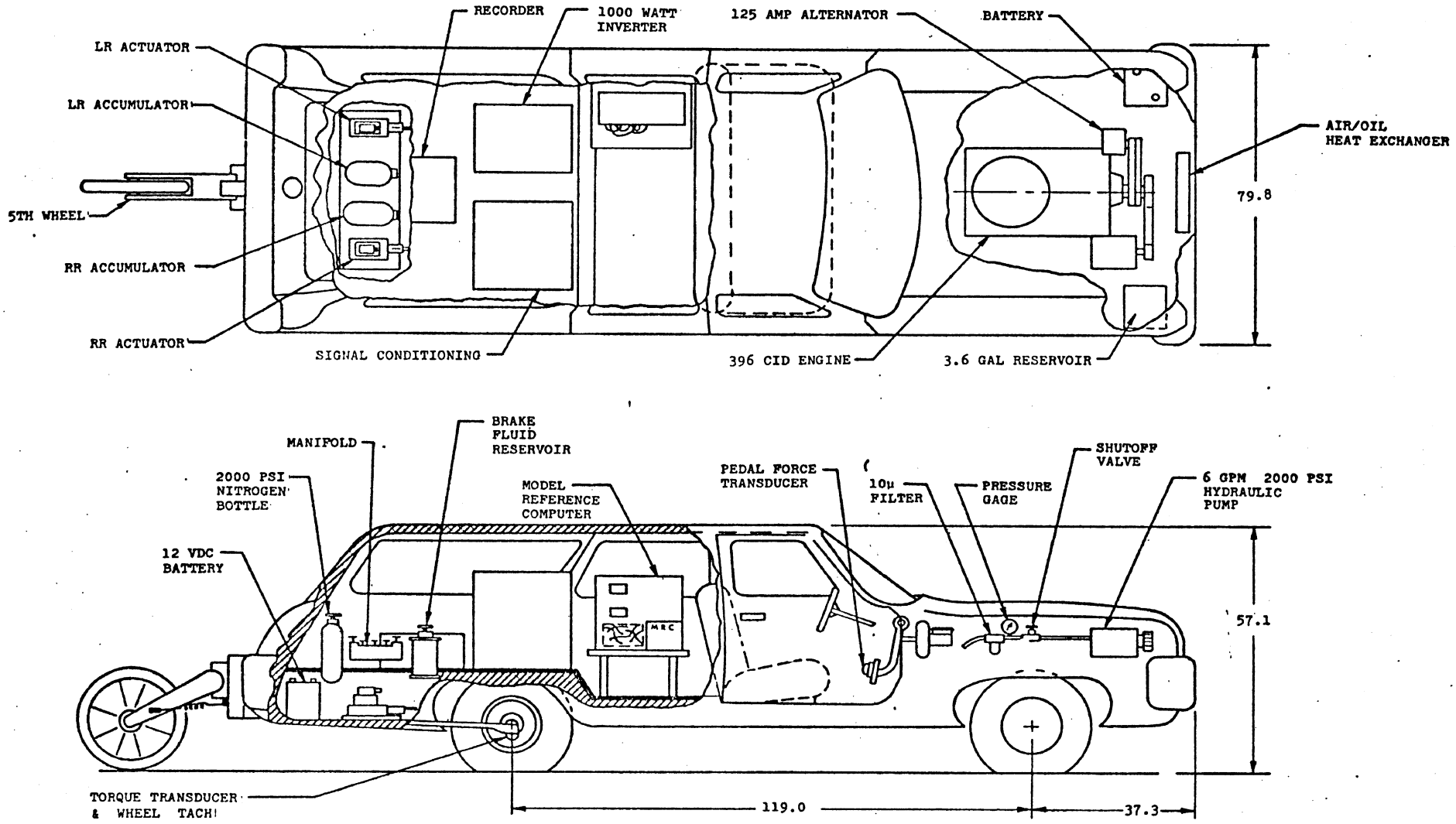

Figure E.2. Major equipment installations in VBV